HEAT TRANSFER TO FREON 12 NEAR THE CRITICAL STATE IN A THERMAL SYPHON TYPE APPARATUS

By

JACK PHILIP HOLMAN

Bachelor of Science in Mechanical Engineering
Southern Methodist University
Dallas, Texas
1955

Master of Science in Mechanical Engineering
Southern Methodist University
Dallas, Texas
1956

Submitted to the faculty of the Graduate School of
the Oklahoma State University of
Agriculture and Applied Science
in partial fulfillment of the
requirements for the degree
of
DOCTOR OF PHILOSOPHY
August, 1958

HEAT TRANSFER TO FREON 12 NEAR THE CRITICAL STATE IN A THERMAL SYPHON TYPE APPARATUS

Thesis Approved:

Thesis Adviser

Dean of the Graduate School

ACKNOWLEDGEMENT

The writer wishes to acknowledge the partial sponsorship of this research by a grant from the General Electric Company. Acknowledgement is also extended to the E.I. du Pont de Nemours Company for donating the Freon 12 used in the research.

The writer is indebted to Professor J.H. Boggs for his helpful guidance during the entire Ph.D. program. The constructive criticism of this thesis by Professors R.N. Maddox, J.R. Norton, and T.B. Thompson was particularly appreciated.

In respect to the construction of the experimental apparatus, the detailed and constructive suggestions of Professor B.S. Davenport as well as the technical competence of laboratory technicians J.A. McCandless and George Cooper, were of immeasurable aid in the research.

The writer was assisted in the research by Gene Nestle, a graduate student. Mr. Nestle's aid in the construction of the apparatus, continuing interest in the progress of the research, calibration of the equipment, and splendid preparation of many of the figures made a definite contribution to this thesis.

Most of all, the writer wishes to thank all those people connected with his academic career who have offered encouragement at various decisive times. This encouragement was often a joke or a light-hearted statement which served to enliven an otherwise exhaustive task. At other times the encouragement was in the form of a blunt and penetrating statement. To these people, who always seem to extract the very best

from life and offer the most important points for consideration in any discussion, the writer extends his gratitude.

TABLE OF CONTENTS

LIST OF TABLES

LIST OF FIGURES

LIST OF FIGURES (Continued)

LIST OF FIGURES (Continued)

LIST OF PLATES

CHAPTER I

INTRODUCTION

Rapidly expanding technological fields of today have created a demand for new and better methods of removing heat from various types of equipment. These methods usually require the knowledge of the heat transfer properties of particular fluids and materials at high temperatures and pressures. This thesis has two objectives which are co-linear with the recent demands on the science of heat transfer; to investigate the characteristics and feasibility of a thermal syphon type apparatus, and to investigate the heat transfer characteristics of Freon 12, dichlorodifloromethane, operating near its critical state in the thermal syphon type of apparatus. Freon 12 is chosen as the fluid to be investigated because of its low critical temperature and pressure and the availability of data on its thermodynamic and physical properties.

The thermal syphon type apparatus is of interest because it requires no circulation pump so that it could prove of significant practical value in an application where containment of the thermodynamic medium is of prime concern. One application for the thermal syphon could be the cooling of a nuclear reactor.

The critical region is of interest because of the high heat transfer film coefficients which may be expected in this region. A qualitative discussion of the critical state will verify this expectation.

In the regions having pressures lower than the critical value, boiling may take place. Boiling usually originates with the formation of small vapor bubbles on the heat transfer surface. After these bubbles are formed they may interact with neighboring bubbles until they are eventually dissipated into the body of the fluid stream. The greater the surface tension the greater may be the size of the bubbles. The greater the size of the bubbles the less the freedom of movement of these bubbles and the less the freedom of movement the smaller is the rate of energy or heat transfer.

As the critical point is approached the surface tension decreases. With this decrease in surface tension smaller bubbles which disseminate very rapidly are formed on the heat transfer surface. At the critical point the surface tension becomes zero and hence a very large number of bubbles is formed. These bubbles have a correspondingly rapid dissipation into the body of the fluid stream. Therefore, very high heat transfer rates may be expected in the immediate vicinity of the critical state.

If a large quantity of energy is removed by the fluid stream its caloric properties will be changed appreciably so that it would not be possible to operate exactly at the critical point. Therefore, the heat transfer rates near the critical state will depend, to a certain extent, on the total quantity of energy removed from the heat transfer surface.

It will be seen that the theory of the thermal syphon type of apparatus does not predict abnormally large values of the heat transfer film coefficient in the critical region. This apparent paradox is in contrast to measured values of the film coefficient presented by previous investigators. (1), (2). However, the thermal syphon type of apparatus

is peculiar in that the flow rate of the fluid is a direct function of the heat transfer rate. The relationships between the heat transfer rates and the flow rates are quite explicit and they are verified experimentally in this thesis.

CHAPTER II

PREVIOUS INVESTIGATIONS IN THE CRITICAL REGION

Only a few investigations into the heat transfer characteristics of fluids operating near the critical state have been conducted. The essential features of these investigations will be discussed in this chapter.

Dickenson and Welch (1) have established the heat transfer characteristics of water operating under forced convection in the critical and supercritical regions. They found that for temperatures below 660°F their data could be correlated by the conventional relation

$$\frac{h d}{k} = 0.023 \left(\frac{\gamma u d}{\mu} \right)^{0.8} \left(\frac{c_p \mu}{k} \right)^{0.4},$$

where

h = heat transfer film coefficient,

d = tube diameter,

k = thermal conductivity,

γ = specific weight of fluid,

u = average fluid velocity,

μ = dynamic viscosity,

c_p = specific heat at constant pressure.

At higher temperatures they did not establish a correlation in terms of dimensionless groups. Instead, they found that the best method to accurately present the data was in the form of a plot of film conductance

h as a function of the surface temperature of the heat transfer tube. The investigators felt that this method of correlation was preferable over a dimensionless correlation because of inadequate property data in the critical region.

In the plots of h as a function of t_s presented by Dickenson and Welch the values of the film conductance increase to extremely large values as the critical temperature is approached. The authors present data for pressures of 3500 psia and 4500 psia and for both of these pressures this large increase of the film conductance is present although for the 3500 psia points it is more pronounced. For surface temperatures above 800°F Dickenson and Welch found that their data could be correlated within ten percent by

$$St = \frac{h}{c_p \gamma u} = \text{constant} = 0.00189,$$

where St is the Stanton number. In the critical region (650°F to 800°F) the authors found a marked decrease in the Stanton modulus by a factor of approximately three.

The range of variables covered in the experiments of Dickenson and Welch were:

Temperature:	220°F to 1000°F
Mass Flow Rates:	1.6×10^6 to 2.5×10^6 lb/hr-ft^2
Heat Flux:	280,000 to 580,000 Btu/hr-ft^2

Doughty and Drake (2) have investigated free convection heat transfer from a horizontal platinum wire to Freon 12 near the critical state. They found that in the superheated vapor region away from the critical state their data could be correlated within fifteen percent by

the curve recommended by McAdams (3). In the critical region they found that the heat transfer coefficients increase tenfold. Because of inadequate property data the authors found that a correlation in terms of dimensionless groups would not suffice. For this reason they presented their results as functions of reduced volume and reduced pressure defined by:

$$\text{reduced volume} = \frac{v}{v_c} = v_R,$$

$$\text{reduced pressure} = \frac{p}{p_c} = p_R.$$

Within three percent of the critical reduced charge they found that the heat transfer film coefficient increases apparently without limit. This same increase occurs within a range of approximately one percent of the critical reduced pressure. According to the data of Doughty and Drake, heat transfer coefficients as high as 350 Btu/hr-ft^2-^{o}F may be expected in the vicinity of the critical point.

Schmidt, Eckert, and Grigull (4) investigated the heat transfer characteristics of ammonia in a thermal syphon type apparatus. The theory developed by these authors is presented in Chapter IV. Due to lack of information on the properties of ammonia near the critical state the authors were not able to verify their theory experimentally. The essential parts of their data presentation were plots of an apparent thermal conductivity defined by

$$k_a \equiv \frac{q\,l}{\Delta t_b A},$$

where

q = heat flow per unit time,

ℓ = one-half of the circumferential length of the loop,

Δt_b = bulk temperature difference in the loop,

A = inside cross sectional area of the tube.

A discussion of this quantity as well as the details of the analysis of Schmidt, Eckert, and Grigull will be given in subsequent chapters.

CHAPTER III

DESCRIPTION OF THE TEST APPARATUS

A test apparatus was constructed to investigate heat transfer characteristics of Freon 12 operating near the critical state. The apparatus operates on the same basic principle as the apparatus used in the experiments of Schmidt, Eckert, and Grigull (4). The apparatus to be discussed in this chapter included several refinements over the apparatus of these authors. These refinements were made in order that more specific data could be collected and hence a better correlation of the data might be realized. The refinements in the apparatus were:

1. Provisions for measuring the mass flow rate of the fluid.

2. Provisions for heating the test section directly instead of wrapping it with heater wire.

3. Provisions for measuring the test section wall temperatures so that a heat transfer film coefficient could be calculated.

A schematic of the apparatus is shown in Figure 1. The fluid is heated in the test section. Due to the decrease in fluid density with an increase in temperature the fluid rises in the left side of the loop. Similarly, the fluid is cooled in the water heat exchanger and falls in the right side of the loop. Hence, a circulation is established due to the difference in temperature on each side of the loop. The principal components indicated in the schematic are: (A) the heat transfer loop proper, (B) the test section and heat transfer element, (C) the power supply and control, (D) the water heat exchanger and control, and

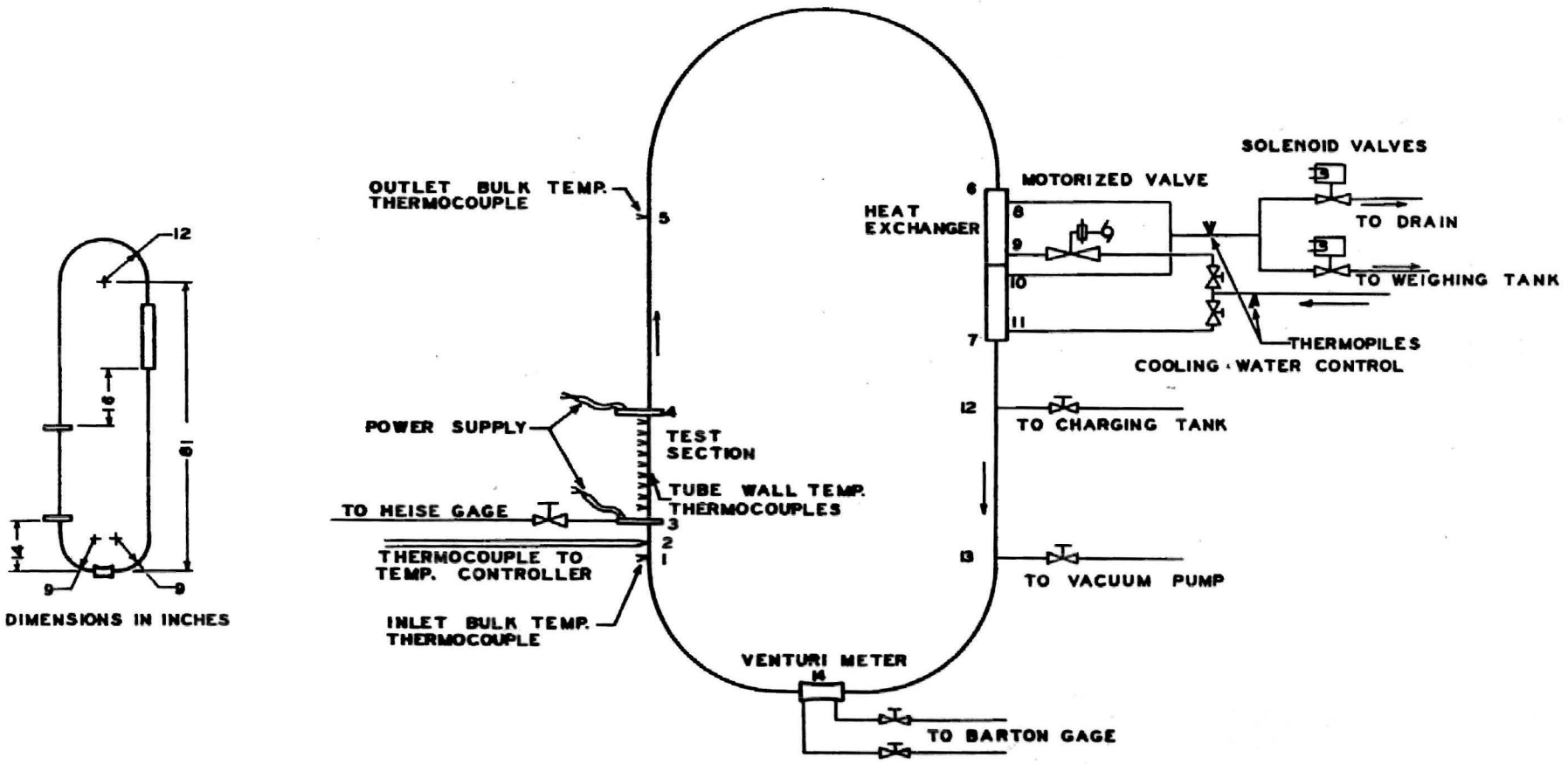

Figure 1

Schematic Diagram of the Thermal Syphon Test Loop

(E) various instrumentation facilities. Each of these components will be described separately.

A. The Heat Transfer Loop Proper

The heat transfer loop proper was constructed of AISI type 304 stainless steel tubing having a 0.500-in. outside diameter and a 0.430-in. inside diameter. All connections were Swagelock type stainless steel fittings.

B. The Test Section and Heat Transfer Element

The test section was also constructed of type 304 stainless steel tubing and was heated by passing an electric current through the tube itself. The details of the connections to this tube are shown in Figure 2. A photograph of the installed section is given in Plate I.

The heat transfer loop was insulated with a one-eighth inch layer of asbestos tape followed by a one and one-half inch layer of Fiberglass blanket. The loop was then wrapped with a layer of aluminum foil to reduce radiative heat loss.

C. The Power Supply and Control

The power supply consisted of a General Electric type K testing transformer rated at eight KVA. The primary voltage was 220 volts and the secondary was so arranged that taps of 2, 4, or 8 volts could be used. A General Electric type MIRS induction voltage regulator was used to vary the primary voltage within approximately plus or minus fifty percent of the nominal value.

D. The Water Heat Exchanger and Control

A detail drawing of the water heat exchanger is shown in Figure 3. As shown, there are two sections for the cooling water flow in order that more precise control on this flow could be achieved. One section is

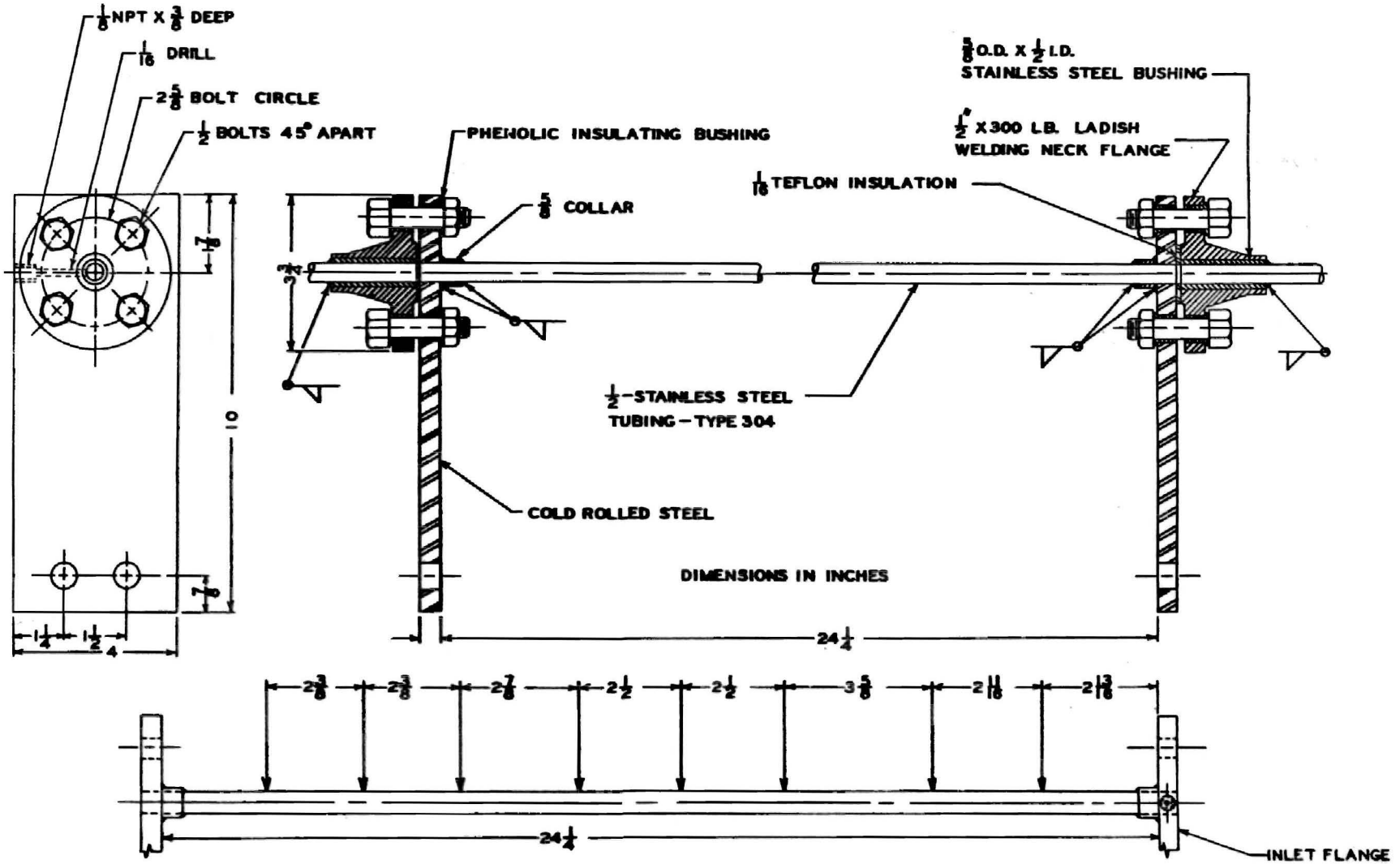

Figure 2. Test Section Detail

PLATE I
TEST SECTION

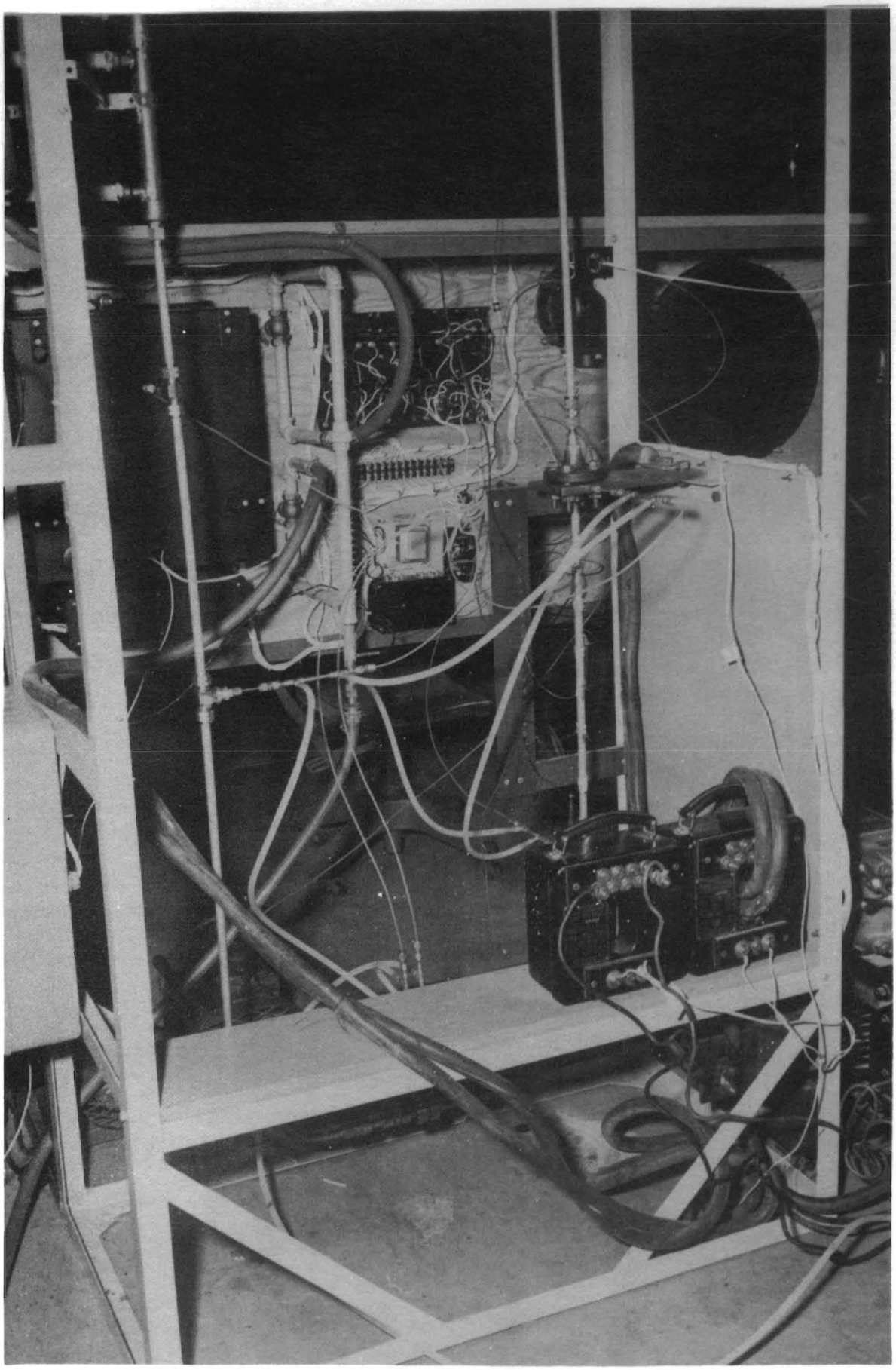

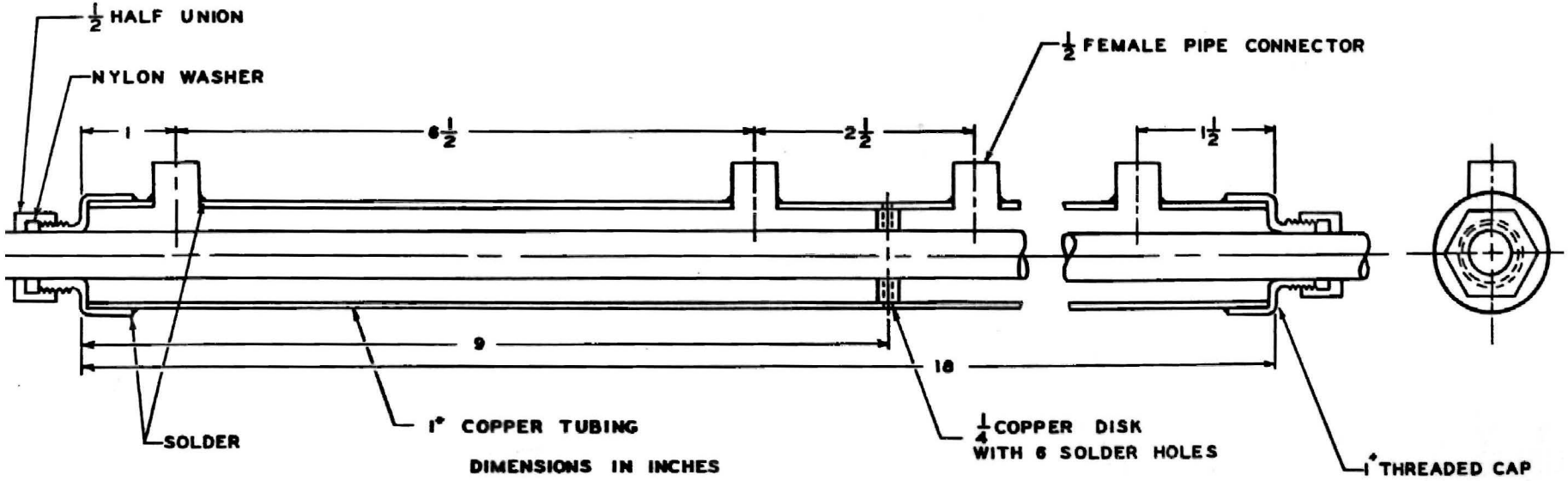

Figure 3

Water Heat Exchanger Detail

controlled entirely by a manually operated one-half inch globe valve. The other section is controlled by a manually operated one-half inch globe valve connected in series with a Minneapolis-Honeywell model K930A motorized valve assembly. The motorized valve assembly is actuated by a Minneapolis-Honeywell circular scale "Electronik" proportional control indicating potentiometer. The controller senses the output of a thermocouple placed on the outside of the tube at the entrance to the test section and compares this output with a manually adjusted set point. As a result of this comparison the motorized valve is opened or closed to maintain a set point temperature at the inlet to the test section. A wiring diagram of this arrangement is shown in Figure 4.

E. Various Instrumentation Facilities

The instrumentation for the test apparatus will be described in respect to the four basic quantities which were to be measured: (1) temperature, (2) pressure, (3) electrical input, and (4) cooling water flow.

1. Temperature Instrumentation

The tube wall temperatures for the test section were obtained by measuring the outputs of No. 30 gage iron-constantan thermocouples which were spot-welded to the outside of the test section tube. The locations of these thermocouples are shown in Figure 2. Two thermocouples were installed at each location, one on either side of the tube. During the initial testing of the apparatus the outputs of the thermocouples on both sides of the tube were measured separately and it was found that they did not differ by more than one degree Fahrenheit. In the light of this minor difference only one of each of the pairs was used for the determination of the outside wall temperature.

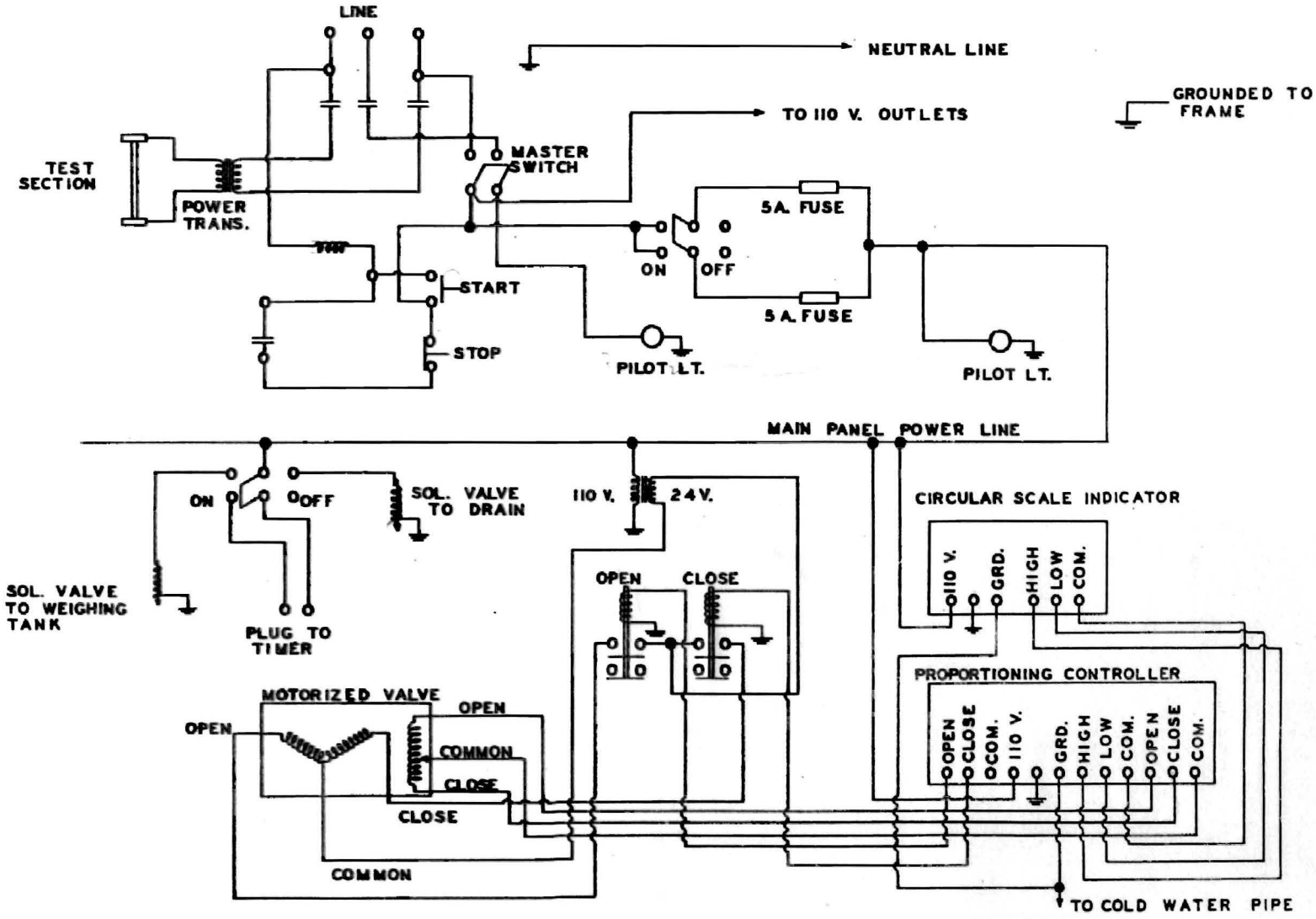

Figure 4

Panel Wiring Diagram

The fluid bulk temperatures were obtained at the locations shown in Figure 1. No mixing chambers were used since such an arrangement would cause an appreciable pressure drop which would in turn directly affect the heat transfer characteristics of the loop. The thermocouples used for measuring the fluid bulk temperatures were Minneapolis-Honeywell "Megopak" type iron-constantan thermocouples sealed in a one-sixteenth inch diameter stainless steel tube. These were inserted into the line using a Swagelock one-half inch tee with an appropriate side fitting to seal the assembly. This arrangement is shown in Figure 5.

Several thermocouples were inserted in the insulation surrounding the loop so that a check could be made on the heat loss to the environment.

The differential temperature across the cooling water heat exchanger was measured by means of two thermopiles consisting of four junctions of No. 30 gage iron-constantan thermocouple wire.

The outputs of the bulk temperature and cooling water thermocouples were measured with a Rubicon type B precision potentiometer. A Leeds and Northrup model 2430-A galvanometer was used in conjunction with this potentiometer.

The tube wall temperatures were measured with a Minneapolis-Honeywell model 153X65 multipoint temperature recorder when the temperatures were below 600°F. Above 600°F the Rubicon potentiometer and a selector switch were used. One set of the wall thermocouples was connected to the recorder while the other set was connected to the potentiometer so that either of the two methods could be used.

All of the wall thermocouples were wrapped one and one-half turns around the tube to minimize any conduction errors. The thermocouples

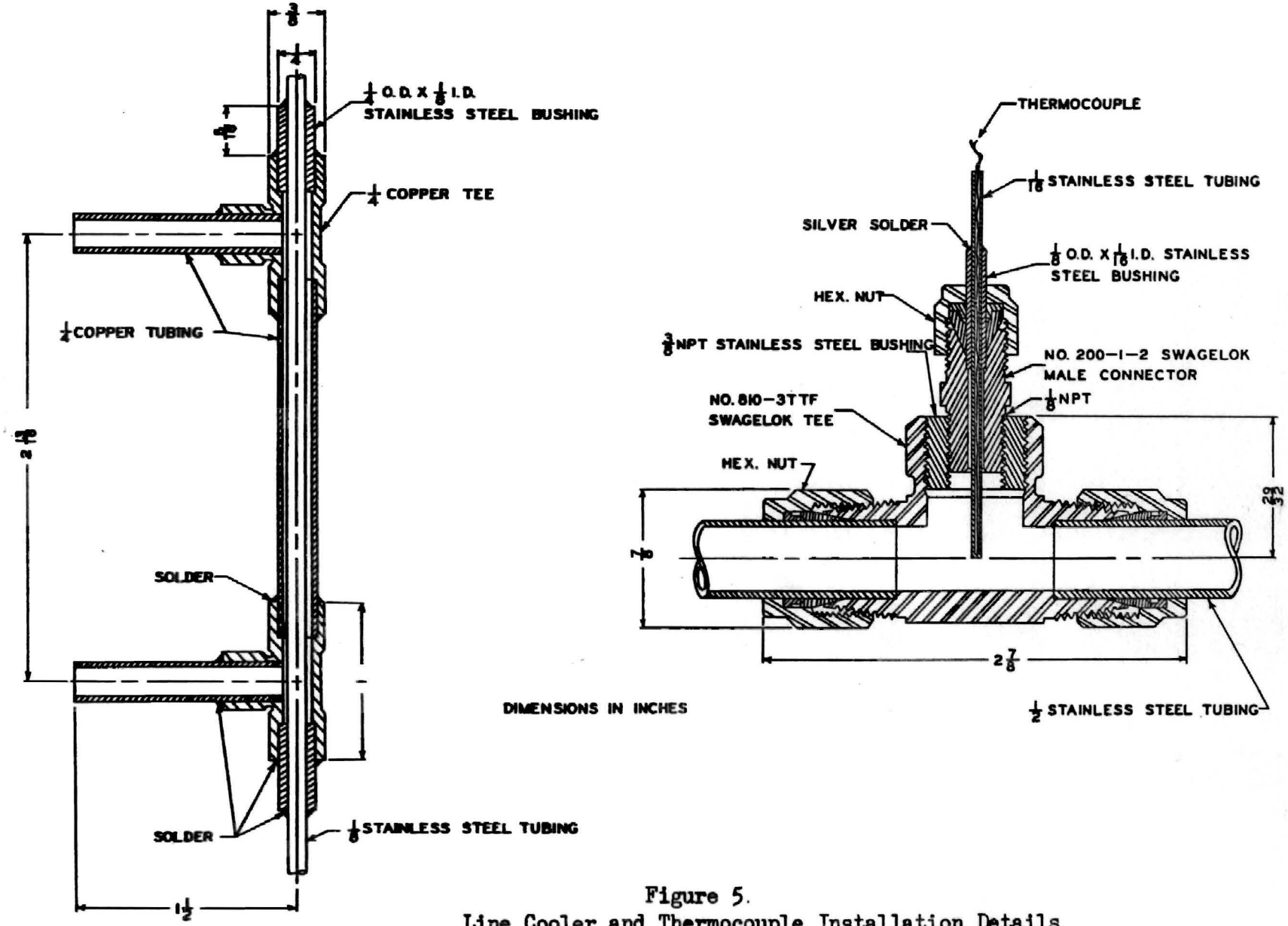

Figure 5.
Line Cooler and Thermocouple Installation Details

were then secured in their position by wrapping them with glass tape.

2. Pressure Instrumentation

The schematic of the pressure instrumentation is shown in Figure 1. A Heise bourdon tube pressure gage having a scale graduated in one psi increments from 0 to 1000 psi was used to measure the system pressure. As shown in the schematic, this pressure is measured at the entrance to the test section. The Heise gage had a calibrated accuracy of 0.1% of the full scale reading.

The flow rate of the fluid in the heat transfer loop was measured by recording the pressure drop across a calibrated venturi. A detailed drawing of this venturi is shown in Figure 6. The pressure drop across the venturi was measured with a Barton model 200 bellows type differential pressure gage graduated in increments of 0.2 inches of water from zero to twenty inches. The accuracy of this instrument is 0.5% of the full scale reading.

All pressure taps coming from the apparatus were cooled by means of the line coolers shown in Figure 5 to insure that the instrument lines were always full of liquid.

3. Electrical Instrumentation

Provisions were made on the control panel for indicating electrical meters and connections for auxiliary precision meters. The details of these connections are shown in Figure 7. The indicating meters were Triplett types. The precision meters were a General Electric AC voltmeter type P-3, 0-15 or 0-30 volt range, accuracy-0.2%, and a General Electric AC ammeter type AP-9, 0-1 or 0-2 ampere range, accuracy-$\frac{1}{2}$%.

Two model C universal current transformers manufactured by the Esterline-Angus Company were used in conjunction with the above ammeter.

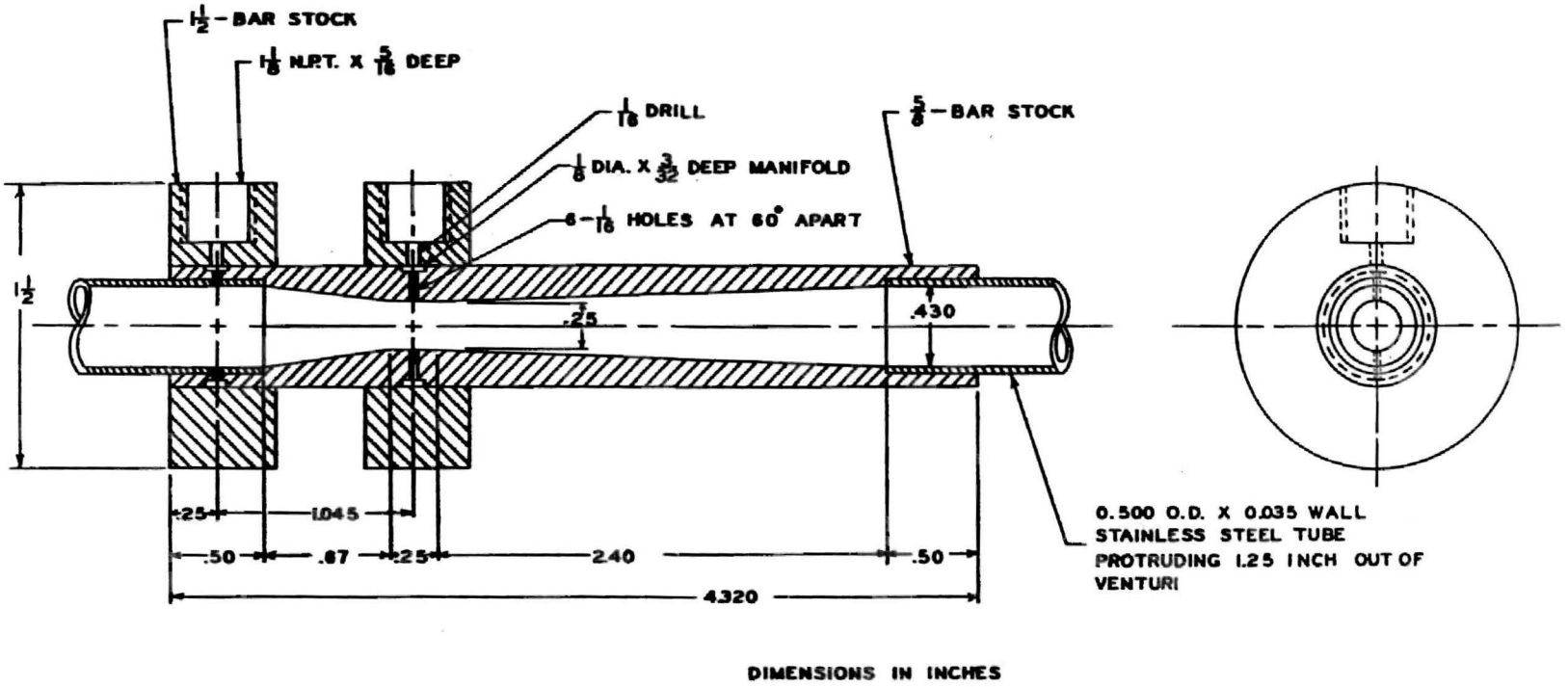

Figure 6

Venturi Detail

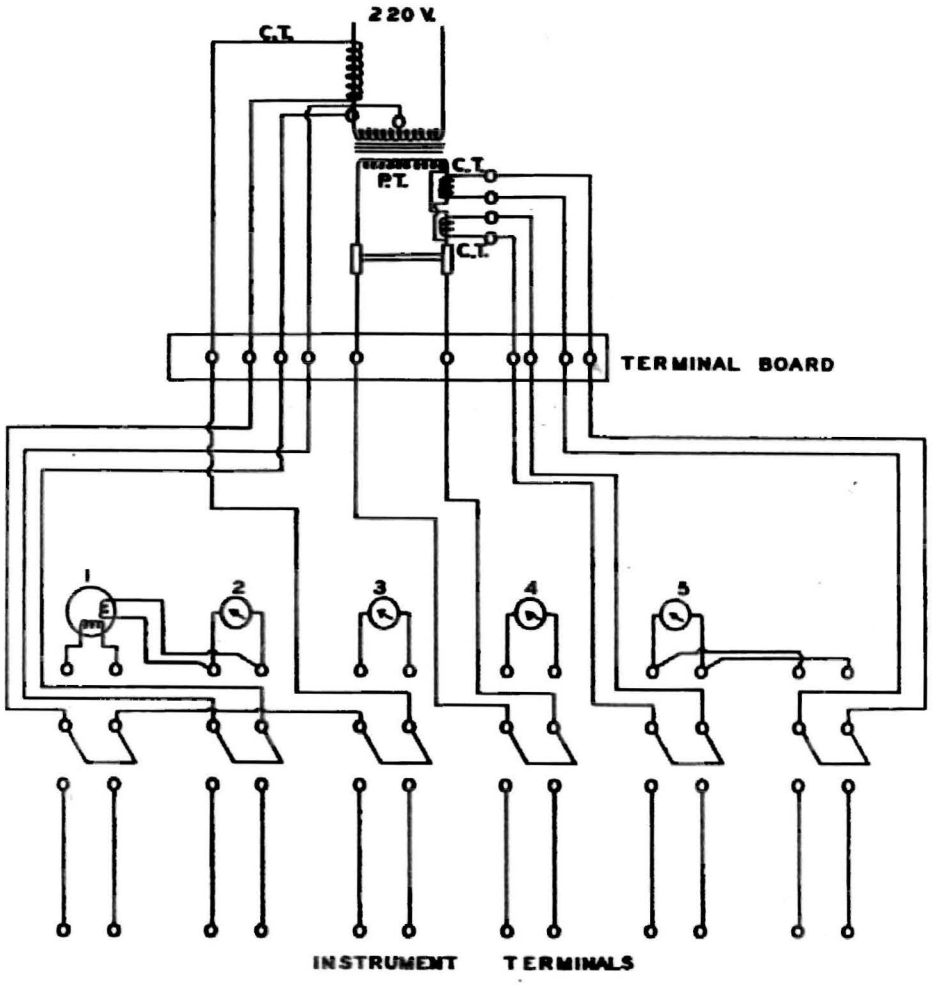

PT - POWER TRANSFORMER
CT - CURRENT TRANSFORMER
1 - WATTMETER
2 - 0-150 VOLTMETER - PRIMARY SIDE
3 - AMMETER - PRIMARY SIDE
4 - 0-10 VOLTMETER - SECONDARY SIDE
5 - AMMETER - SECONDARY SIDE

Figure 7

Instrument Wiring Diagram

4. Cooling Water Flow Measurement

Cooling water flow to the water heat exchanger was measured by recording the time required to collect a certain quantity of the cooling water. The discharge from the heat exchanger was diverted from the drain to a weighing tank by means of two solenoid valves as shown in Figures 1 and 4. As shown in Figure 4 electrical provisions were made so that when the flow of water to the weighing tank was started an electric timer was started. Correspondingly, when the water was again allowed to flow to the drain the timer was stopped.

The heat transfer fluid used in the thermal syphon loop was Freon 12, dichlorodifloromethane, a product of the E.I. du Pont de Nemours Company, Inc. The specifications as furnished by the manufacturer (5) are:

Maximum water content, ppm by weight	10
Maximum non-absorbable gas, percent by volume in the vapor	1.5
Boiling point at one atmosphere pressure, ^{o}F	-21.6
Maximum boiling range, ^{o}F	0.5
Maximum high boiling impurities, percent by volume	0.01
Chloride content	None

The critical constants for Freon 12 are:

$$t_c = 233.2\ ^{o}F$$

$$p_c = 596.8\ \text{psia}$$

$$v_c = 0.02870\ lb_m/ft^3$$

Front and rear views of the complete test apparatus are shown in Plates II and III.

PLATE II
FRONT VIEW OF TEST APPARATUS

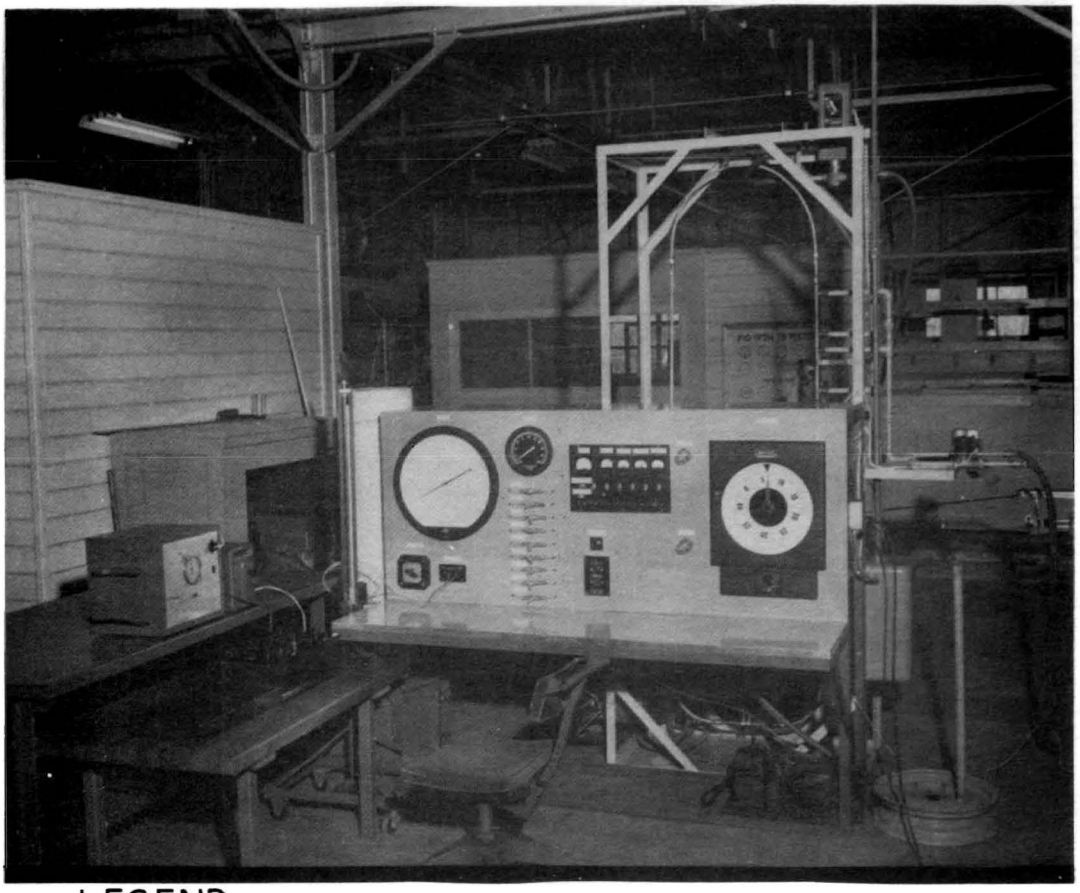

LEGEND

1 – FRAME
2 – LOOP
3 – HEAT EXCHANGER
4 – MOTORIZED VALVE
5 – OUTLET TO SOLENOID VALVES
6 – TEMPERATURE CONTROLLER
7 – COOLING WATER VALVES
8 – TERMINAL BOARD
9 – PILOT LIGHT
10 – START - STOP SWITCH
11 – LINE CONTROL VALVES
12 – THERMOCOUPLE PLUG BOARD
13 – THERMOCOUPLE SELECTOR SWITCH
14 – HEISE GAGE
15 – BARTON GAGE
16 – FREON TANK
17 – MANOMETER
18 – POTENTIOMETER
19 – GALVANOMETER
20 – TIMER
21 – VACUUM PUMP

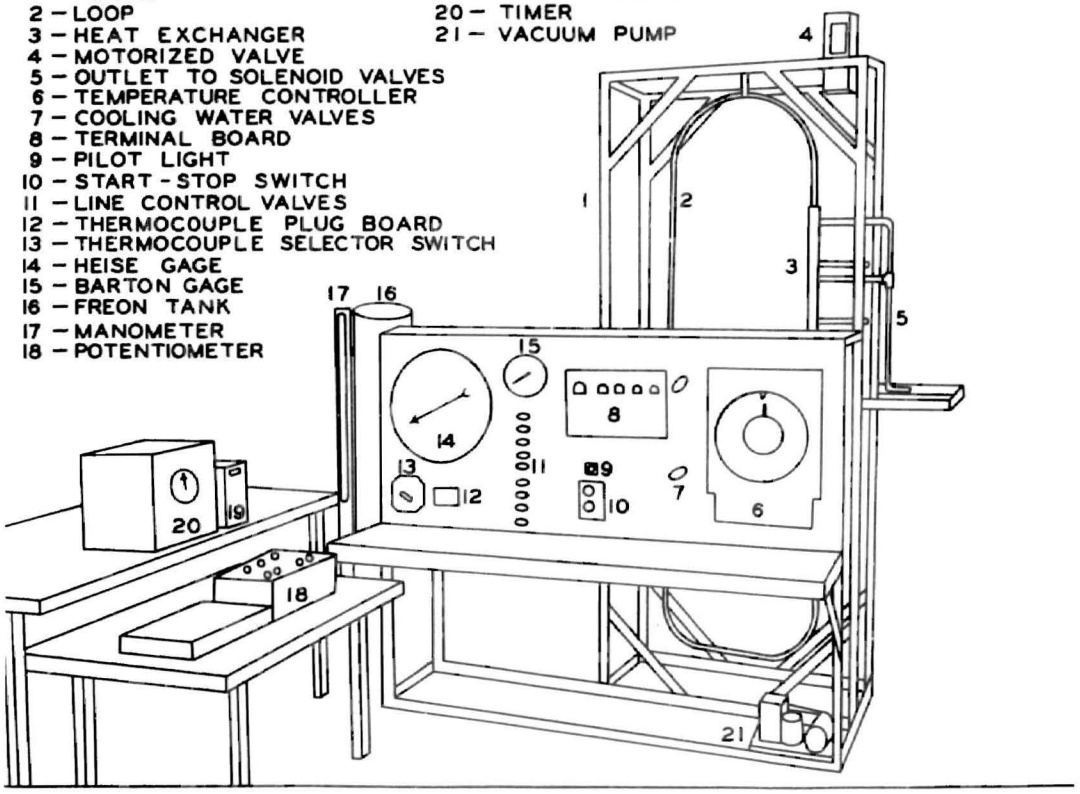

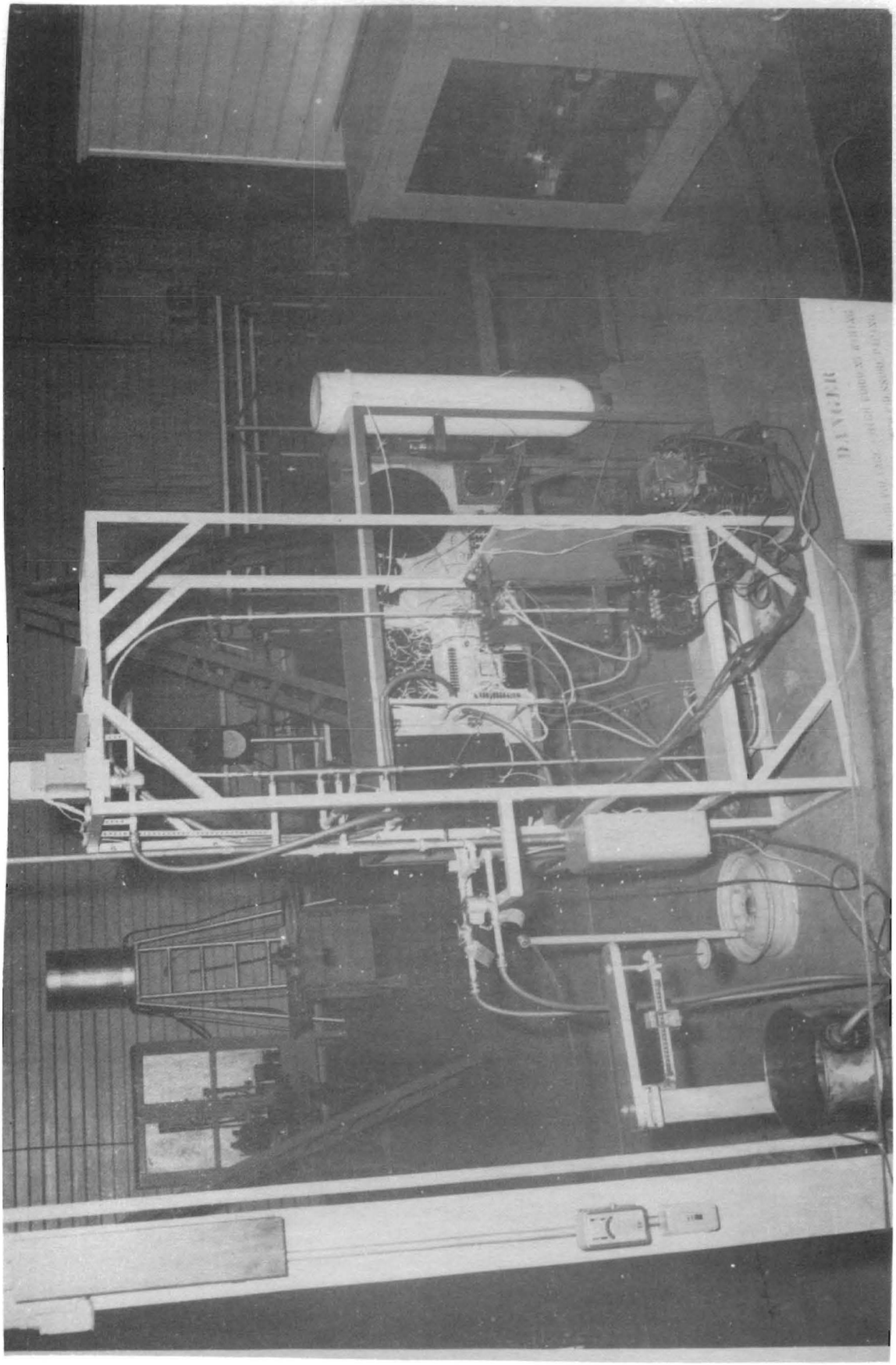

CHAPTER IV

THEORY OF THE THERMAL SYPHON

Before developing the theory for the thermal syphon type apparatus it is well to review the general behavior of the properties of a fluid in the vicinity of its critical point. In this way, the derived relationships for the thermal syphon may be considered in their proper perspective.

The trends of the properties of a fluid near the critical state are:

$$\beta = \frac{1}{v}\left(\frac{\partial v}{\partial T}\right)_p \longrightarrow \infty$$

$$c_p = \left(\frac{\partial h}{\partial T}\right)_p \longrightarrow \infty$$

viscosity becomes indeterminate,

thermal conductivity becomes indeterminate,

surface tension $\longrightarrow$ 0.

The hypothesis that the viscosity and thermal conductivity become indeterminate is taken in consideration of the generalized correlations for these properties as presented by Comings and Egly (6) and Comings and Nathan (7). In these generalized correlations the viscosity and thermal conductivity may change by one hundred percent across the critical region. This is analogous to the change that takes place across the saturation region from the saturated liquid to the saturated vapor.

The effect of the above trends on the operating characteristics of the thermal syphon will be discussed in subsequent paragraphs.

The original development of the theory for the thermal syphon was given by Schmidt, Eckert, and Grigull (4). The initial development here follows closely their method of attack. An expansion of the theory of these authors will be given in the latter sections of the analytical development.

A schematic diagram of the thermal syphon is shown in Figure 8. The driving pressure due to the difference in fluid density on each side of the loop is

$$\Delta p = y\left[\frac{\gamma_3+\gamma_4}{2} - \frac{\gamma_1+\gamma_2}{2}\right] = y\,\gamma_m \Delta t_b \beta_m , \qquad \text{IV-1}$$

where

$$\Delta t_b = t_{2b} - t_{1b} = t_{3b} - t_{4b} ,$$

y = vertical distance between center of test section and center of heat exchanger,

γ = specific weight of the fluid,

γ_m = mean specific weight of fluid evaluated at the arithmetic mean bulk temperature in the thermal syphon loop,

β_m = mean volume coefficient of expansion evaluated at the arithmetic mean bulk temperature.

The heat absorbed by the fluid is given by

$$q = w\, c_p\, \Delta t_b \qquad \text{IV-2}$$

or

$$q = \gamma_m A_i u\, c_p\, \Delta t_b , \qquad \text{IV-3}$$

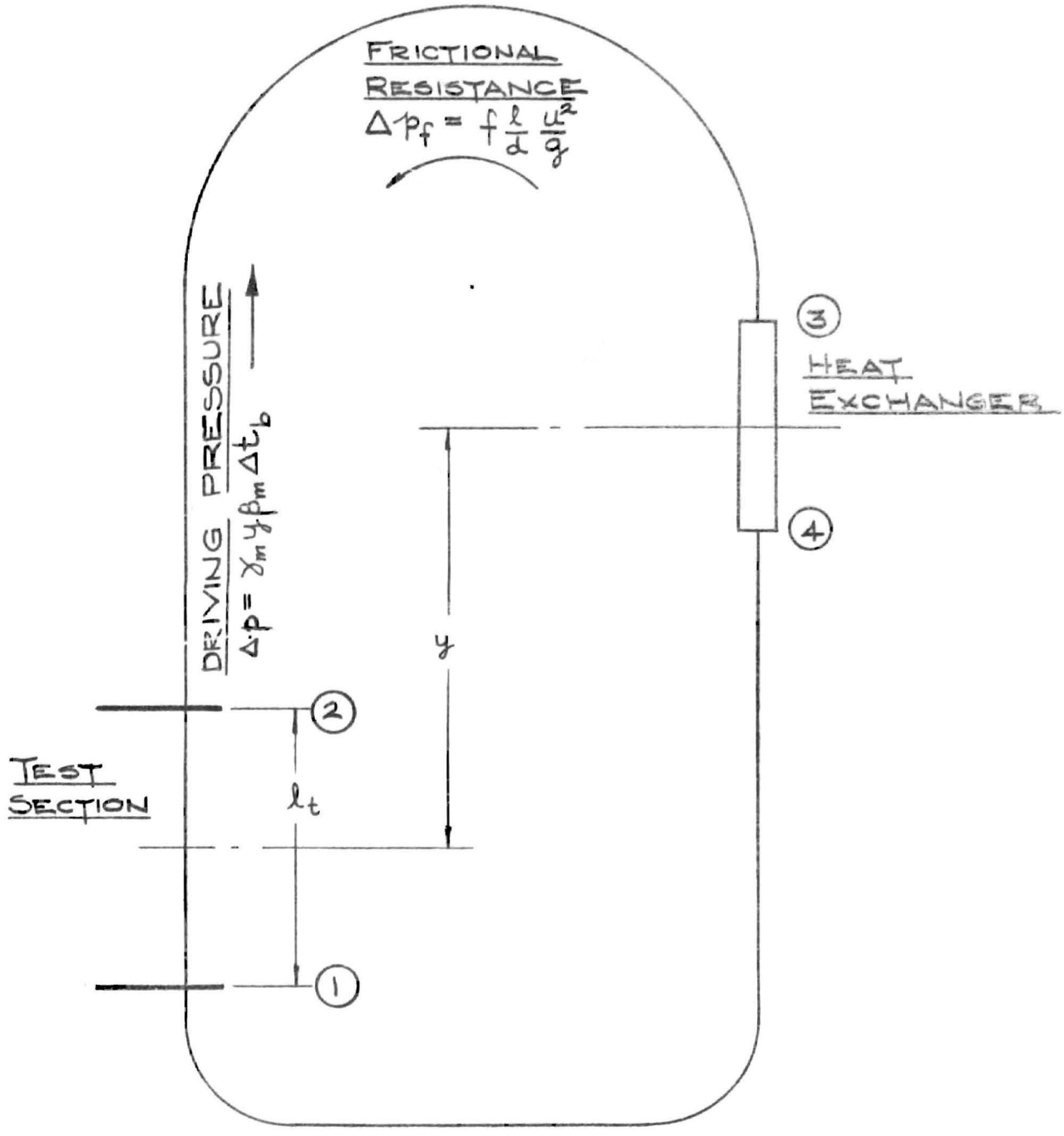

Figure 8

Schematic of Thermal Syphon

where

q = total heat added in the heating section per unit time,

w = weight rate of flow of fluid in the thermal syphon,

c_p = specific heat at constant pressure,

A_i = inside cross sectional area of the tube,

u = mean fluid velocity.

An apparent thermal conductivity may be defined by

$$q = k_a \Delta t_b \frac{A_i}{l} , \qquad \text{IV-4}$$

where l is one-half the circumferential length of the heat transfer loop. Then

$$k_a \equiv \frac{q l}{A_i \Delta t_b} . \qquad \text{IV-5}$$

The pressure differential due to the difference in fluid density is balanced by the frictional pressure loss. The frictional pressure loss may take one of two forms. For laminar flow

$$\Delta p_f = \frac{64 \mu u l}{d_i^2} , \qquad \text{IV-6}$$

where

μ = dynamic viscosity evaluated at the arithmetic mean bulk temperature.

For turbulent flow the Blasius law

$$\Delta p_f = 0.316 \left(\frac{\gamma u d}{\mu}\right)^{-1/4} \gamma_m \frac{u^2 l}{g d} \qquad \text{IV-7}$$

is recommended (8), where g is the gravitational constant. In either case a dimensionless ratio of k_a/k may be formed, where k is the thermal conductivity evaluated at the arithmetic mean bulk temperature.

For the turbulent case

$$k_a = \frac{q\,l}{A_i\,\Delta t_b} = \gamma_m u\, c_p\, l, \qquad \text{IV-8}$$

$$y\,\gamma_m \Delta t_b \beta_m = 0.316 \left(\frac{\gamma_m d}{\mu}\right)^{-1/4} \frac{\gamma_m l}{g d}\, u^{7/4}, \qquad \text{IV-9}$$

and

$$u = \left(\frac{y g d}{l}\right)(0.316)^{-4/7} \left(\frac{\gamma_m d}{\mu}\right)^{1/7} \left(\Delta t_b \beta_m\right)^{4/7}, \qquad \text{IV-10}$$

so that

$$\frac{k_a}{k} = \frac{\gamma_m u\, c_p\, l}{k}. \qquad \text{IV-11}$$

Combining equations IV-10 and IV-11,

$$\frac{k_a}{k} = (Pr)(Gr_b)^{4/7}(y/l)(0.316)^{-4/7}(l/d), \qquad \text{IV-12}$$

where

$$Pr = \frac{c_p \mu}{k} = \text{Prandtl number}$$

and

$$Gr_b = \frac{g \beta_m \Delta t_b d^3 \gamma_m^2}{\mu^2} = \text{Grashof number evaluated at the bulk temperature difference.}$$

In the laminar case the expression which is equivalent to equation IV-12 is

$$\frac{k_a}{k} = \frac{1}{64}(Gr_b)(Pr)(y/d). \qquad \text{IV-13}$$

Equations IV-1 and IV-2 may be used to extend the analysis of Schmidt, Eckert, and Grigull to a formulation for the heat transfer film coefficient in the heated section. This coefficient is defined by

$$h \equiv \frac{q}{A_d \Delta t_f} , \qquad \text{IV-14}$$

where

$A_d = \pi d_i l_t =$ surface area of the heat transfer surface,

$l_t =$ length of the test section tube.

For the turbulent case the pressure balance gives

$$0.316 \left(\frac{\gamma_m u d}{\mu}\right)^{-1/4} \gamma_m \frac{u^2 l}{g d} = y \gamma_m \Delta t_b \beta_m . \qquad \text{IV-15}$$

Solving for the bulk temperature difference the relation

$$\Delta t_b = \frac{q}{\gamma_m A_i u c_p} = \frac{0.316 \left(\frac{\gamma_m u d}{\mu}\right)^{-1/4} u^2 l}{g d y \beta_m} \qquad \text{IV-16}$$

is obtained. Correspondingly,

$$q = \frac{0.316 \left(\frac{\gamma_m u d}{\mu}\right)^{-1/4} u^2 l \gamma_m A_i u c_p}{g d y \beta_m} . \qquad \text{IV-17}$$

Hence, and expression for the heat transfer film coefficient may be written as

$$h = \frac{0.316 \left(\frac{\gamma_m u d}{\mu}\right)^{-1/4} u^2 l \gamma_m A_i u c_p}{g d y \beta_m A_d \Delta t_f} \qquad \text{IV-18}$$

or

$$h = \frac{\frac{0.316}{4} \left(\frac{\gamma_m u d}{\mu}\right)^{-1/4} u^3 l \gamma_m c_p}{g y \beta_m l_t \Delta t_f} . \qquad \text{IV-19}$$

Collecting terms,

$$h = \frac{0.079 \left(\frac{\gamma_m u d}{\mu}\right)^{-1/4} u^3 d^3 \gamma_m c_p \frac{\gamma_m^2}{\mu^2} \left(l/l_t\right)}{y \left(\frac{g d^3 \beta_m \Delta t_f \gamma_m^2}{\mu^2}\right)} . \qquad \text{IV-20}$$

Introducing $Gr_f = \frac{g d^3 \beta_m \Delta t_f \gamma_m^2}{\mu^2}$,

$$h = \frac{0.079 \left(\frac{\gamma_m u d}{\mu}\right)^{-1/4} \frac{u^3 \gamma_m^3 d^3 c_p}{\mu^2}}{Gr_f} \left(\frac{l}{l_t}\right)\left(\frac{1}{y}\right). \qquad \text{IV-21}$$

This expression may be further simplified by the introduction of the Nusselt, Prandtl, and Reynolds numbers so that

$$Nu = 0.079 (Re)^{11/4} (Pr) (Gr_f)^{-1} \left(\frac{l}{l_t}\right)\left(\frac{d}{y}\right), \qquad \text{IV-22}$$

where

$Nu = \frac{hd}{k}$ = Nusselt number,

$Re = \frac{\gamma_m u d}{\mu}$ = Reynolds number.

For the laminar case,

$$\frac{64 \mu u l}{d^2} = y \gamma_m \Delta t_b \beta_m \qquad \text{IV-23}$$

and

$$\Delta t_b = \frac{64 \mu u l}{d^2 y \gamma_m \beta_m} = \frac{q}{\gamma_m A_i u c_p}, \qquad \text{IV-24}$$

so that

$$q = \frac{64 \mu u^2 c_p l A_i}{d^2 y \beta_m} \qquad \text{IV-25}$$

and

$$h = \frac{64 \mu u^2 c_p l A_i}{d^2 y \beta_m A_d \Delta t_f}. \qquad \text{IV-26}$$

This expression reduces to

$$h = \frac{16 \mu u^2 c_p}{y \beta_m d \Delta t_f} \left(\ell / \ell_t \right), \qquad \text{IV-27}$$

which may be simplified by the introduction of dimensionless groups. The resulting simplified expression is

$$Nu = 16 (Re)^2 (Pr) (Gr_f)^{-1} (\ell / \ell_t) (d / y). \qquad \text{IV-28}$$

According to the above theory the apparent thermal conductivity should become very large as the critical state is approached. This was verified by Schmidt, Eckert, and Grigull (4). An experimental verification for Freon 12 will be presented in this thesis.

The trend of the heat transfer film coefficient as the critical state is approached is not so clear. Since the heat transfer film coefficient is a function of the ratio $\frac{c_p}{\beta_m}$ and both the specific heat and the volume coefficient of expansion become extremely large in the immediate vicinity of the critical point, an analysis of the behavior of the film coefficient must involve a comparison of the rates of change of these two properties as the critical state is approached. The property data is not sufficiently accurate to make this comparison. Therefore, as in many cases, the problem reduces to one which must be solved by experimentation.

A few statements regarding the general validity of the relationships developed in this chapter are in order. The primary assumptions involved in the derivations presented above are:

a. The loop is composed of a smooth tube so that the frictional pressure drop may be evaluated with one of the expressions given.

b. The thermal syphon effect may be described in terms of mean

property values.

Assumption (a) seems entirely proper. A possible modification is that which would be necessary to account for the pressure loss in fittings or flow measuring equipment. This type of modification would probably take the form of a substitution of an equivalent length for pressure drop in place of the physical length of the heat transfer loop. Hence, for a particular thermal syphon loop, this modification would change only the constant term in the expression.

Assumption (b) is a necessity if one is to predict the behavior of the thermal syphon in terms of dimensionless parameters. It is convenient to evaluate mean property values at the arithmetic mean bulk temperature. This evaluation assumes that the properties follow a linear variation in the region in question. Of course, this is not entirely correct but in the region near the critical state the bulk temperature difference for a given heat input is small so that a linear relationship may be assumed. In the superheat region away from the critical state the bulk temperature difference would be larger but in this region the property values are very nearly linear so that the assumption still seems valid.

The overall validity of both (a) and (b) must be verified experimantally. This verification will be described in the chapters to follow.

CHAPTER V

EXPERIMENTAL PROCEDURE

Before beginning the experiments the entire apparatus was charged to 900 psia with compressed air and allowed to stand for three days. No variations in pressure were observed other than those which could be attributed to changes in room temperature. It was therefore concluded that the apparatus was airtight.

The system was then evacuated by connecting it to a Cenco Hyvac vacuum pump operating in conjunction with a small mercury diffusion pump. The vacuum pump was allowed to run until an absolute pressure of sixty microns was established in the test setup.

The apparatus was charged with an arbitrary quantity of fluid by heating the Freon 12 supply tank so that the saturation pressure in the tank was greater than the saturation pressure corresponding to the temperature of the loop. The temperature of the loop was room temperature when no power was applied. For the room temperatures involved, the saturation pressure of Freon 12 is about 85 psia. It was usually sufficient to heat the supply tank to a point such that a pressure of 100 psia was established in the system. This insured that the system was charged entirely with liquid Freon 12.

After the system was charged power was applied to the test section and a cooling water flow was maintained to establish a particular test section inlet temperature. Runs were made with a constant charge in the

apparatus for several different inlet temperatures to the test section. The procedure was repeated for successively smaller charges by bleeding part of the Freon 12 back into the supply tank. For each constant charge in the loop different power inputs were used with variations in the inlet temperature. For a particular charge an upper limit to the amount of power which could be applied was set by the upper pressure limits of the system. It was usual procedure not to exceed 900 psia in the unit. Since the upper pressure was fixed then the factor which established the limit on the energy input was the ability of the water heat exchanger to maintain a sufficiently low average temperature in the loop. For much of the compressed liquid region large energy inputs were not possible since the temperature difference between the Freon 12 and the cooling water was not large enough to handle the higher heat fluxes.

It was usually necessary to wait from ten to thirty minutes for the apparatus to reach equilibrium on each run. Three indications that a steady state had been established were used. These indications were the set point of the cooling water controller, the system pressure, and the record of the wall temperatures on the temperature recorder. When all of these indications remained constant over a period of time of two to three minutes the apparatus was presumed to be in a steady state. It was found that the record of the wall temperatures was most indicative of an equilibrium state.

Once a steady state was established in the system the various temperatures and pressures were recorded. Usually, only about five minutes were required to collect all of the data for a particular run.

CHAPTER VI

EXPERIMENTAL OBSERVATIONS

When operating quite close to the critical state it was found that an increase in the cooling water flow over that quantity necessary to maintain equilibrium near the critical pressure caused a marked increase in the test section wall temperature. Although the increased cooling water flow presents a lower fluid bulk temperature at the entrance to the test section, this is more than counterbalanced by the lower fluid flow rate which prevails at the new bulk temperature. In conjunction with this phenomenon it was found that in order to start the loop in operation from normal room temperatures when charged to critical or supercritical densities only very mild heating rates could be applied until the system had reached the critical pressure. Because of the conditions described above it was usual practice to charge the system to densities greater than the critical value and then bleed part of the fluid back into the supply tank to maintain a desired pressure in the system.

A rather unusual phenomenon was observed when the apparatus was operating in the superheated vapor region. A very slow, regular variation in the venturi pressure drop was observed. A total variation between the limits of three and five inches of water was not unusual. These variations were very regular and they occurred over a length of time of one to two minutes. During the occurrence of this phenomenon all of

the conditions for steady state were satisfied so that the variations could not be attributed to nonequilibrium conditions of operation. The pressure drop which was recorded in the runs involving these variations was the average of the two limiting values. To fully analyze the variations in the venturi pressure drop some type of recording pressure instrument would have to be used. Such an instrument was not available for these tests.

In the experimental regions where the fluid was superheated and the smaller power inputs were used, a problem in the control of the cooling water was encountered. The temperature difference between the Freon 12 and the cooling water in this region was rather large so that only a small quantity of cooling water was required. At the smaller power inputs it was extremely difficult for the electronic controller to assume a steady state position due to the fact that the flow control valve was being controlled between the closed position and a position which was only slightly open. In these regions of operation no data was collected when it was not possible to maintain steady conditions without oscillations of the temperature controller.

In the regions close to the critical state, fluctuations in pressure on the order of twenty to thirty psi were observed. Accompanying these fluctuations was an intense vibration of the test apparatus. When the rate of cooling water was increased so that the pressure in the apparatus was reduced the fluctuations subsided. However, if the cooling water flow rate was decreased or more power was applied the fluctuations became more severe and did not subside until the pressure in the apparatus had risen to a value well above the critical value. In many instances the pressure fluctuations did not subside until a pressure

of 750 to 800 psia had been attained.

The apparatus was quite stable and responded nicely to the modes of control applied except in the regions of operation described above.

CHAPTER VII

REDUCTION OF DATA

The reduction of the experimental test data is concerned with the determination of the heat transfer film coefficients and the establishment of a suitable correlation of these coefficients which may be used to predict the results of future test data.

Two types of heat transfer film coefficient were calculated; a local film coefficient and an average film coefficient defined by the equations:

$$h_{local} = \frac{q}{A(t_s - t_b)} \qquad \text{VII-1}$$

and

$$h_{avg.} = \frac{q}{A(t_{s_{avg.}} - t_{b_{avg.}})} \cdot \qquad \text{VII-2}$$

The calculation of the film coefficients was based on the assumption that uniform heat flux was generated in the test section tube. On the basis of this assumption the bulk temperature could be assumed to vary linearly from the entrance to the exit of the tube. This is equivalent to stating that the specific heat of the fluid does not vary appreciably in this range. This statement is not true when applied to a fluid operating in the critical region. However, it is not possible at this time to delineate the detailed behavior of the specific heat in this region. Thus, the assumption of a linear variation in the bulk

temperature seems a reasonable one in the light of the present property information available.

The equation presented by Kreith and Summerfield (9) was used to calculate the inside wall temperature from the measured outside wall temperatures. This equation is

$$\Delta t = t_o - t_i = \frac{m}{k_o \rho_o}\left\{(\Delta x)^2 + \frac{1}{3 r_o}(\Delta x)^3 + (\Delta x)^4\left[\frac{m(3\alpha + 4\alpha\beta t_o + \beta)}{6(1+\beta t_o)(1+\alpha t_o)} + \frac{1}{4 r_o^2}\right]\right\} \qquad \text{VII-3}$$

where

$$m = \frac{3.413\, \rho_m^2 I^2}{2\pi^2 (r_o^2 - r_i^2)^2}\,, \qquad \text{VII-4}$$

ρ = electrical resistivity,

ρ_o = electrical resistivity at 0°F,

k_o = thermal conductivity at 0°F,

t_o = outside wall temperature,

t_i = inside wall temperature,

Δx = wall thickness,

α = temperature coefficient of electrical resistivity,

β = temperature coefficient of thermal conductivity,

I = electric current.

$$\rho_m = \rho_o\left[1 + \alpha t_m\right] = \rho_o\left[1 + \frac{\alpha}{r_o - r_i}\int_{r_i}^{r_o} t_r\, dr\right], \qquad \text{VII-5}$$

where

t_m = mean radial temperature,

t_r = temperature as a function of radius.

When the constants are evaluated equation VII-3 becomes

$$\Delta t = 0.46248\, m + 6.2647\times10^{-7} m^2 \left[\frac{0.002377 + 0.01282\, t_o}{(1+5.17\times10^{-4} t_o)(1+6.2\times10^{-4} t_o)}\right], \qquad \text{VII-6}$$

where

$$m = 1.353\times10^{7} \rho_m^2 I^2 \qquad \text{VII-7}$$

and

$$\rho_m = 2.265\times10^{-6}(1+0.00062\, t_m). \qquad \text{VII-8}$$

The temperature drop across the tube wall was computed for several different values of the outside wall temperature and electric current by means of an IBM 650 computer. The computation was performed first with the value of the outside wall temperature inserted in place of t_m. Then, with a value Δt_i calculated on this basis the calculation was repeated using as the mean radial temperature

$$t_m = t_o - 1/2\, \Delta t_i \qquad \text{VII-9}$$

The results of these calculations are shown in Figure 16. The temperature drop across the wall was always rounded to the nearest degree Fahrenheit when calculating the inside tube wall temperature.

The average wall temperature was calculated by the trapezoidal rule

$$t_{avg.} = \frac{1}{2L}\left[t_1 \Delta l_1 + t_2(\Delta l_1 + \Delta l_2) + \cdots + t_n \Delta l_{n-1}\right], \qquad \text{VII-10}$$

where $\Delta l_1, \Delta l_2, \cdots \Delta l_{n-1}$ are the distances between the respective thermocouples, and L is the distance between the first and last thermocouple used in the calculation. The average bulk temperature was evaluated over this same length so that an average film temperature drop could be calculated. The average bulk temperature used for the evaluation of the properties in the Reynolds, Prandtl, Grashof, and Nusselt numbers was the arithmetic mean of the measured entrance and exit bulk temperatures. The bulk temperatures used for the calculation of the local film coefficients were evaluated at the location of the particular wall temperature thermocouples. Values of reduced specific volume and reduced pressure defined by

$$v_R = \frac{v_m}{v_c}$$

and

$$p_R = \frac{p}{p_c}$$

were also calculated for the purpose of presenting the data, where

v_m = mean specific volume evaluated at arithmetic mean bulk temperature,

p = system pressure,

p_c = critical pressure,

v_c = critical specific volume.

It was determined that the heat loss through the insulation surrounding the heat transfer loop was of the order of one percent of the total heat flux. The heat flux used in the calculation of the heat transfer film coefficients was corrected for this loss.

A summary of the test data is given in Table I. A detailed outline

of the various sources of property data for Freon 12 is given in Appendix C.

TABLE I

SUMMARY OF TEST DATA

Run	Remarks	P_R	V_R	$t_{b_{in}}$ (°F)	$t_{b_{out}}$ (°F)	I (amp.)	q/A B/hr-ft^2	Δt_{avg} (°F)	Re x 10^{-4}
1		1.206	0.829	244.36	254.98	256.8	15820	151	12.52
2		1.164	1.018	245.14	255.57	262.7	16600	157	13.40
3		1.042	1.244	235.11	238.38	255.4	16030	142	15.99
4	b	0.921	0.675	222.66	223.25	258.1	16180	195	18.49
5	b	0.838	0.634	214.98	215.17	271.0	17420	109	18.49
6		0.903	2.073	146.35	180.47	215.7	10460	69	1.75
7		1.267	0.494	162.67	194.81	208.0	9893	129	1.796
8		1.040	0.507	154.65	187.74	209.4	10130	122	1.761
9		1.194	0.499	156.05	196.04	235.5	12740	158	1.942
10		1.406	0.494	163.80	206.43	244.0	14100	173	2.043
11		1.583	0.489	169.33	214.62	251.8	15230	191	2.091
12	b	0.601	0.513	152.86	181.09	219.0	10490	24	2.031
13		0.901	0.529	168.53	200.16	213.3	10200	47	1.808
14		1.039	0.537	175.70	206.50	206.9	9843	116	1.811
15		1.240	0.525	177.69	218.41	253.3	15370	176	2.189

TABLE I (Continued)

Run	Remarks	P_R	V_R	$t_{b_{in}}$ (°F)	$t_{b_{out}}$ (°F)	I (amp.)	q/A B/hr-ft^2	Δt_{avg} (°F)	Re x 10^{-4}
16		1.396	0.527	183.39	228.74	273.9	17950	206	2.371
17		1.571	0.519	190.31	237.73	280.8	37160	219	2.427
18	b	0.720	0.544	171.83	197.31	214.6	10260	21	2.030
19	b	0.885	0.547	183.76	211.22	210.6	9906	32	1.845
20		1.055	0.565	189.80	219.42	204.2	9557	110	1.804
21		1.189	0.537	188.67	231.45	283.2	19360	200	2.423
22		1.396	0.551	197.41	241.68	289.8	20460	210	6.518
23		1.605	0.542	206.13	253.74	299.2	22200	236	6.193
24	b	0.737	0.557	178.38	202.97	219.4	10500	21	12.92
25		0.982	0.561	189.53	216.42	209.4	9948	120	7.445
26		0.953	0.590	196.66	223.64	207.8	9869	118	8.668
27		1.466	0.547	206.06	240.34	240.8	13990	170	5.067
28		1.508	0.549	203.49	247.53	294.1	21440	223	6.193
29	b	0.880	0.604	203.38	222.43	215.8	10160	14	13.92
30		1.055	0.602	213.08	233.02	206.6	9659	105	7.594
31	a	1.349	0.611	221.32	250.96	252.6	15450	158	6.804

TABLE I (Continued)

Run	Remarks	P_R	V_R	$t_{b_{in}}$ (°F)	$t_{b_{out}}$ (°F)	I (amp.)	q/A B/hr-ft^2	Δt_{avg} (°F)	Re x 10^{-4}
32		1.143	0.598	204.05	239.52	314.9	23950	163	9.364
33	a	1.365	0.611	215.11	254.85	331.5	26250	195	8.24
34	a	1.533	0.624	223.38	267.01	333.1	27210	247	8.486
35		1.122	0.862	228.74	244.39	202.9	9483	94	8.509
36		1.039	0.696	219.91	239.49	251.7	15110	133	10.42
37		1.039	0.703	215.24	247.92	282.2	19160	155	13.42
38		1.044	0.675	212.20	239.23	332.5	26530	223	12.89
39	a	1.223	0.664	224.91	251.55	286.4	20070	182	9.913
40	a	1.421	0.699	237.46	265.41	282.9	19610	185	10.26
41		1.499	0.879	249.52	276.49	284.6	20340	173	12.67
42	a	1.114	0.699	226.09	245.80	310.2	23580	187	14.24
43		1.303	0.810	237.53	262.89	311.2	23990	186	14.55
44	b	0.838	0.619	206.50	217.93	268.6	17160	151	20.22
45		0.947	0.691	220.93	229.88	246.6	14900	231	16.11
46	a	1.064	0.680	227.53	240.27	253.3	15320	128	13.56
47	a	1.240	0.750	237.40	254.33	250.7	15070	145	10.82

TABLE I (Continued)

Run	Remarks	P_R	V_R	$t_{b_{in}}$ (°F)	$t_{b_{out}}$ (°F)	I (amp.)	q/A B/hr-ft^2	Δt_{avg} (°F)	Re_{-4} x 10^{-4}
48		1.407	0.837	247.73	268.68	250.6	15120	153	10.87
49		1.550	0.902	257.20	280.08	244.8	14650	158	10.01
50		0.854	0.631	217.27	217.95	253.1	15830	265	19.02
51		0.938	0.680	226.58	228.12	253.3	15850	227	17.73
52	a	1.039	0.810	233.51	238.02	261.3	16480	142	13.92
53	a	1.092	0.788	237.14	244.13	260.8	16510	146	13.53
54		1.236	0.936	247.30	260.31	258.1	16210	158	13.11
55		1.365	1.088	257.30	275.02	256.0	16110	172	11.95
56		1.491	1.138	266.55	289.23	255.8	16230	184	11.10
57	a	1.022	0.888	230.27	238.67	345.3	29120	266	20.50
58	a	1.067	0.870	232.82	242.63	345.6	29290	265	16.25
59	a	1.047	0.893	236.35	238.67	206.2	9669	93	12.89
60		0.963	0.781	230.93	230.93	255.0	16020	229	13.85
61	a	1.002	0.995	234.65	235.63	258.4	16280	176	11.44
62	a	1.025	1.266	236.45	238.64	258.1	16220	164	13.78
63	a	1.072	0.951	240.31	245.76	257.3	16200	171	13.09

TABLE I (Continued)

Run	Remarks	P_R	V_R	$t_{b_{in}}$ (°F)	$t_{b_{out}}$ (°F)	I (amp.)	q/A B/hr-ft^2	Δt_{avg} (°F)	Re_{-4} x 10^4
64		1.223	1.088	251.55	263.15	252.2	15500	179	12.09
65		1.323	1.235	261.42	280.12	249.8	15480	190	10.74
66	a	1.022	1.382	234.62	241.45	314.4	25140	275	15.66
67		1.030	1.476	237.69	254.49	270.4	18130	220	12.48
68		1.081	1.598	242.53	264.23	271.8	18210	212	14.87
69		1.131	1.643	247.43	274.13	271.2	18220	210	14.56
70		1.173	1.583	252.60	283.25	269.6	18060	214	13.32
71		1.216	1.674	256.45	291.33	269.9	18110	217	13.13
72		1.072	1.903	257.83	268.03	266.7	17590	191	11.97
73		1.014	2.073	254.75	260.64	267.2	17560	184	12.04
74		1.131	1.903	267.99	283.28	264.6	17410	204	11.92
75		1.230	1.674	271.03	293.45	262.7	17230	208	11.82
76		1.039	1.833	248.38	258.18	281.6	20080	241	13.36
77		1.097	1.733	252.27	267.66	281.6	19980	241	12.78
78		1.032	2.073	244.03	280.21	254.9	16150	224	12.88
79		1.081	2.037	250.67	294.36	255.7	16300	210	13.59

TABLE I (Continued)

Run	Remarks	P_R	V_R	$t_{b_{in}}$ (°F)	$t_{b_{out}}$ (°F)	I (amp.)	q/A B/hr-ft^2	Δt_{avg} (°F)	Re_{-4} x 10^4
80		1.151	2.013	260.90	313.39	255.0	16140	205	13.27
81		1.278	1.924	280.28	345.32	251.5	15930	200	12.52
82		1.064	2.453	253.84	342.70	253.6	15930	217	13.70
83		1.089	2.436	259.30	354.76	253.1	15850	224	14.27
84	a	1.064	0.815	227.36	243.54	354.2	30820	279	18.99
85	a	1.168	0.879	234.72	257.30	353.9	30780	265	16.25
86		1.508	1.006	254.03	289.23	348.8	30410	285	14.00
87		1.424	1.006	248.91	285.34	379.7	36320	317	17.21
88	a	1.141	0.862	235.99	255.28	384.8	36390	293	18.26
89		1.267	0.904	241.45	267.73	383.2	36280	315	18.12
90		1.367	1.201	253.94	287.53	378.4	35590	326	17.27
91		1.121	1.018	242.10	254.75	338.9	27650	236	18.15
92		1.114	1.018	239.46	255.47	378.4	35340	289	19.61
93		1.245	1.235	249.03	274.23	374.4	34950	303	17.28
94		1.429	1.088	262.37	298.71	367.7	34310	352	14.45
95		1.045	1.733	241.48	259.30	369.3	34190	384	16.34

TABLE I (Continued)

Run	Remarks	P_R	V_R	$t_{b_{in}}$ (°F)	$t_{b_{out}}$ (°F)	I (amp.)	q/A B/hr-ft^2	Δt_{avg} (°F)	Re_{-4} x 10^4
96		1.168	1.576	251.68	283.19	366.9	33900	387	16.03
97		1.295	1.445	260.73	301.95	369.0	33940	326	14.93
98		1.432	1.445	272.37	326.17	368.6	33850	324	14.70
99		1.055	1.957	242.63	282.34	364.5	32910	325	15.06
100		1.159	1.873	253.48	306.75	363.2	32780	305	16.18
101		1.282	1.768	264.59	333.72	363.2	33050	302	14.84
102		1.035	2.137	239.46	294.53	401.6	40820	364	17.72
103		1.144	1.990	249.23	320.58	399.2	40230	348	17.51
104		1.295	1.863	264.39	356.79	391.2	39240	356	15.99
105		1.347	1.968	270.44	366.82	389.9	38940	362	15.24
106		1.047	2.277	240.47	318.03	366.4	33700	325	16.56
107		1.156	2.163	253.97	353.00	366.4	33480	305	16.18
108		1.238	2.086	263.51	371.30	360.8	33060	311	17.93
109		1.315	2.013	271.00	393.53	358.4	32730	315	15.36
110		1.055	2.561	240.73	368.42	401.6	41160	341	18.44
111		1.151	2.489	252.73	409.51	402.4	41370	306	19.89

TABLE I (Continued)

Run	Remarks	P_R	V_R	$t_{b_{in}}$ (^oF)	$t_{b_{out}}$ (^oF)	I (amp.)	q/A B/hr-ft^2	Δt_{avg} (^oF)	Re_{-4} x 10^4
112		1.055	2.765	244.10	401.17	362.1	32900	308	17.81
113		1.156	2.599	259.46	435.62	357.0	32320	334	16.42
114		1.064	3.110	243.87	486.34	412.0	44670	387	20.26
115		1.029	0.781	222.33	238.80	267.8	17550	173	11.89
116		1.019	0.730	218.41	238.02	300.2	22040	216	13.10
117		1.156	0.675	222.85	249.03	333.9	27010	260	11.54
118		1.474	0.725	239.07	275.18	346.6	29500	277	14.01

Remarks:

[a] Property values particularly in doubt in this region.

[b] Boiling took place in some part of the test section.

CHAPTER VIII

TEST RESULTS AND CORRELATION OF DATA

In Chapter IV a theoretical analysis of the thermal syphon was presented. The expression derived to represent the behavior of the heat transfer film coefficient for the conditions of turbulent flow was

$$Nu = 0.079\,(Re)^{11/4}\,(Gr_f)^{-1}\,(Pr)\left(\frac{\ell}{\ell_t}\right)\left(\frac{d}{y}\right). \qquad \text{IV-22}$$

The values of the constant factors for the particular test loop are:

ℓ = 109.3-in.

ℓ_t = 25.25-in.

d = 0.430-in.

y = 37.0-in.

When these values are inserted in equation IV-22 the predicted correlation for the particular test loop is obtained as

$$\frac{Nu)(Gr_f)}{(Pr)} = 0.00397\,(Re)^{11/4}. \qquad \text{IV-22a}$$

One would expect the experimental data to follow the form of this equation. Figures 9, 10, and 11 show that this expectation is justified. For the regions where $\frac{v_m}{v_c} < 1$ the correlation

$$\frac{Nu)(Gr_f)}{(Pr)} = 0.000560\,(Re)^{2.99} \qquad \text{VIII-1}$$

is obtained. For the regions where $\frac{v_m}{v_c} > 1$ the relation

$$\frac{(Nu)(Gr_f)}{(Pr)} = 0.00494\,(Re)^{11/4} \qquad \text{VIII-2}$$

is obtained. Figure 11 shows a comparison of these two expressions with the analytically predicted correlation. The two different correlations depending on the value of the reduced specific volume may be justified on the basis that the viscosity changes abruptly across the critical region. The correlations do not change so abruptly. This may be explained by the fact that most of the influence of the viscosity in the dimensionless correlation is canceled out. This cancellation is caused by the artificial way in which all but the one-fourth power of the viscosity originally in the Blasius law is entered in the relationship to make it dimensionless. As a matter of fact, the thermal conductivity is also artificially inserted into the equation.

The scatter of data and the conflicting values of the slopes and constant terms of the correlations as compared with the analytically predicted values may be easily attributed to the uncertainty of the property values used. Indeed, with the large uncertainties of the properties in the critical and supercritical regions it is remarkable that the correlation of the data was as successful as shown in the figures.

It is possible that the constant term in the correlation must be determined by using an equivalent length for pressure drop through the loop and fittings instead of the physical circumferential length.

The scatter of data in the correlation for the regions of $\frac{v_m}{v_c} > 1$ may be partly attributed to the slow oscillatory phenomenon in the flow rate as described on page 35.

Figure 12 shows the inadequacy of the conventional relationship

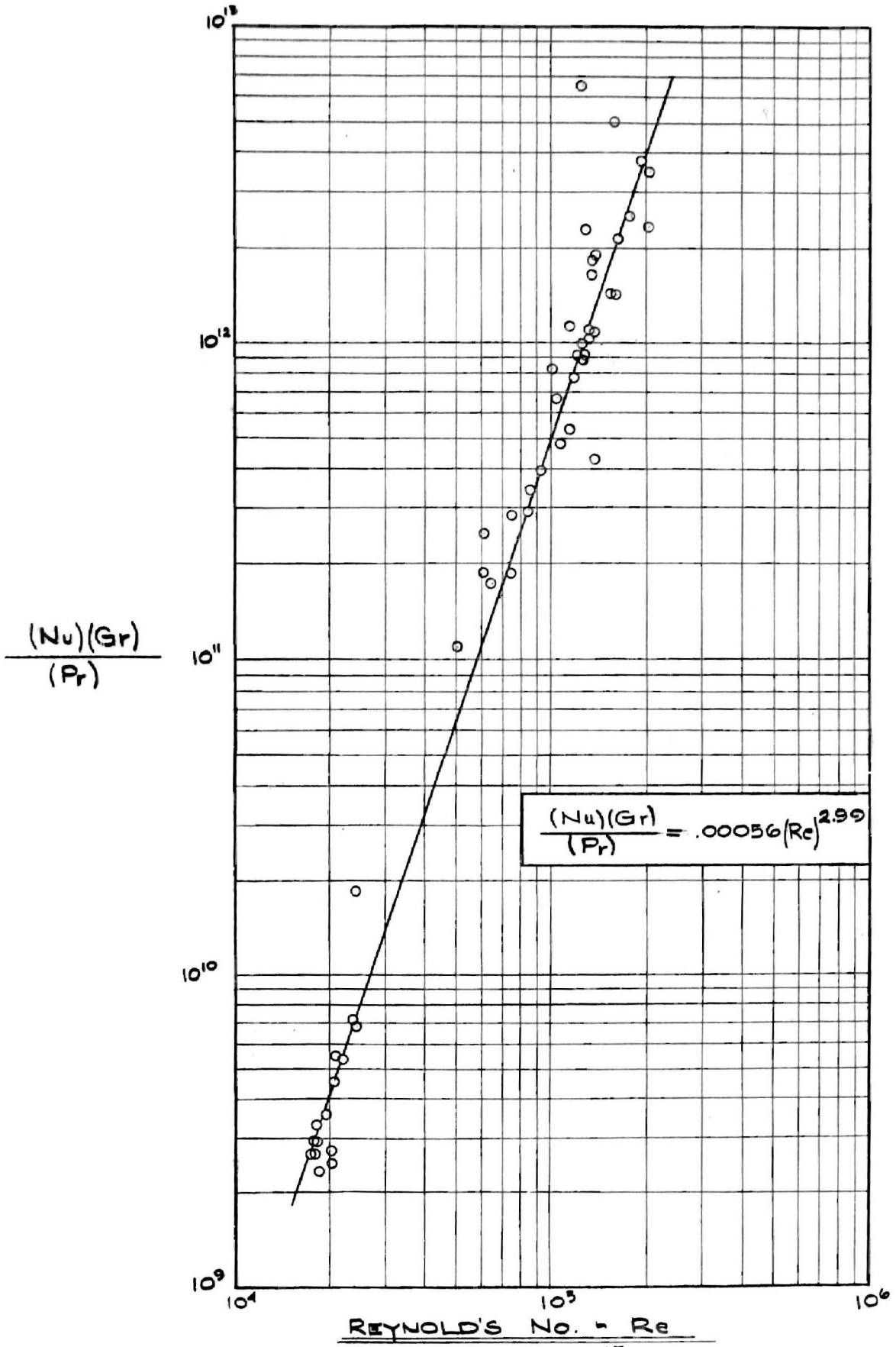

Figure 9. Correlation for $\frac{v_m}{v_c} < 1$

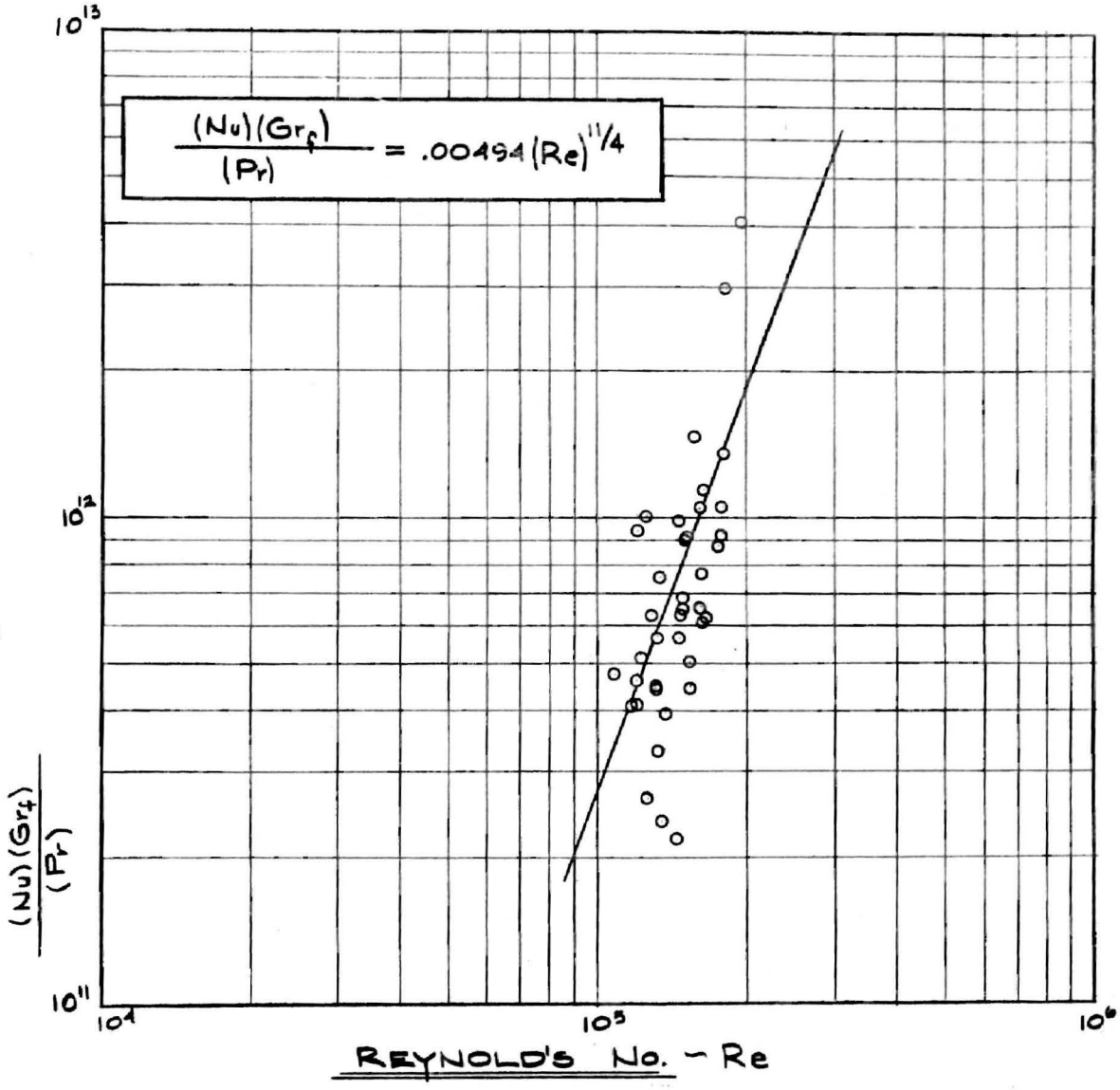

Figure 10. Correlation for $\frac{\sigma_m}{\sigma_c} > 1$

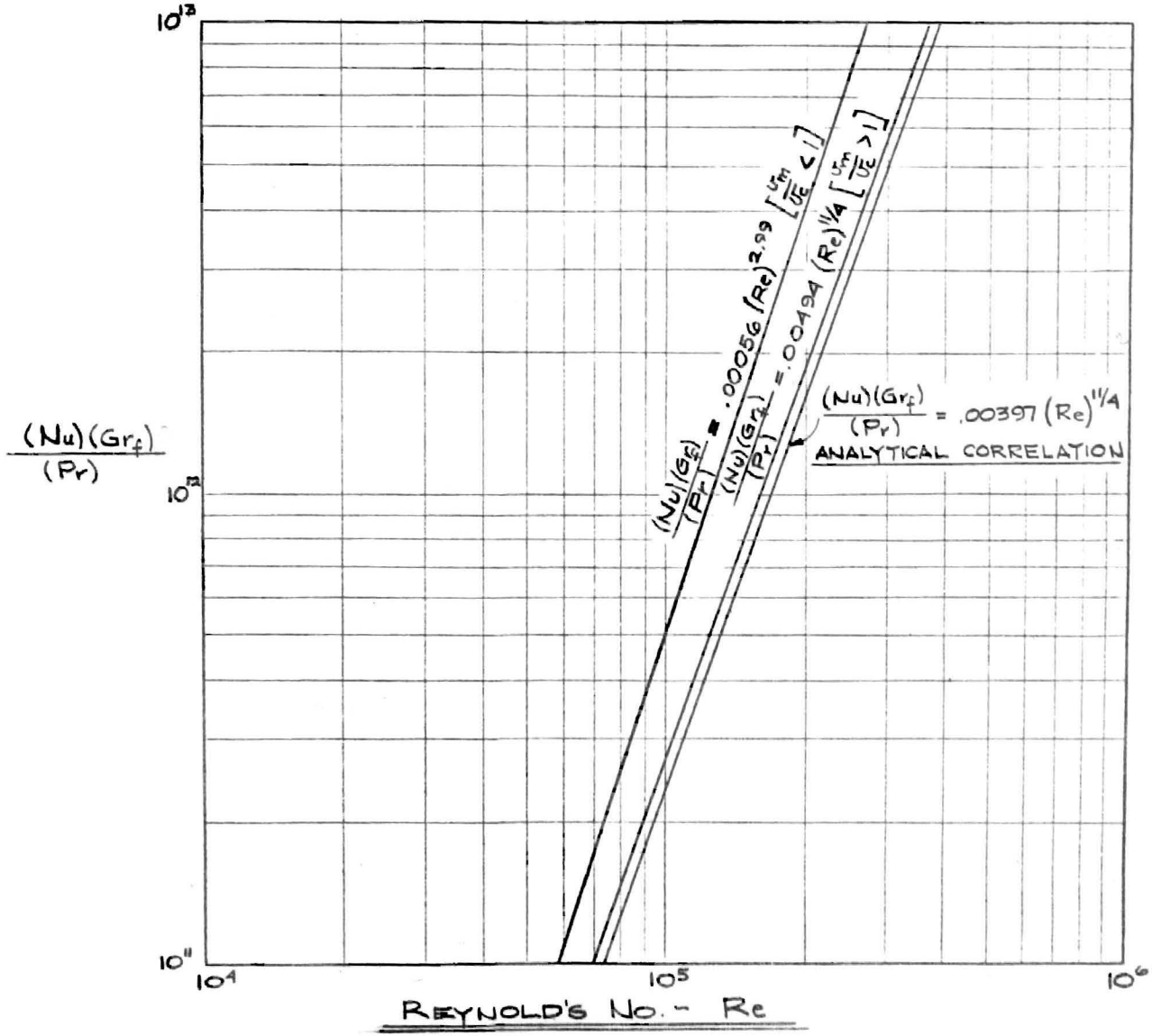

Figure 11. Comparison of Experimental Correlations with Analytical Prediction

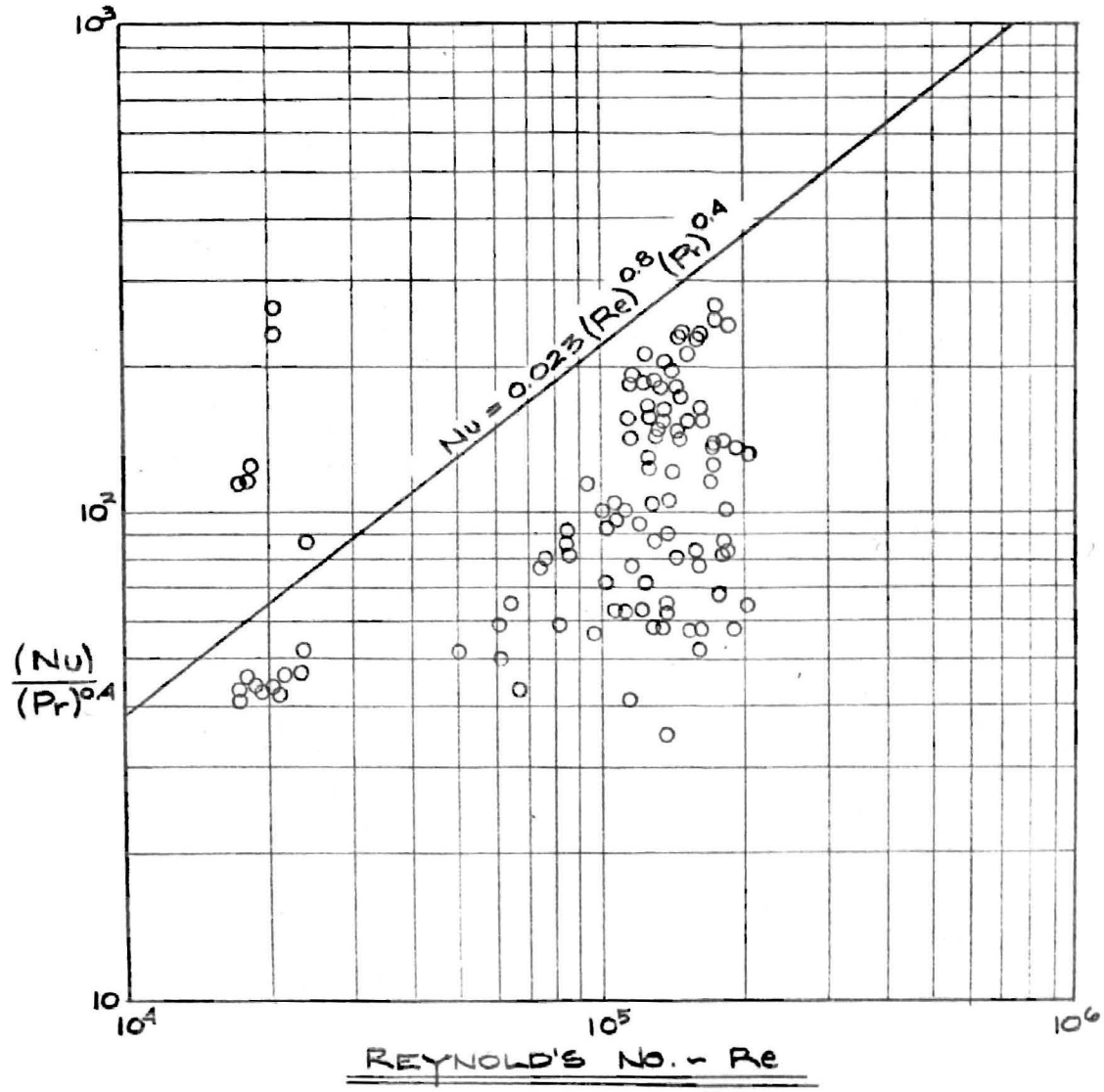

Figure 12. Plot of Experimental Data Showing Inadequacy of Conventional Forced Convection Relation to Predict Behavior of the Thermal Syphon

$$Nu = 0.023 (Re)^{0.8} (Pr)^{0.4}$$

to predict the behavior of the thermal syphon. Even though the convection phenomena which occur in the heat transfer loop are of the forced type, the flow rate and heat flux are not independent variables as in most cases of forced convection. The flow rate is an explicit function of the heat flux as well as the viscous properties of the fluid. This differs from the conventional case where the fluid flow rate is dependent only on the viscous characteristics of the fluid.

Figure 13 is a plot of selected values of the apparent thermal conductivities. The trends of the curves in the supercritical region agree with the trends presented by Schmidt, Eckert, and Grigull (4). The boiling trend is shown for the subcritical pressures.

Figure 14 is a plot of selected values of the average heat transfer film coefficients. In this figure the influence of boiling at pressures below the critical value is very pronounced. For supercritical pressures the course of the film coefficient curves is very nearly constant.

Complete plots of the local heat transfer film coefficients are shown in Figure 15. Extreme nonuniformity in the local film coefficient values may be seen. However, there is a distinct pattern to this nonuniform behavior. For $\frac{\sigma_m}{\sigma_c} < 1$ the film coefficients increase in an oscillatory manner along the length of the tube. The oscillations become more severe as the critical value of $\frac{\sigma_m}{\sigma_c} = 1$ is approached. For $\frac{\sigma_m}{\sigma_c} > 1$ the oscillations become less severe as the region of operation is further removed from the critical state. Also, in the superheated vapor region the local film coefficients decrease along the length of the tube.

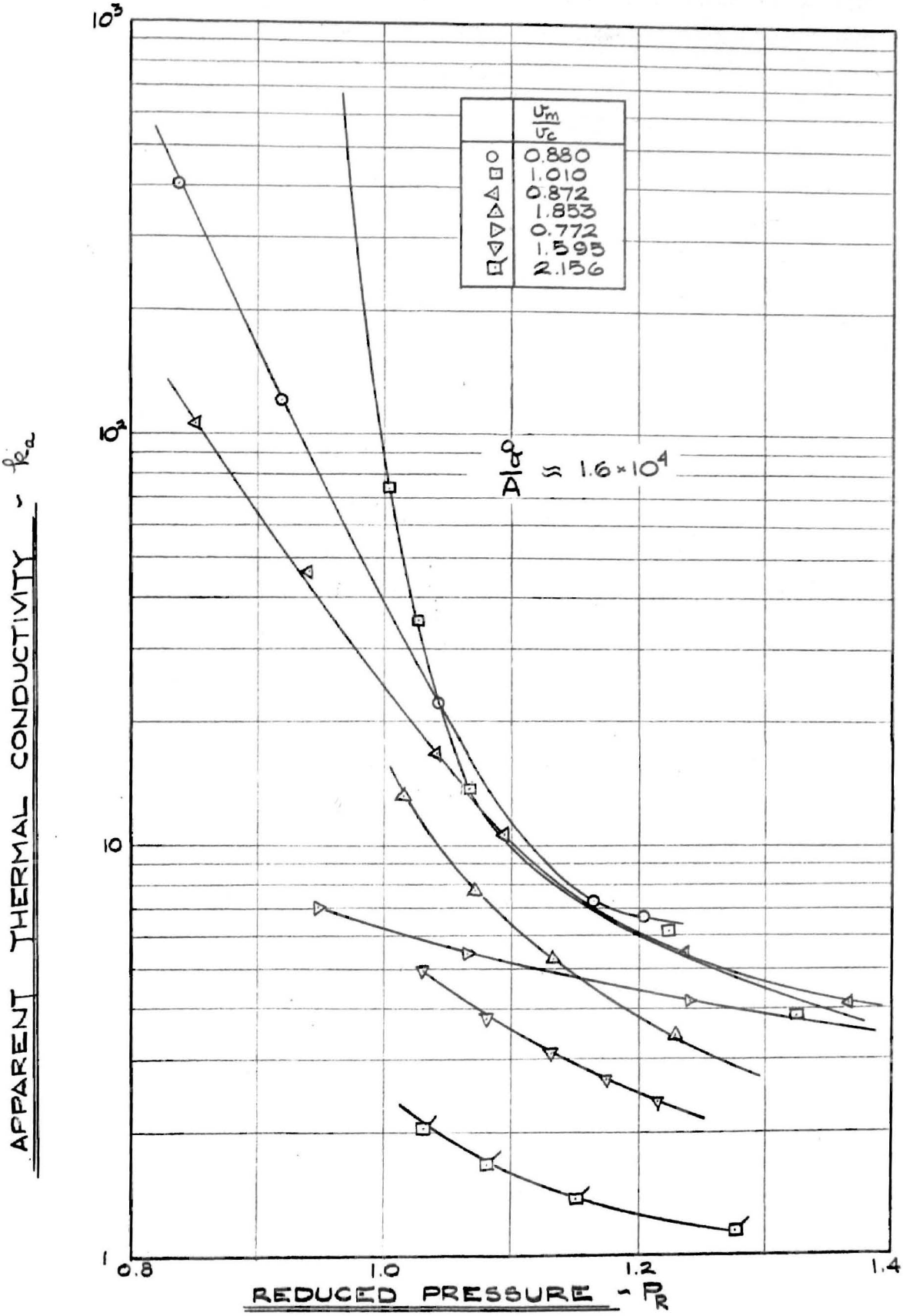

Figure 13. Plot of Selected Apparent Thermal Conductivities

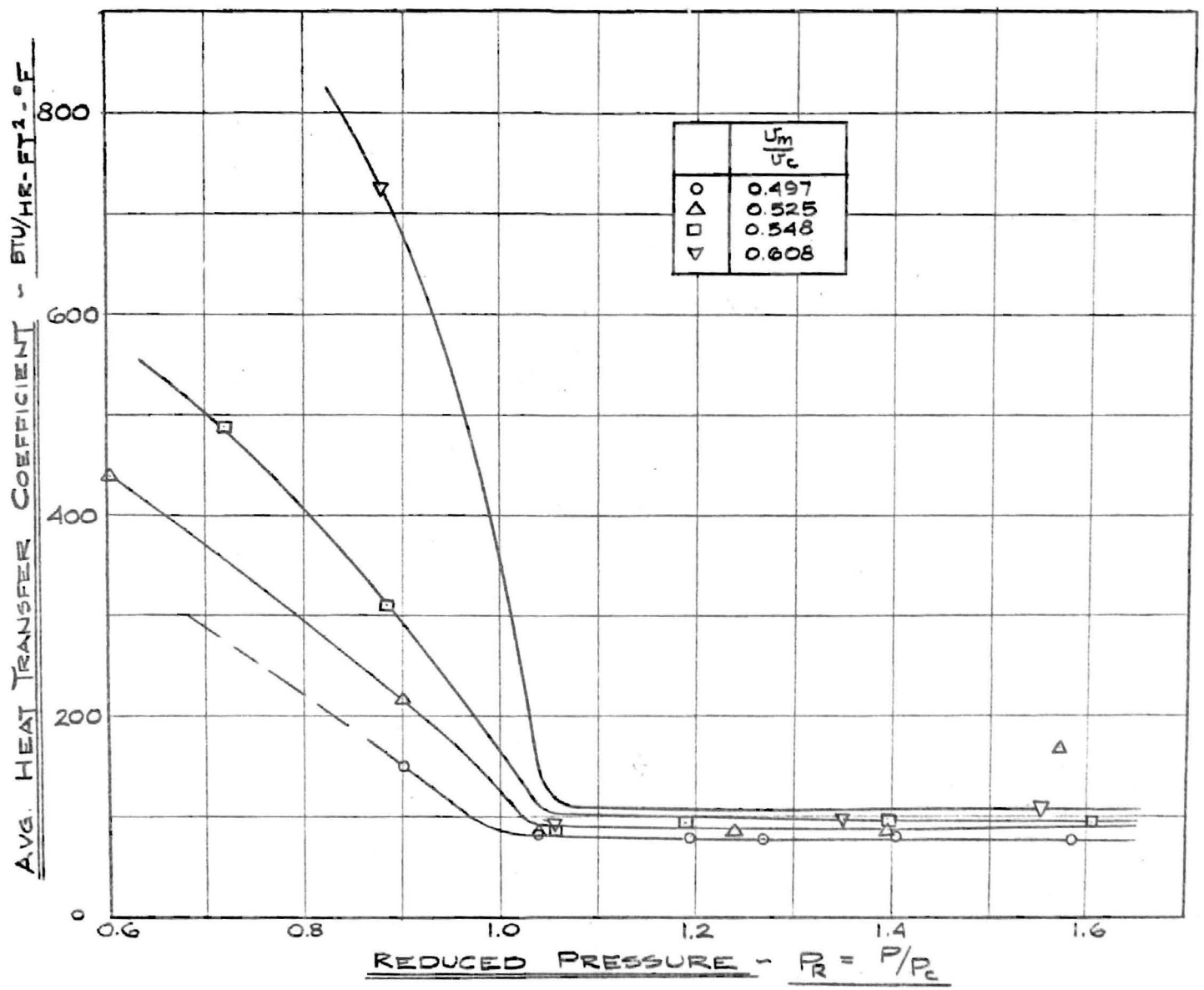

Figure 14. Plot of Selected Average Heat Transfer Film Coefficients

The increase of the film coefficient along the length of the tube in the regions for $\frac{v_m}{v_c} < 1$ and the corresponding decrease in the regions for $\frac{v_m}{v_c} > 1$ indicate that the highest values of the heat transfer film coefficient may be expected in the immediate vicinity of the critical state. This fact clarifies the discussion on page 31 concerning the uncertainties involved in predicting the trends to be expected near the critical point. In respect to that discussion it would seem that the specific heat capacity increases at a faster rate than the volume coefficient of expansion.

The oscillatory nature of the curves may be attributed to the rapid change of the property values in the neighborhood of the critical state. In the regions of $\frac{v_m}{v_c} < 1$ the film conditions may be close to the critical state even if the bulk conditions are not. As the values of $\frac{v_m}{v_c}$ are increased the entire bulk of the fluid reaches the unstable critical region and more violent oscillations persist. As the fluid progresses into the superheated vapor region a more stable situation is experienced. In this region the film conditions will be further removed from the critical state than the bulk of the fluid since the heat transfer boundary layer has a higher temperature than the bulk temperature. If one considers the oscillations in the local film coefficient values to be the result of violent transitions in the hydrodynamic boundary layer, then it is easily seen that the rapid change of viscosity across the critical state explains the intimate connection of the oscillations with the critical region.

In view of the large errors which may be present in the property values used in the calculations as well as the unstable nature of the critical state, it seems that the comparison presented in Figure 11 is

entirely conducive to acceptance of the analytical expression

$$\frac{(Nu)(Gr_f)}{(Pr)} = 0.00397\,(Re)^{11/4} \qquad \text{IV-22a}$$

as indicative of the heat transfer characteristics of the thermal syphon tested. It is presumed that there was no dissociation of the Freon 12 during the experiments.

CHAPTER IX

ANALYSIS OF EXPERIMENTAL ERRORS

Errors which may be present in the experiments described above will be discussed in this chapter. Two errors are presented; the errors which are present because of the inherent inaccuracies of the instruments, and realistic estimates of the actual errors considering operating conditions of the apparatus, etc. The effect that these errors may have on the final test data will be discussed in subsequent paragraphs. Table II gives the minimum error which would be present in the experimental data considering the accuracy of the instruments, and the estimated accumulative errors due to all experimental inaccuracies. The estimated errors presented in Table II are valid only for those regions of operation which were stable. Larger errors would be present in the regions close to the critical state where large fluctuations in pressure were encountered.

Any error in the calculation of the difference in temperature across the tube wall due to the variation in wall thickness may certainly be discounted since the differential temperatures were always rounded to the nearest degree Fahrenheit.

The maximum error in the heat transfer film coefficient due to errors in the bulk temperature, wall temperature, and power measurements may be calculated as

$$\text{Max. Error} = \left[1 - \frac{\left(\frac{.995}{1.000}\right)\left(\frac{.990}{1.000}\right)}{\left(\frac{150}{146}\right)} \right] \times 100 = 4.12\%,$$

TABLE II

SUMMARY OF EXPERIMENTAL ERRORS

Variable	Minimum Error	Estimated Accumulative Error
Bulk temperature	± 0.1 °F	± 2.0 °F
Wall temperature	± 1.0 °F	± 3.0 °F
System pressure	± 1 psi	± 2 psi
Venturi differential pressure	± 0.1-in. H_2O	± 0.2-in. H_2O
Electric current	± 1/2 %	± 1 %
Voltage across test section	± 0.03 volts	± 0.05 volts
Cooling water temperature difference	± 0.1 °F	± 0.3 °F
Cooling water flow rate	± 1/2 %	± 1 %
Tube wall diameter	-	± 0.0002-in.

assuming a film temperature difference of 150°F. Of course, this error would be larger for the ranges where the film temperature drop was smaller than this value. With the exception of three runs, the film temperature drop was always greater than 100°F.

The assumptions involved in the derivation of the Kreith-Summerfield equation presented on page 39 were an adiabatic outer tube surface, a linear variation of the thermal conductivity and electrical resistivity with temperature, and no axial heat flow along the tube. The heat loss through the insulation was of the order of one percent so that the error due to a nonadiabatic wall condition would be completely absorbed in the rounding of the temperature differences to the nearest degree Fahrenheit. As shown in Figures 30 and 31 the second assumption is fulfilled. The third assumption must be checked. Considering two points along the tube a distance of three inches apart, having a difference in temperature of 100°F, the axial heat flow may be calculated as

$$q_{axial} = k A \frac{\Delta t}{\Delta x} = \frac{(10)(\pi)(1/2)(.035)(100)}{(144)(.25)} = 1.52 \text{ Btu/hr}$$

which is certainly negligible. Therefore, it may be concluded that the conditions imposed on the use of the Kreith-Summerfield equation are fulfilled.

In consideration of the above discussion it is believed that the heat transfer film coefficients have been determined within an accuracy of plus or minus five percent. The correlations of these coefficients may involve sources of error other than the ones discussed above. These other errors were discussed on pages 36 and 60.

CHAPTER X

CONCLUSIONS AND RECOMMENDATIONS

As stated on page 61 it appears entirely suitable to accept the analytical relation

$$Nu = 0.079\,(Pr)\,(Gr_f)^{-1}\,(Re)^{11/4}\left(\ell/\ell_t\right)\left(d/y\right) \qquad \text{IV-22}$$

as the characteristic equation of the thermal syphon apparatus. With the discussions presented in Chapters VI and VIII in mind specific conclusions may be stated as follows:

1. Very large heat transfer film coefficients of the order of 1500 Btu/hr-ft^2-^{o}F may obtained when the conditions for boiling are satisfied. These coefficients are limited to the regions where the heat flux is rather low since at high heat flux the fluid becomes superheated in the upper end of the test section.

2. Slightly higher heat transfer film coefficients may be experienced near the critical state than in the compressed liquid or superheat regions.

3. The trends of an apparent thermal conductivity defined by equation IV-6 agree with the trends presented by Schmidt, Eckert, and Grigull (4).

4. The experimental data may be correlated within plus or minus twenty-five percent by the following relations:

$$\frac{(Nu)(Gr_f)}{(Pr)} = 0.00056\,(Re)^{2.99}, \qquad \frac{v_m}{v_c} < 1 \qquad \text{VIII-1}$$

$$\frac{(Nu)(Gr_f)}{(Pr)} = 0.00494\,(Re)^{11/4}, \qquad \frac{v_m}{v_c} > 1 . \qquad \text{VIII-2}$$

5. Instabilities of operation were experienced in the vicinity of the critical point. These instabilities were described on page 36.

In view of the above conclusions it is believed that the thermal syphon may be used as an effective method of removing heat from various sources. It would be particularly valuable in an application where containment of the heat transfer fluid is of primary concern as in a nuclear reactor.

Before the thermal syphon principle may be used for a practical application further experimentation should be conducted to resolve some of the following points.

a. A thorough understanding of the slow oscillation phenomena described on page 35 should be developed. This may best be accomplished by careful experimental measurements with recording pressure instruments.

b. A thorough analysis of the pressure drops around the thermal syphon loop should be made. This will also require recording pressure instrumentation.

c. An investigation of the detailed pressure drop along the test section tube may clarify the oscillatory nature of the heat transfer film coefficients along the length of the tube.

d. A temperature controller with a faster response time would be of value.

In connection with the above recommendations for future research it is believed that a thermal syphon apparatus should be constructed to investigate the heat transfer characteristics of water near its

critical state. This would be of definite interest since water would probably be the fluid used in a practical application of the thermal syphon principle. Also, more information is available on the thermodynamic and physical properties of water than for Freon 12 so that a better analysis of the experimental data should be possible.

SELECTED BIBLIOGRAPHY

1. Dickenson, N.L., and C.P. Welch, "Heat Transfer to Supercritical Water", Trans. Amer. Soc. Mech. Engrs., Vol. 80, pp. 746-52, (1958).

2. Doughty, D.L., and R.M. Drake, "Free Convection Heat Transfer from a Horizontal Right Cylinder to Freon 12 Near the Critical State", Trans. Amer. Soc. Mech. Engrs., Vol. 78, pp. 1843-50, (1956).

3. McAdams, W.H., Heat Transmission, McGraw-Hill, New York, N.Y., 3rd Edition, (1954), p. 176.

4. Schmidt, E., E. Eckert, and U. Grigull, "Heat Transfer by Liquids Near the Critical State", AAF Translation No. 527, Air Materiel Command, Wright Field, Dayton, Ohio.

5. "Kinetic" Chemicals Division, E.I. du Pont de Nemours & Co., Wilmington, Delaware, "Quality Specifications for the Freon Fluorinated Hydrocarbon Refrigerants", Bull. B-8S.

6. Comings, E.W., and R.S. Egly, "Viscosities of Gases and Vapors at High Pressures", Ind. Eng. Chem., Vol. 32, pp. 714-8, (1940).

7. Comings, E.W., and M.F. Nathan, "Thermal Conductivity of Gases at High Pressures", Ind. Eng. Chem., Vol. 39, pp. 964-70, (1947).

8. Eckert, E.R.G., Introduction to the Transfer of Heat and Mass, McGraw-Hill, New York, N.Y., (1950), p. 81.

9. Kreith, F., and M. Summerfield, "Heat Transfer to Water at High Flux Densities With and Without Surface Boiling", Trans. Amer. Soc. Mech. Engrs., Vol. 71, pp. 805-15, (1949).

10. Eiseman, B.J., R.L. McHarness, and J.J. Martin, "The New Thermodynamic Properties of Freon 12", Ref. Eng., Vol. 63, No. 9, pp. 31-44, (Sept. 1955).

11. Lenoir, J.M., "Thermal Conductivity of Gases at Atmospheric Pressure", Univ. of Ark. Experiment Sta., Bull. 18, (Aug. 1953).

12. Benning, A.F., and W.H. Markwood, "Thermal Conductances and Heat Transmission Coefficients of Freon Refrigerants", Kinetic Chemicals Inc., Wilmington, Del., (1942).

13. Benning, A.F., and W.H. Markwood, "The Viscosities of Freon Refrigerants", Ref. Eng., Vol. 37, p. 243, (1939).

14. American Society for Metals, Metals Handbook, p. 314, (1948).

APPENDIX A

LOCAL HEAT TRANSFER FILM COEFFICIENTS

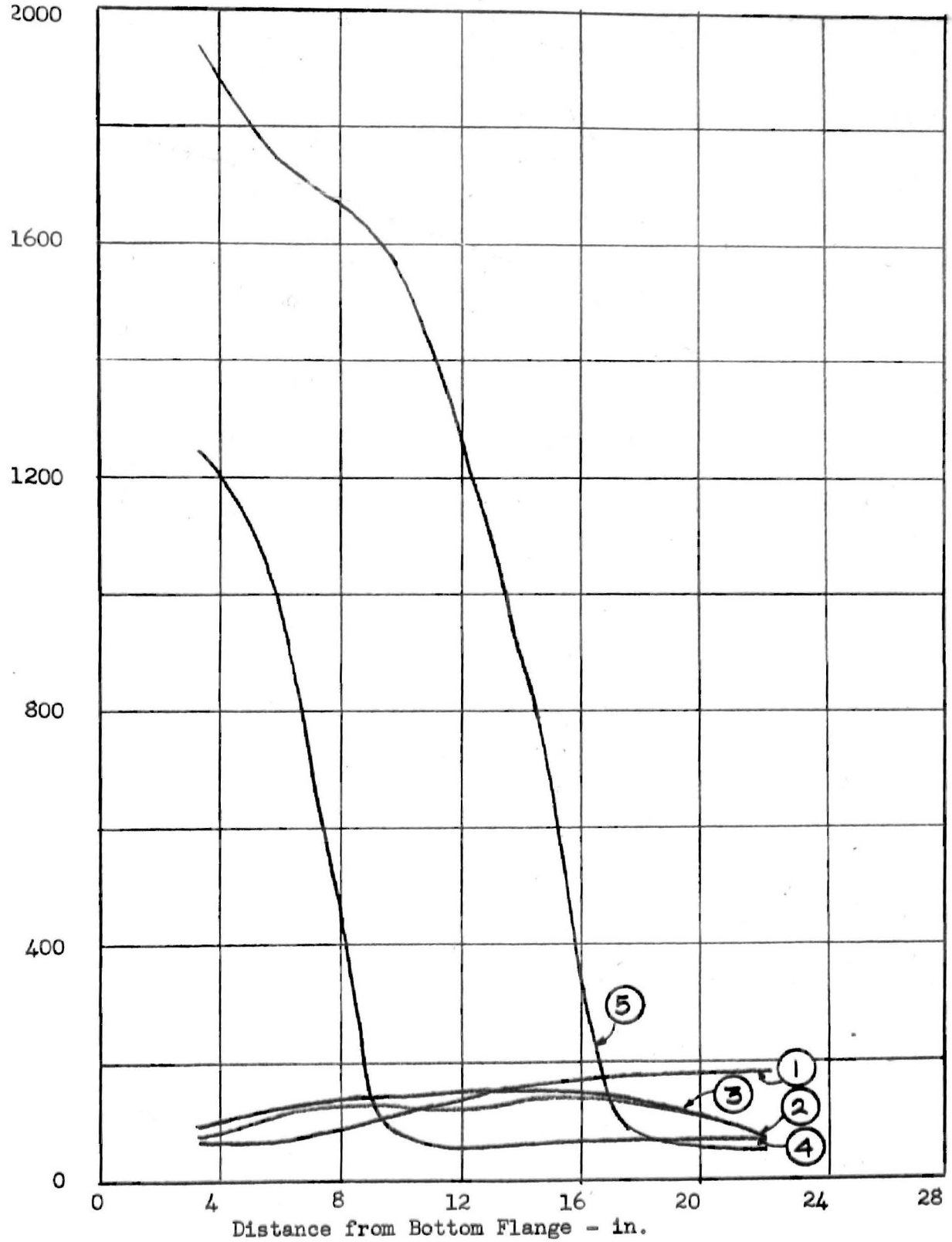

Figure 15(a). Local Heat Transfer Film Coefficients Runs 1-5, V_R = 0.880

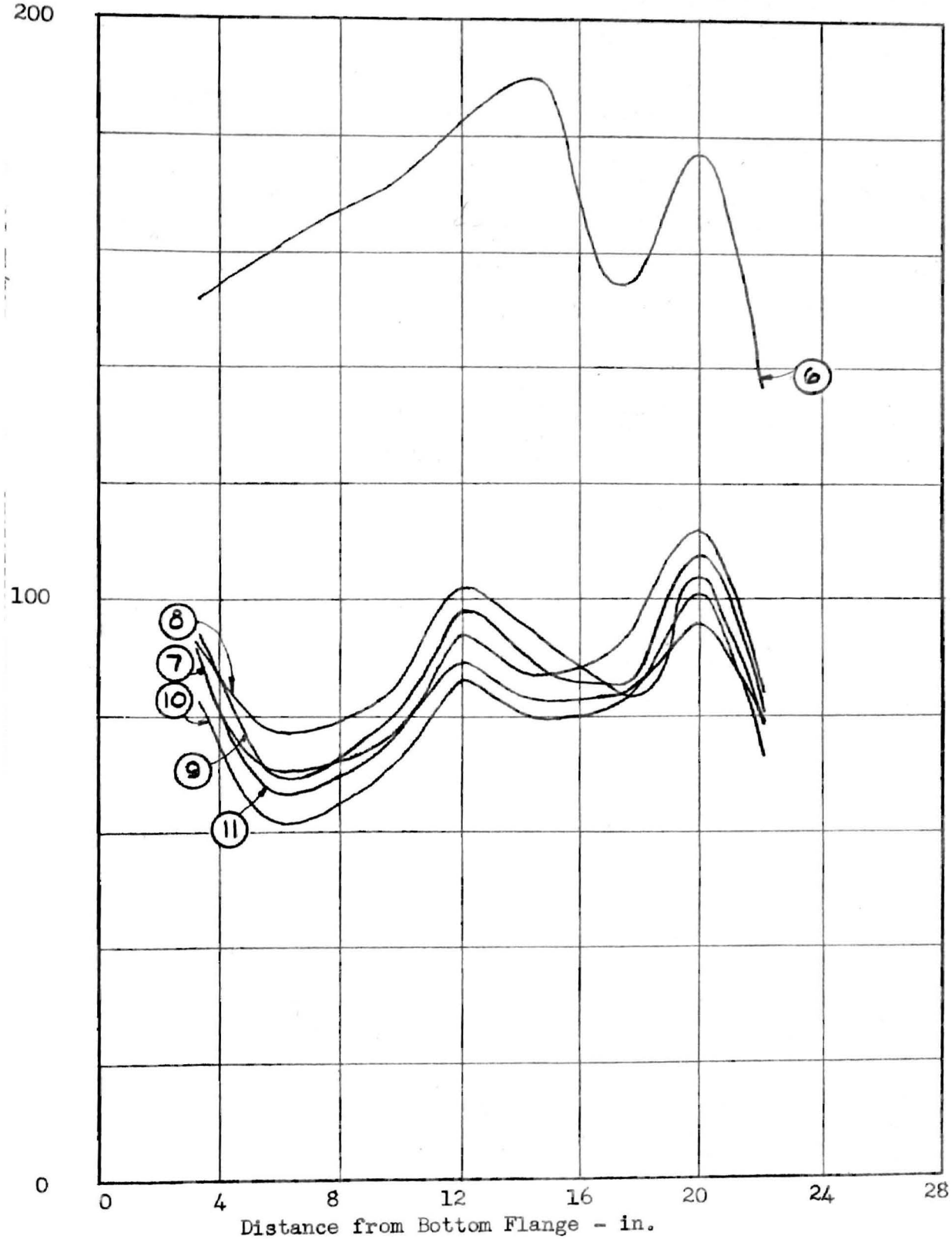

Figure 15(b). Local Heat Transfer Film Coefficients
Runs 6-11, V_R = 0.497

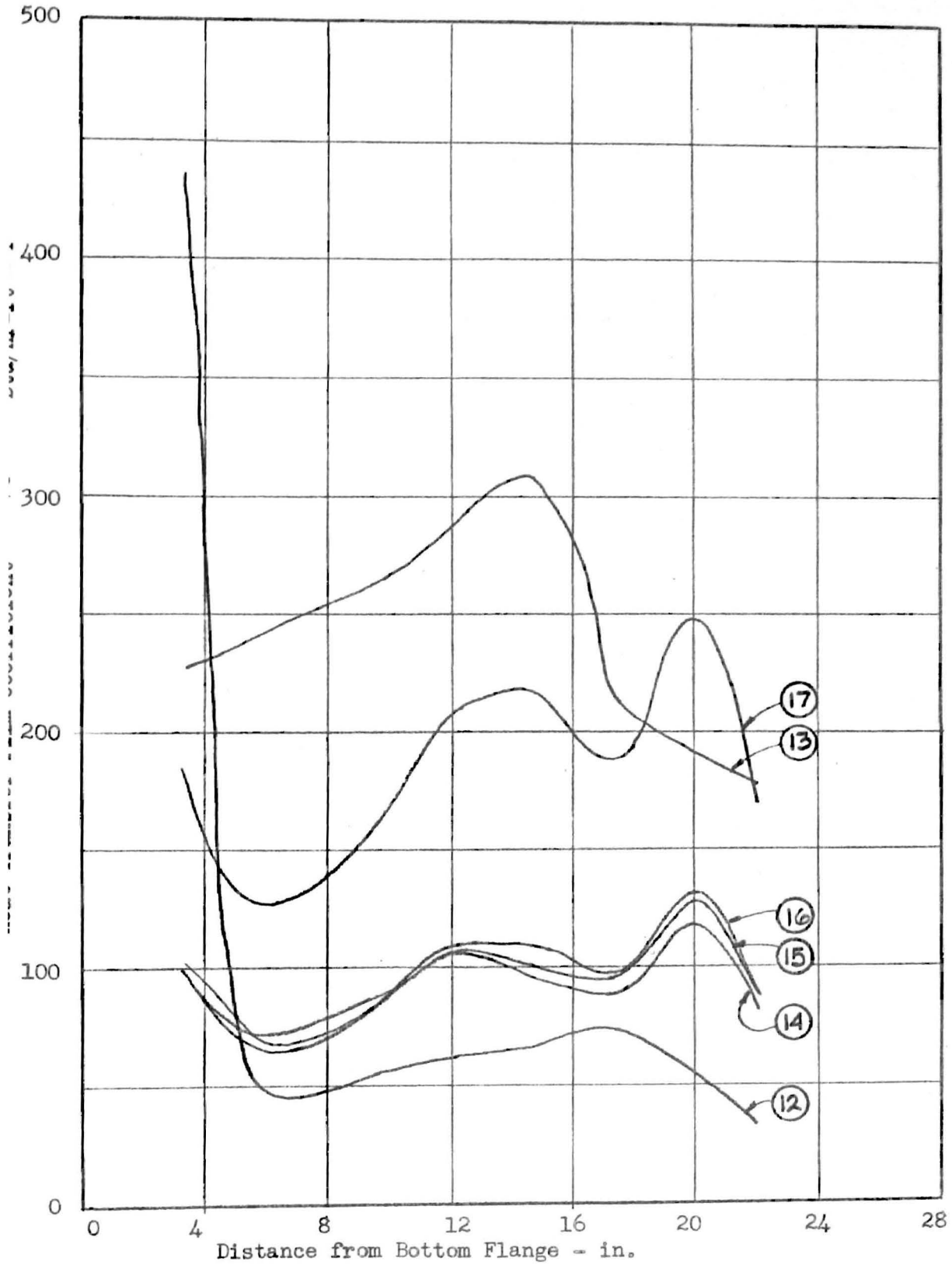

Figure 15(c). Local Heat Transfer Film Coefficients
Runs 12-17, V_R = 0.525

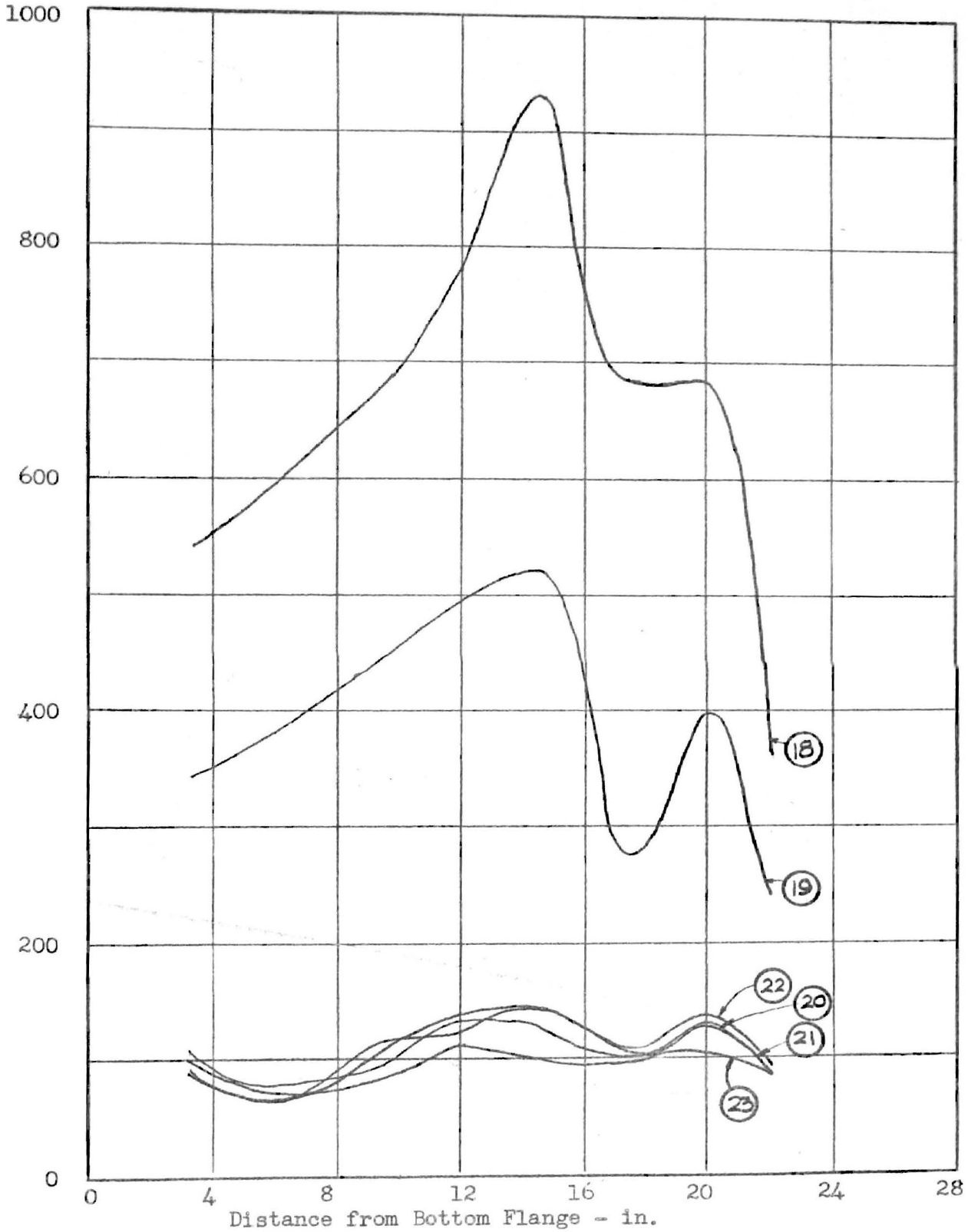

Figure 15(d). Local Heat Transfer Film Coefficients
Runs 18-23, $V_R = 0.548$

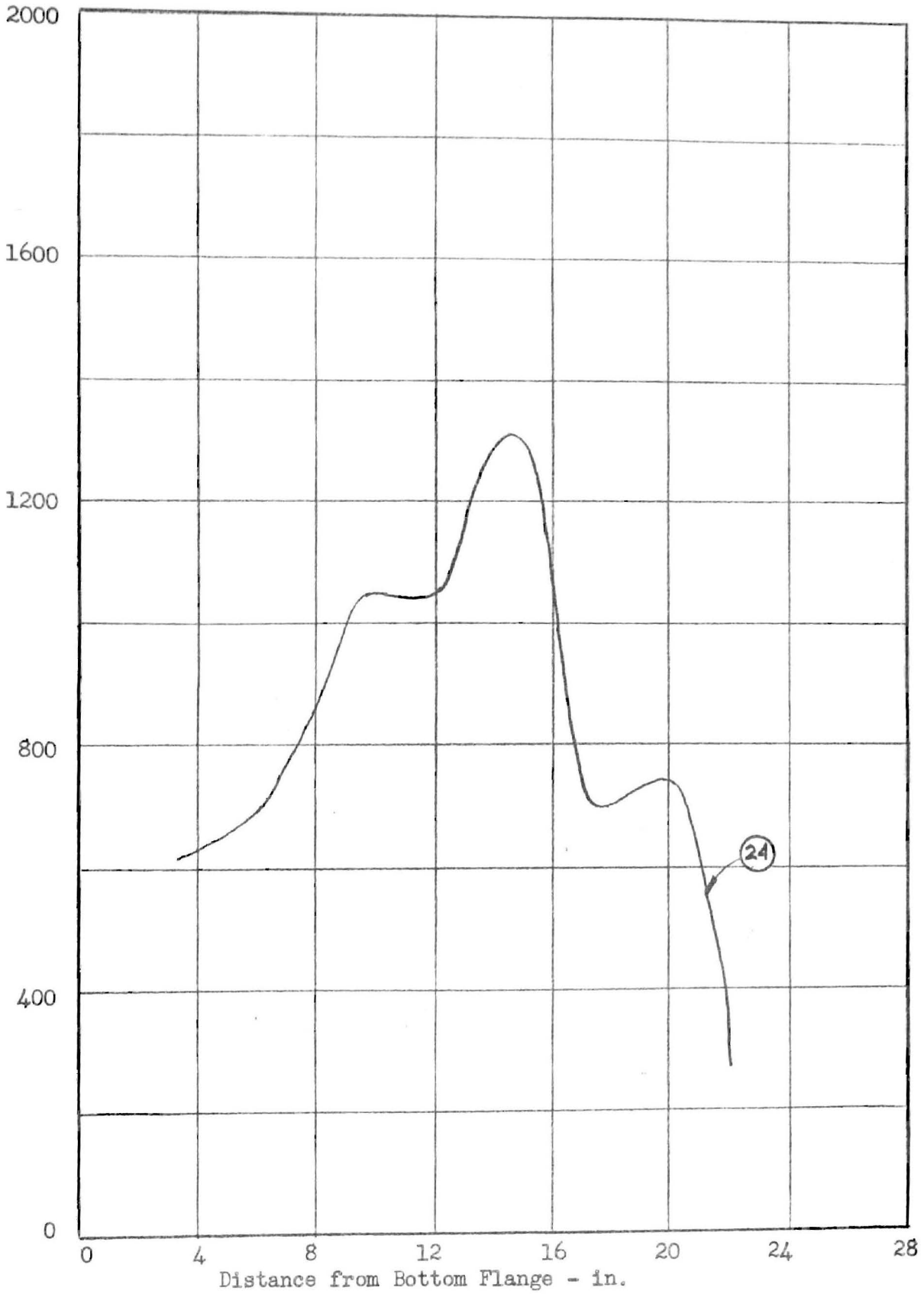

Figure 15(e). Local Heat Transfer Film Coefficients
Run 24, V_s = 0.561

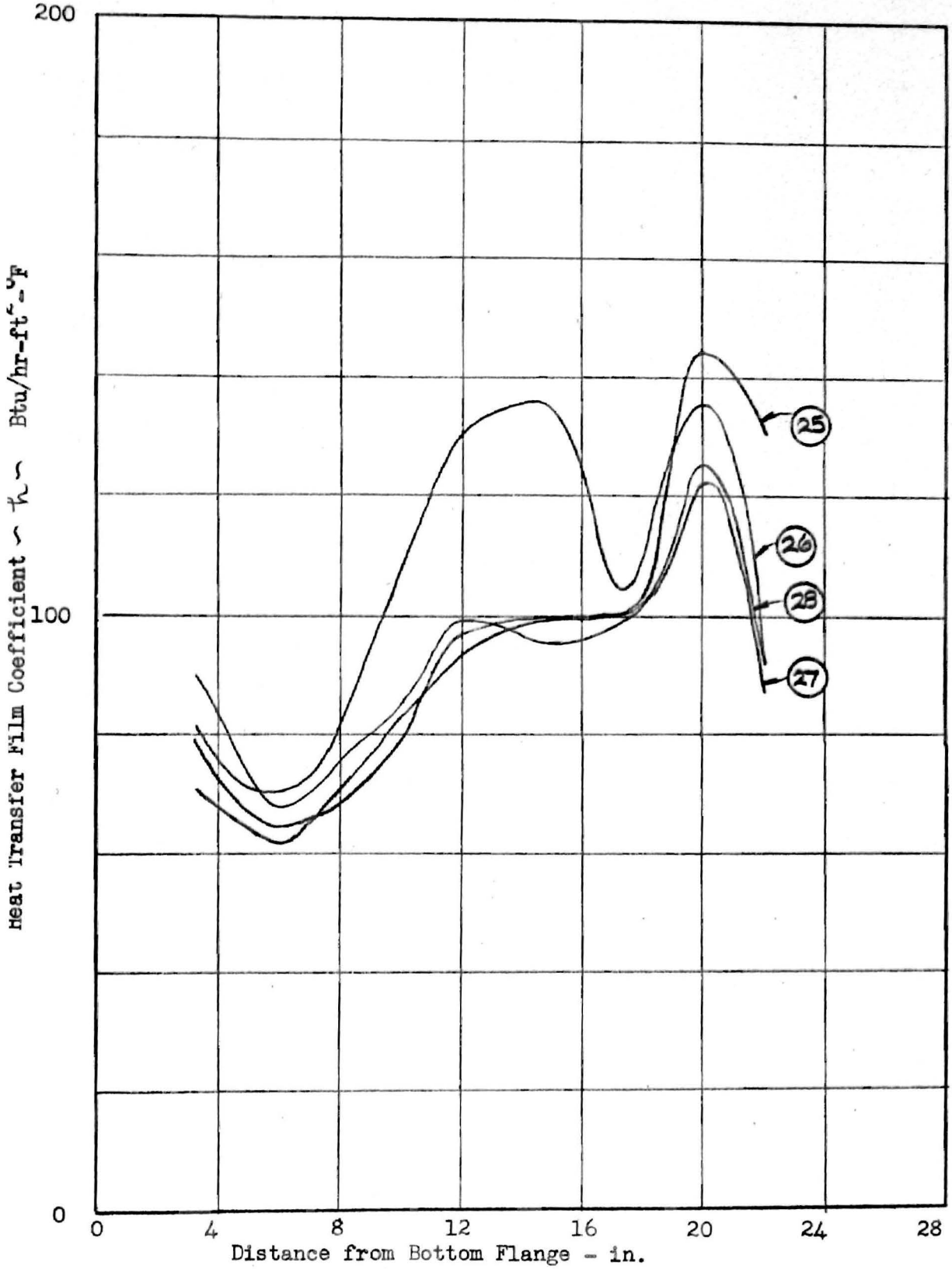

Figure 15(f). Local Heat Transfer Film Coefficients
Runs 25-29, V_R = 0.561

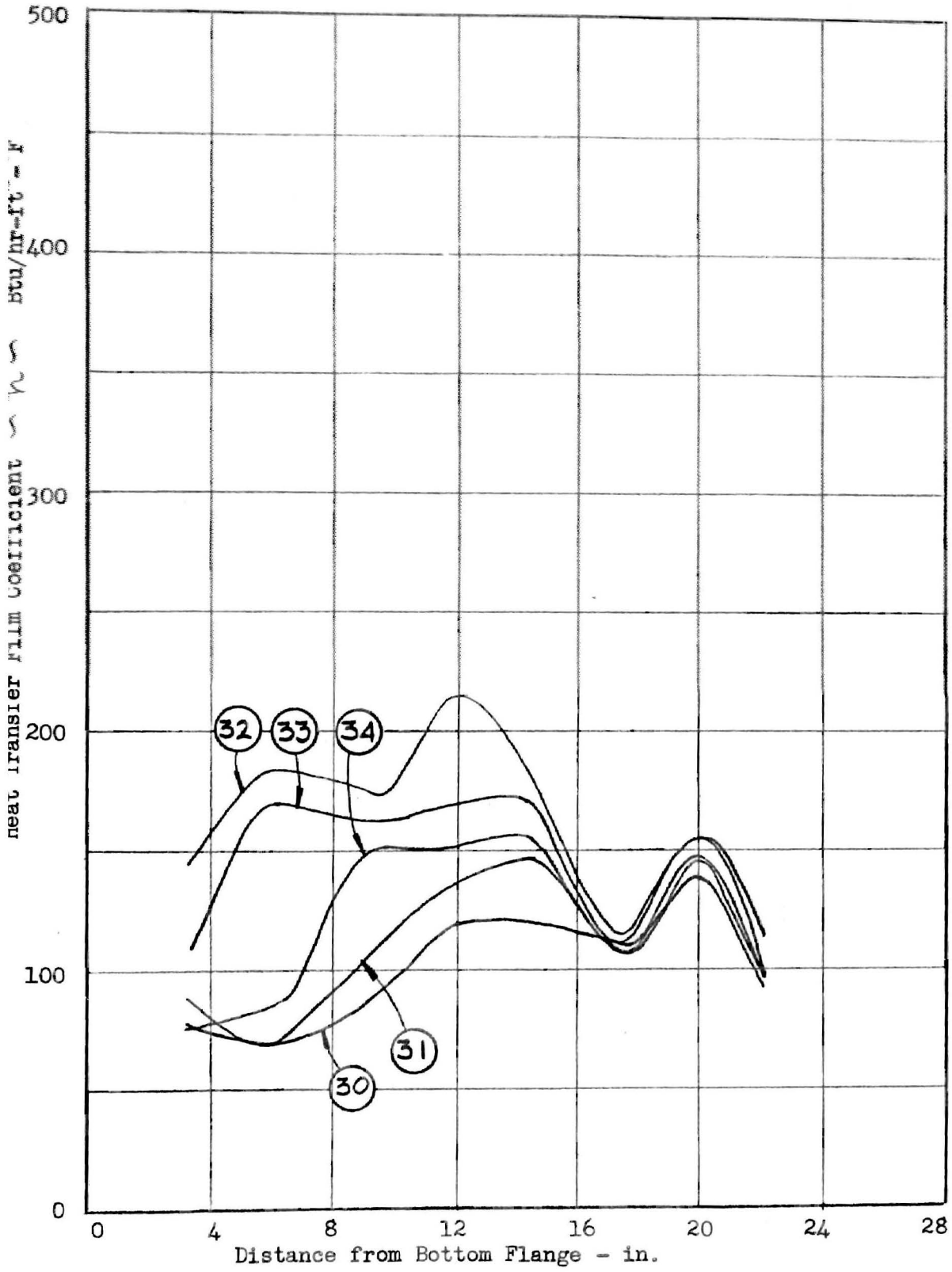

Figure 15(g). Local Heat Transfer Film Coefficients
Runs 30-34, V_R = 0.608

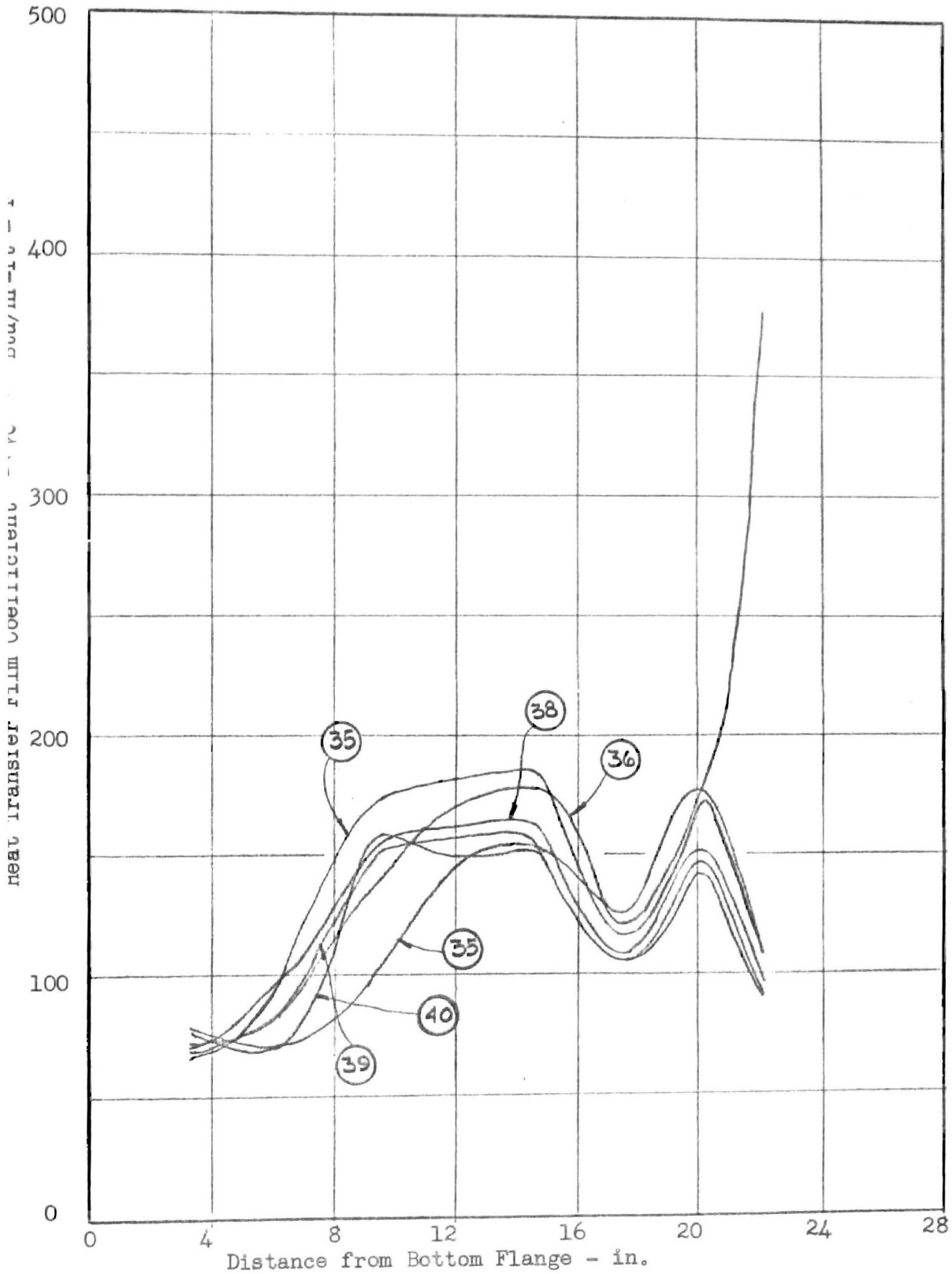

Figure 15(h). Local Heat Transfer Film Coefficients
Runs 35-40, V_R = 0.716

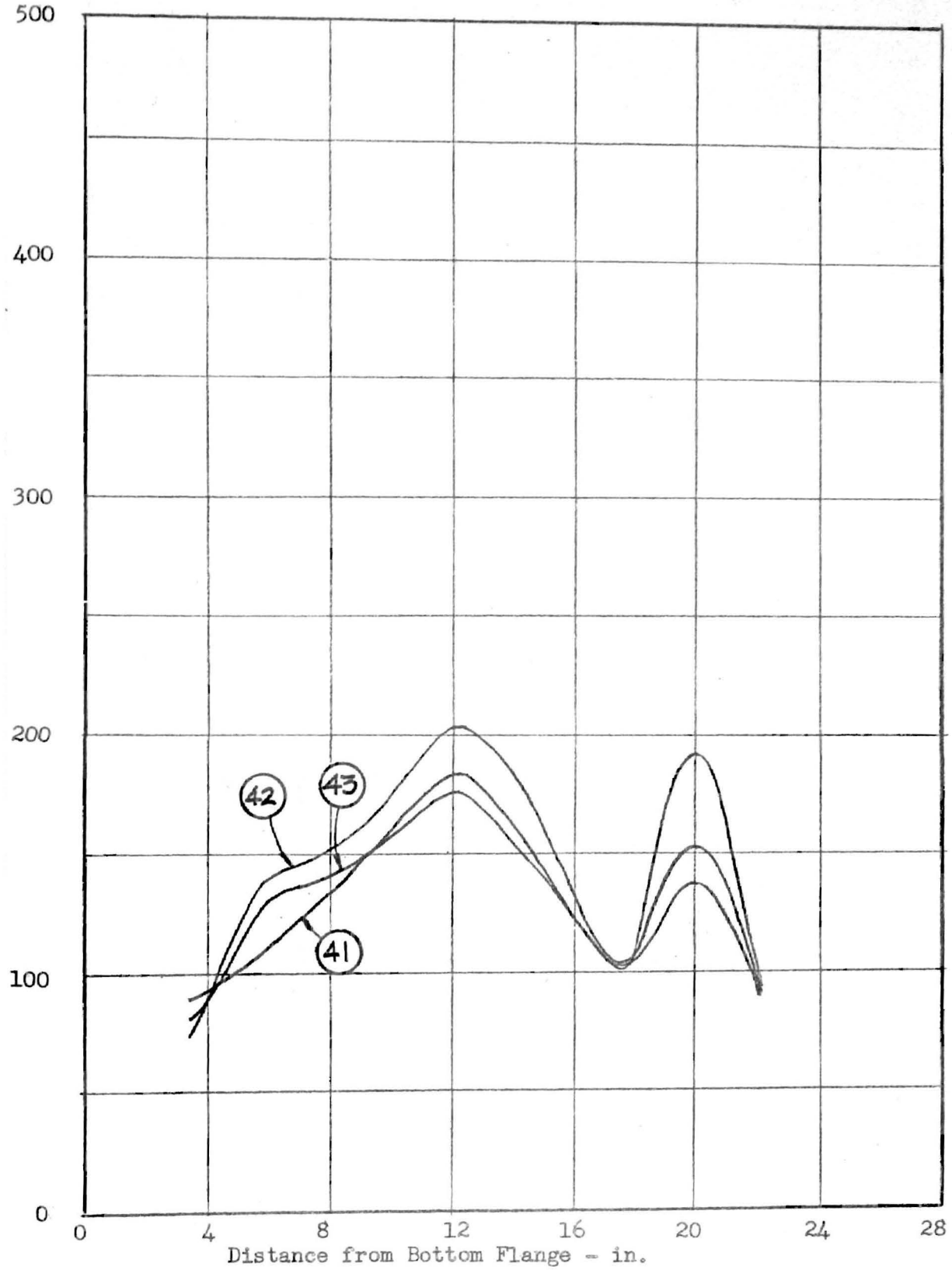

Figure 15(i). Local Heat Transfer Film Coefficients
Runs 41-43, V_R = 0.752

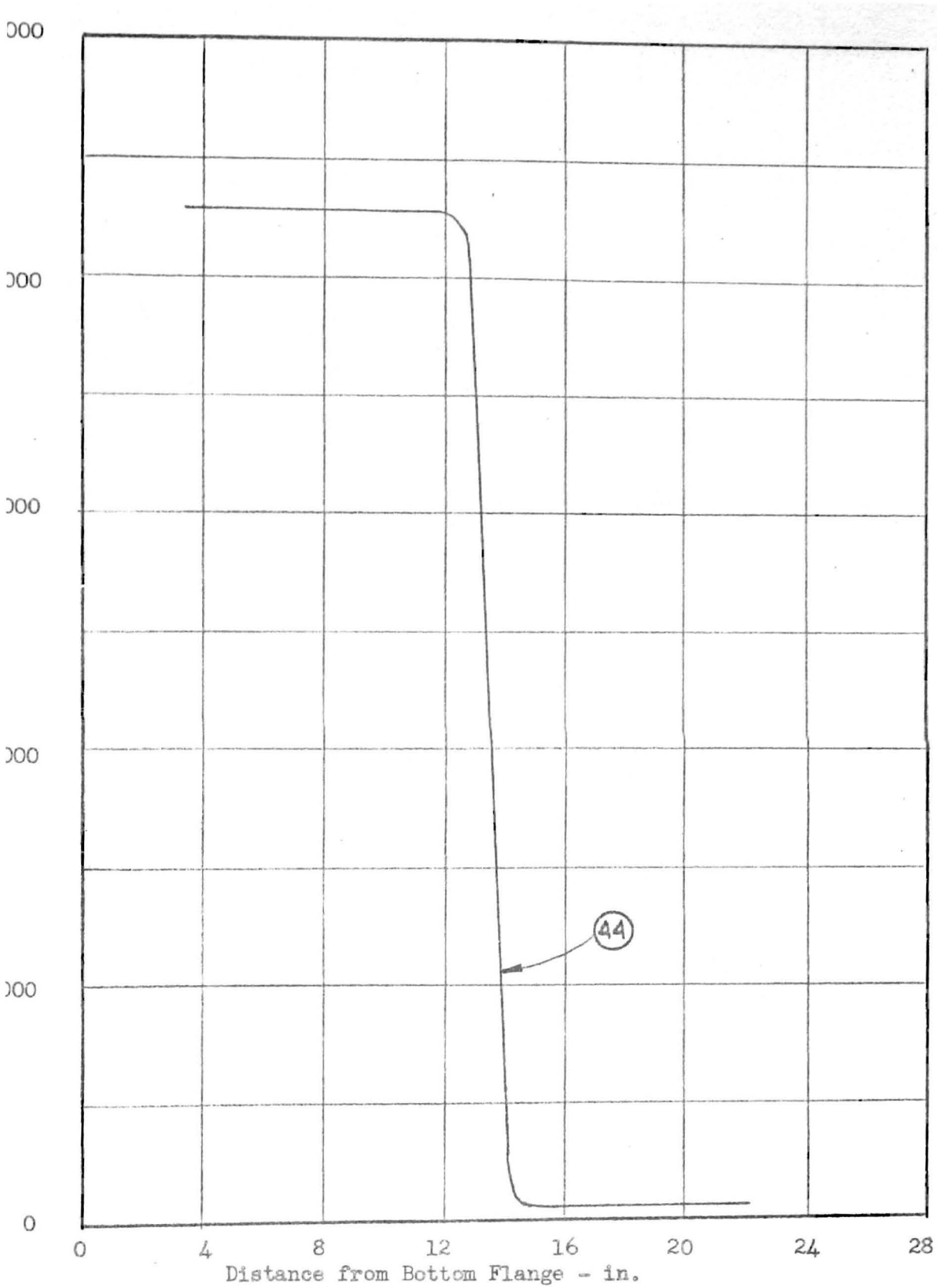

Figure 15(j). Local Heat Transfer Film Coefficients
Run 44, V_R = 0.752

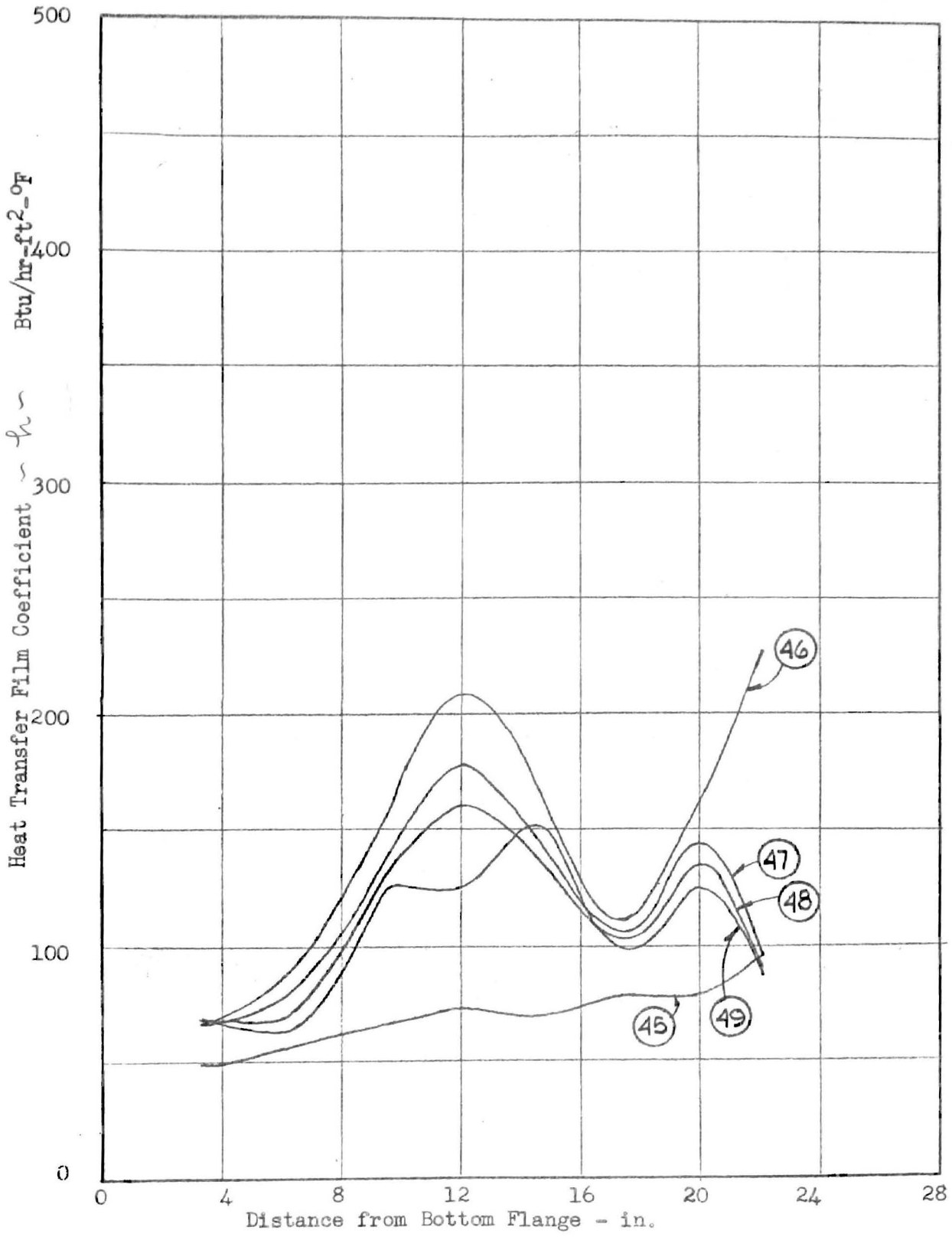

Figure 15(k). Local Heat Transfer Film Coefficients
Runs 45-49, V_R = 0.772

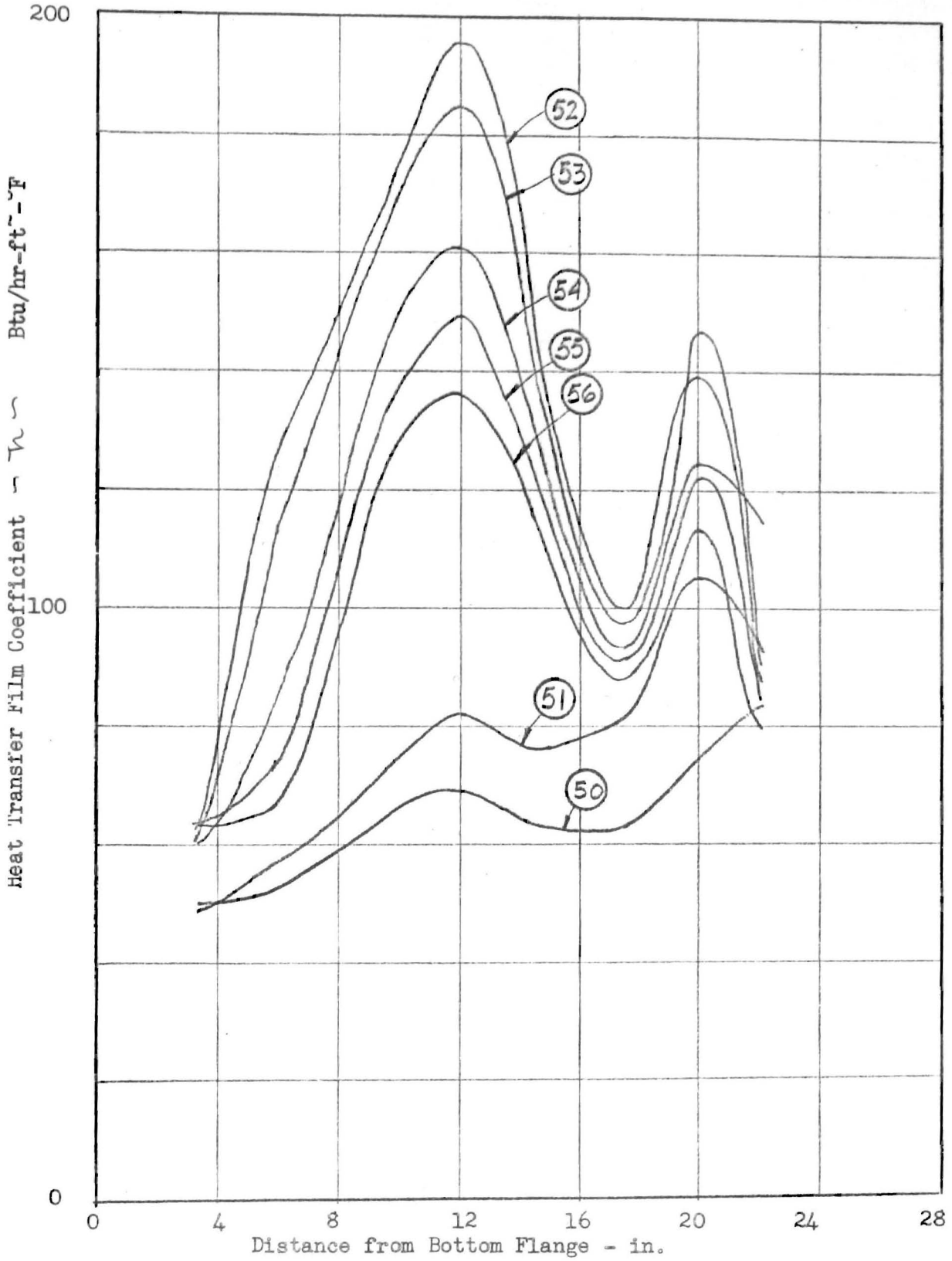

Figure 15(1). Local Heat Transfer Film Coefficients
Runs 50-56, V_R = 0.872

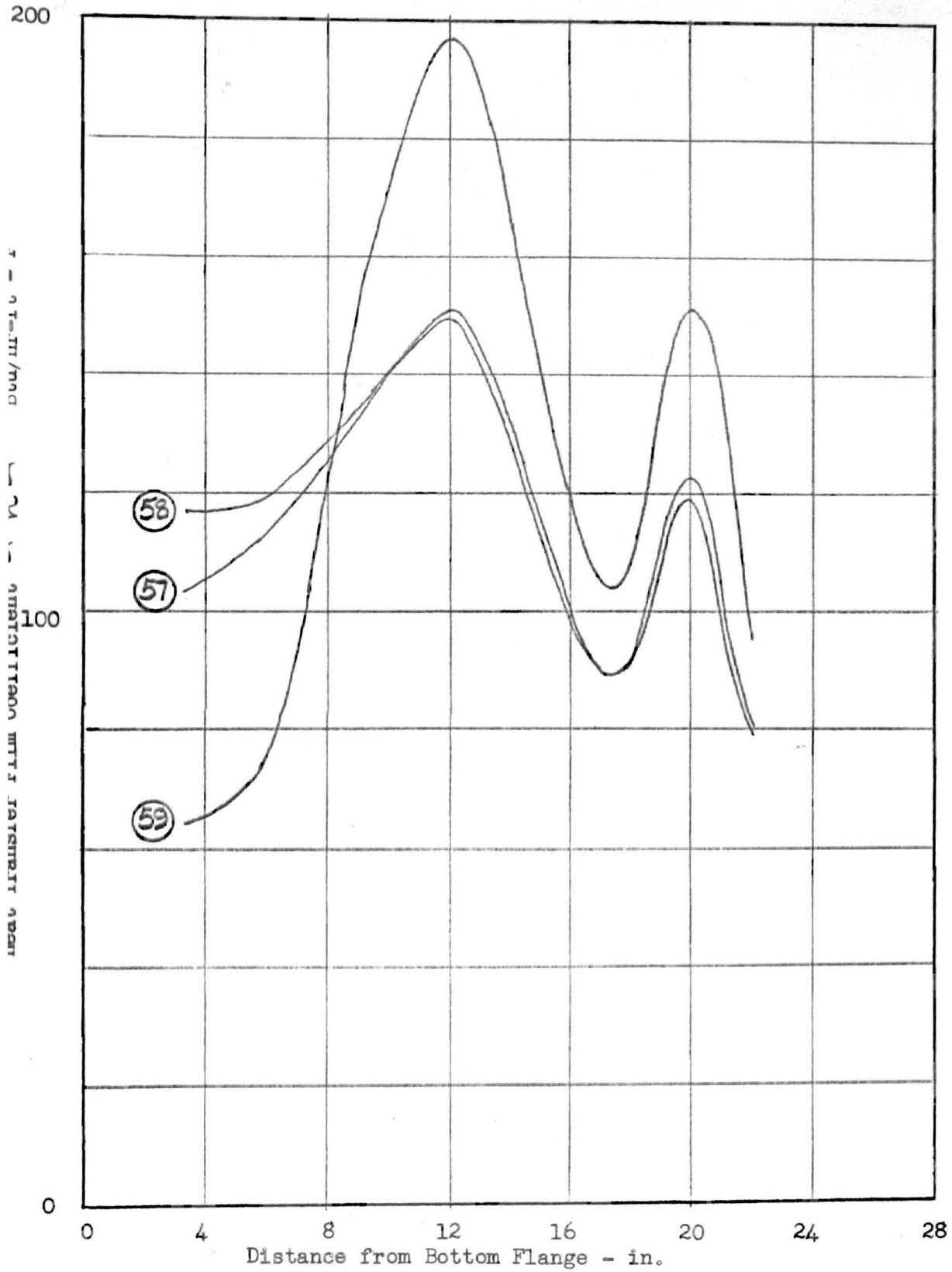

Figure 15(m). Local Heat Transfer Film Coefficients
Runs 57-59, V_R = 0.872

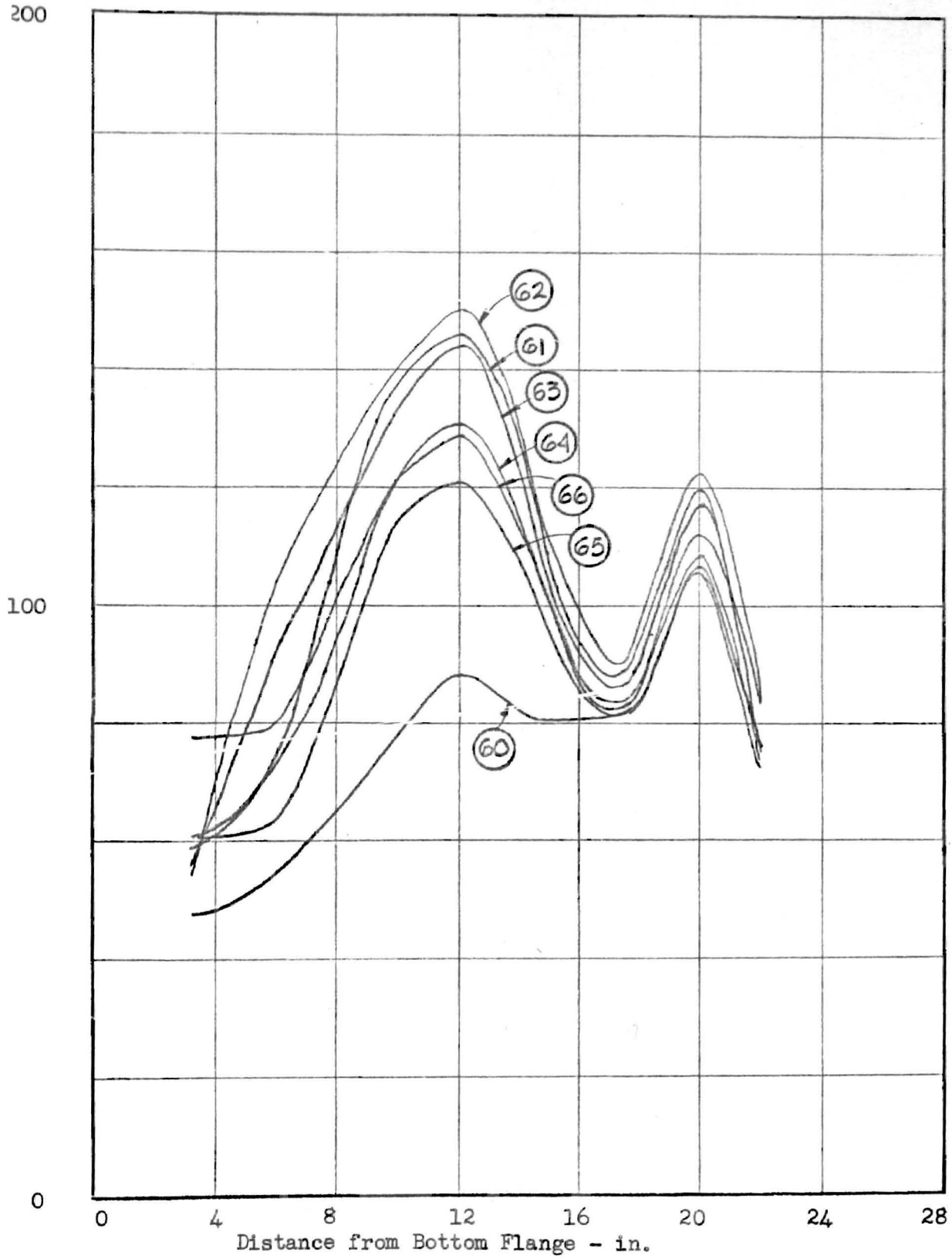

Figure 15(n). Local Heat Transfer Film Coefficients
Runs 60-66, V_R = 1.010

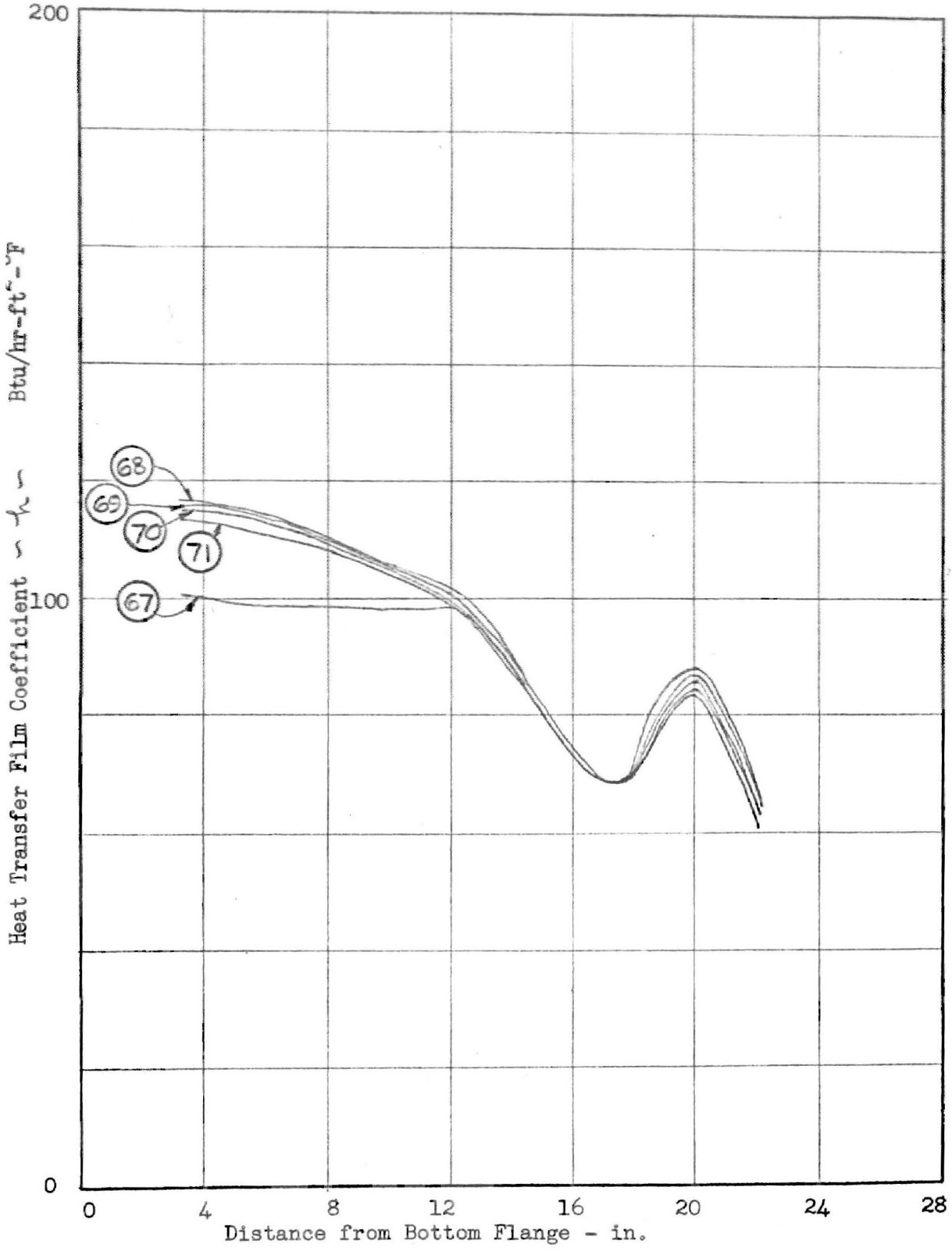

Figure 15(o). Local Heat Transfer Film Coefficients
Runs 67-71, V_R = 1.595

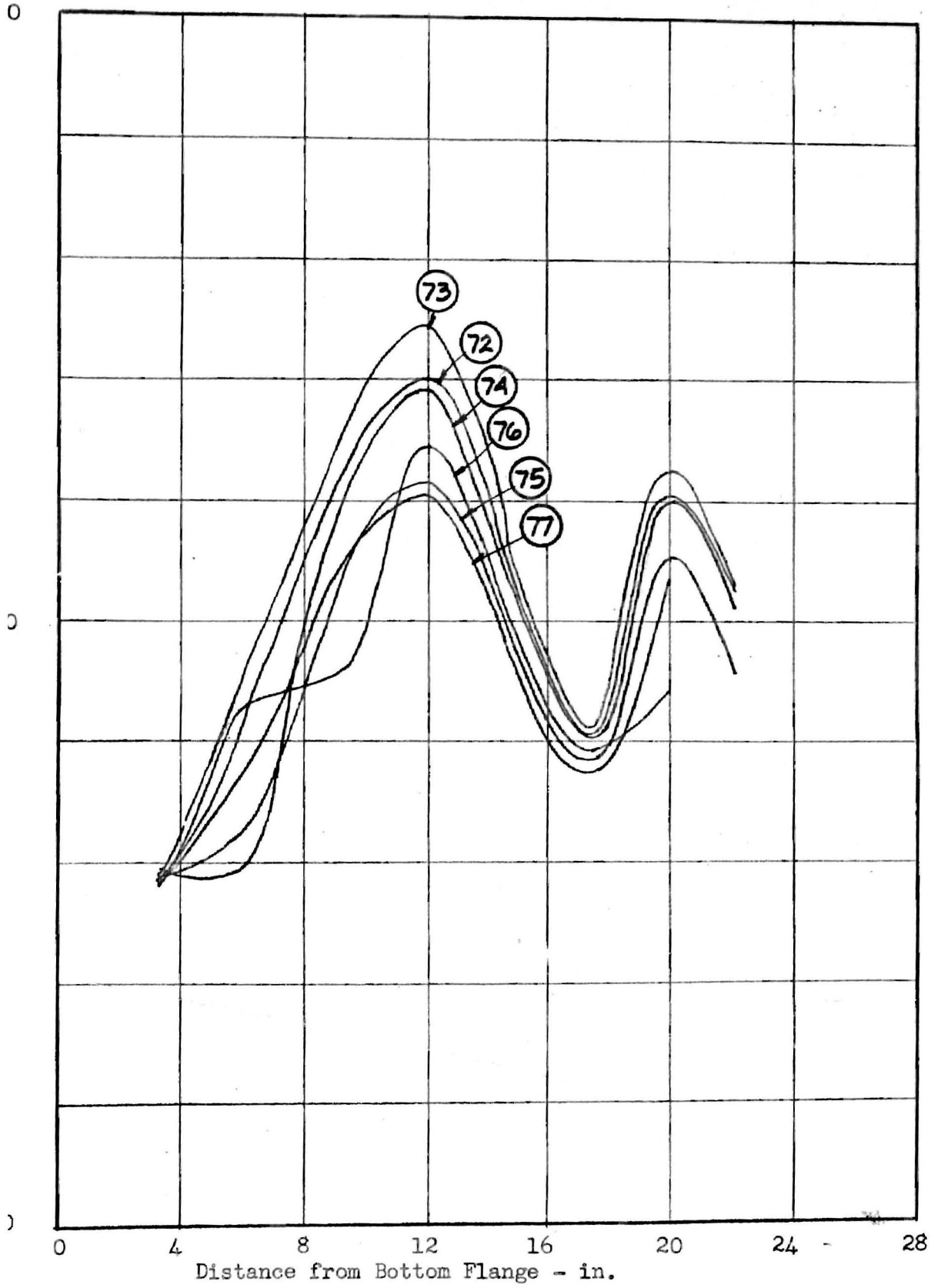

Figure 15(p). Local Heat Transfer Film Coefficients
Runs 72-77, V_R = 1.853

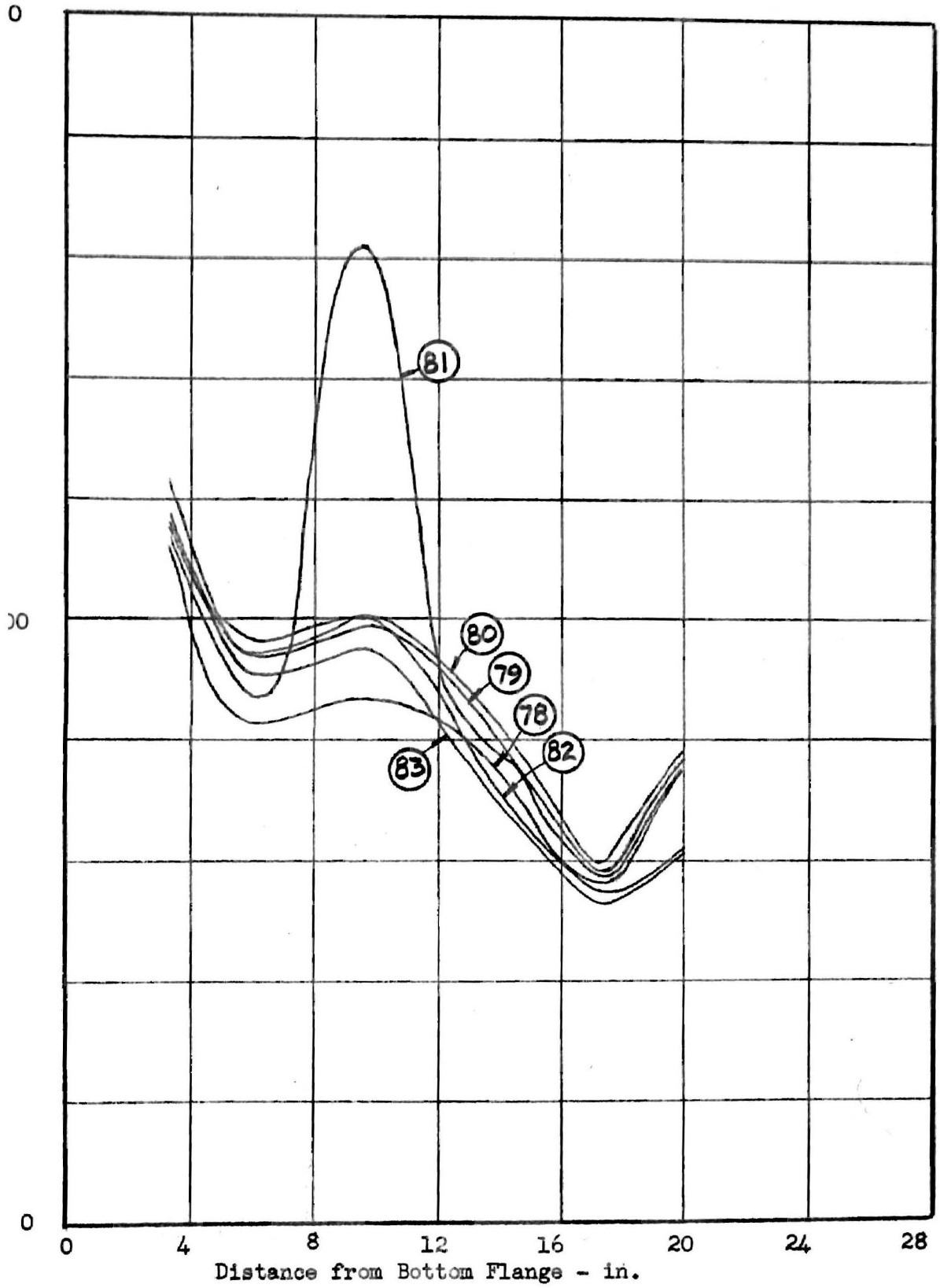

Figure 15(q). Local Heat Transfer Film Coefficients
Runs 78-83, $V_R = 2.156$

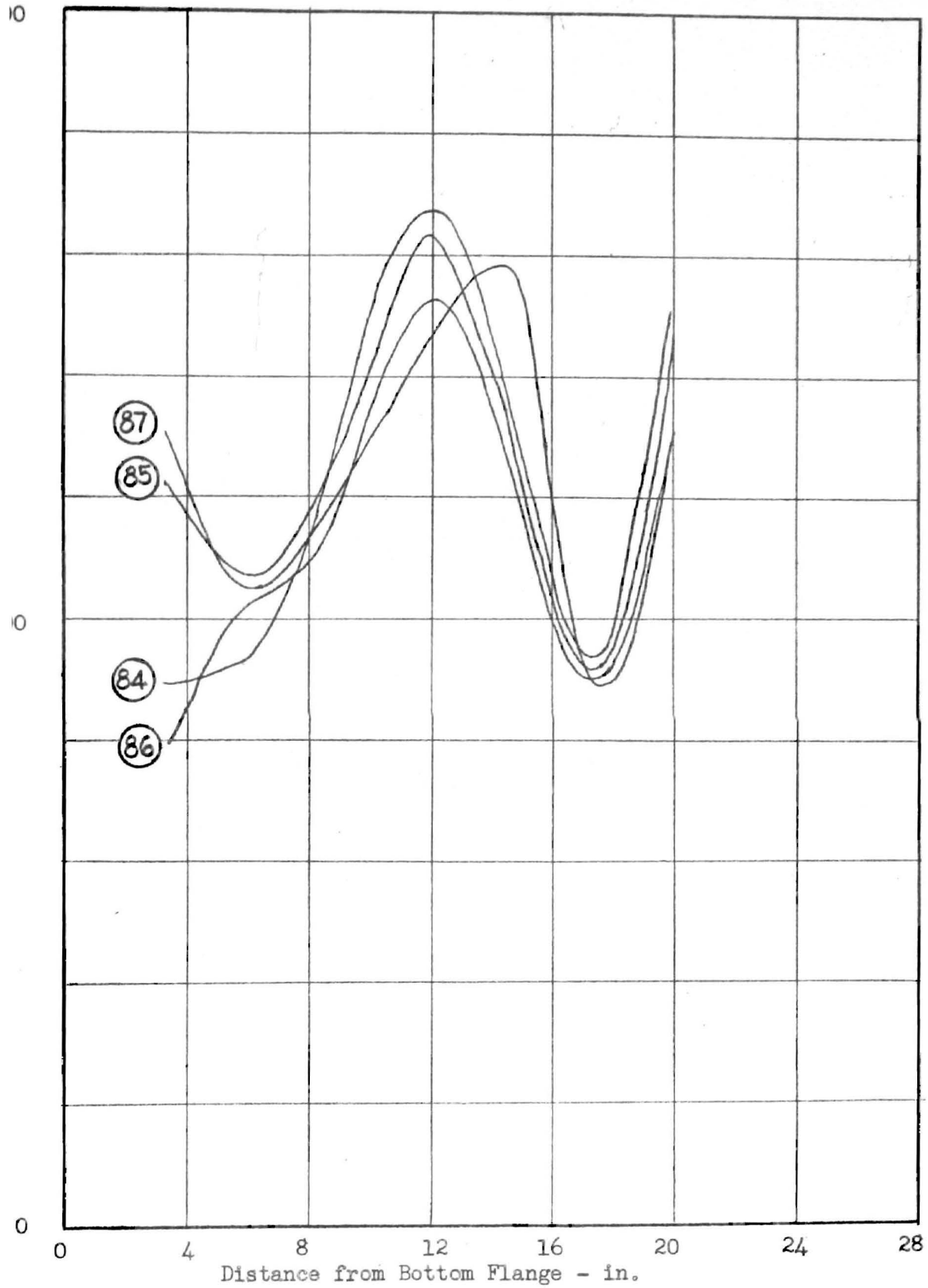

Figure 15(r). Local Heat Transfer Film Coefficients
Runs 84-87, V_R = 0.926

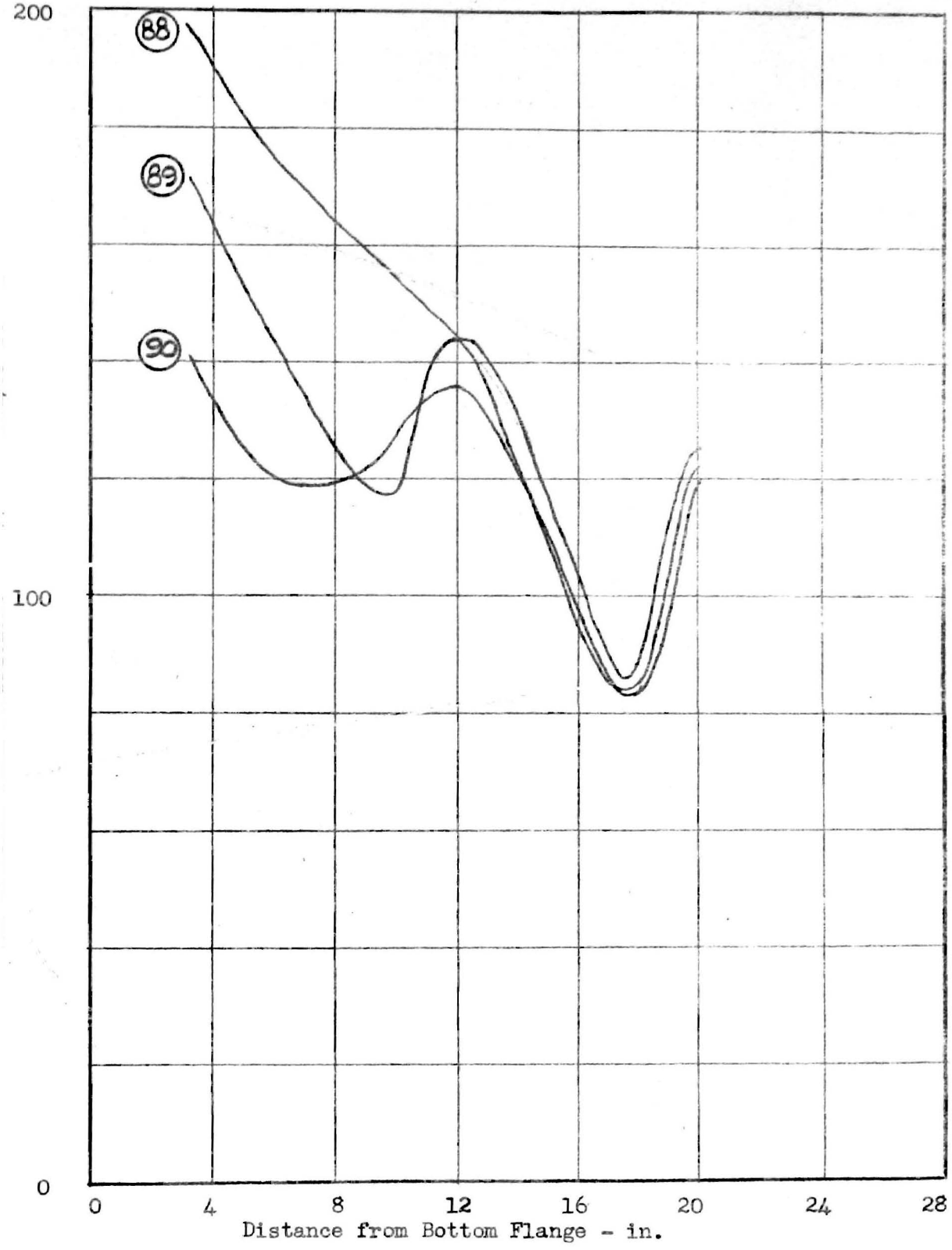

Figure 15(s). Local Heat Transfer Film Coefficients
Runs 88-91, V_R = 0.989

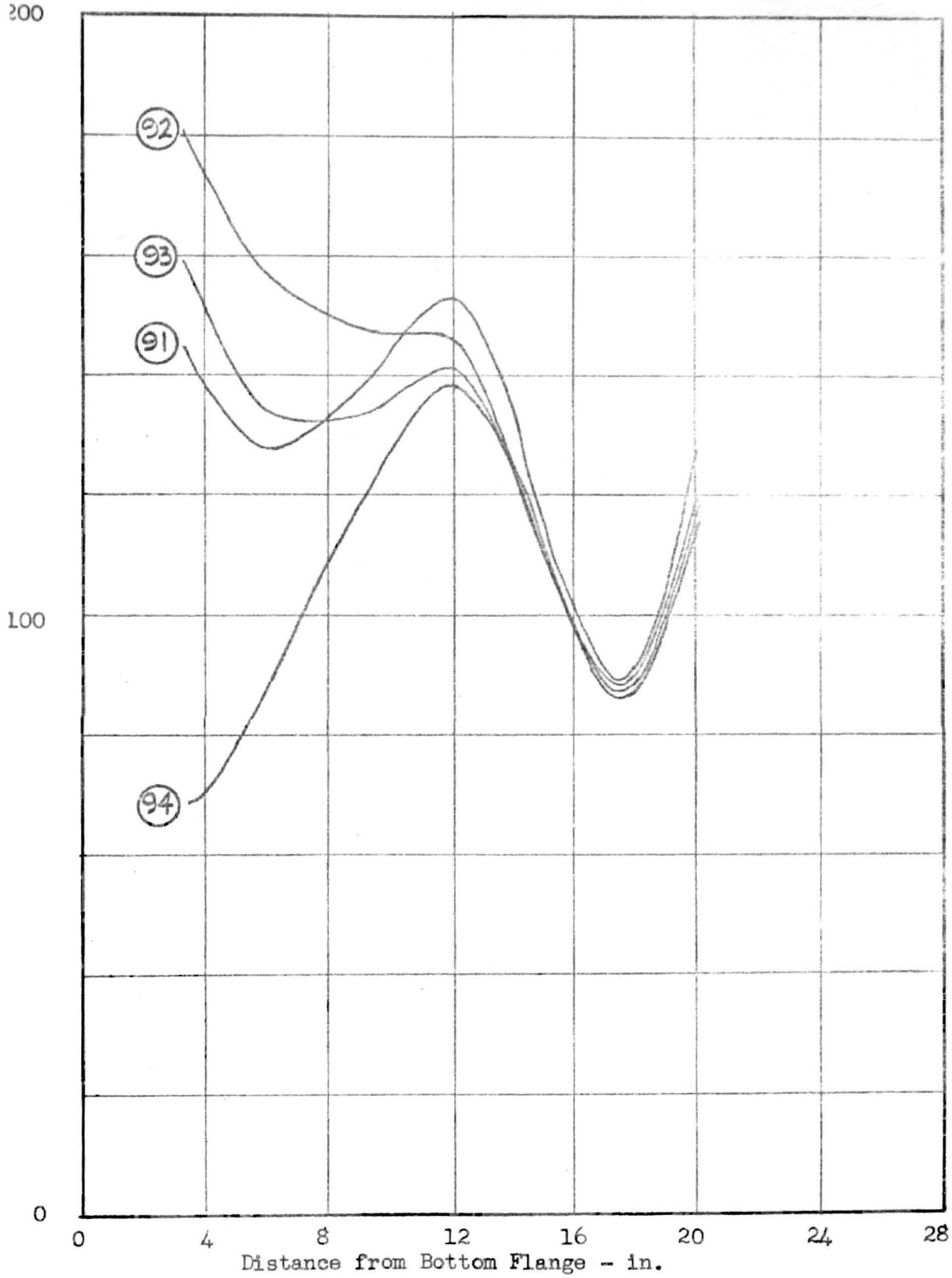

Figure 15(t). Local Heat Transfer Film Coefficients
Runs 92-94, V_R = 1.090

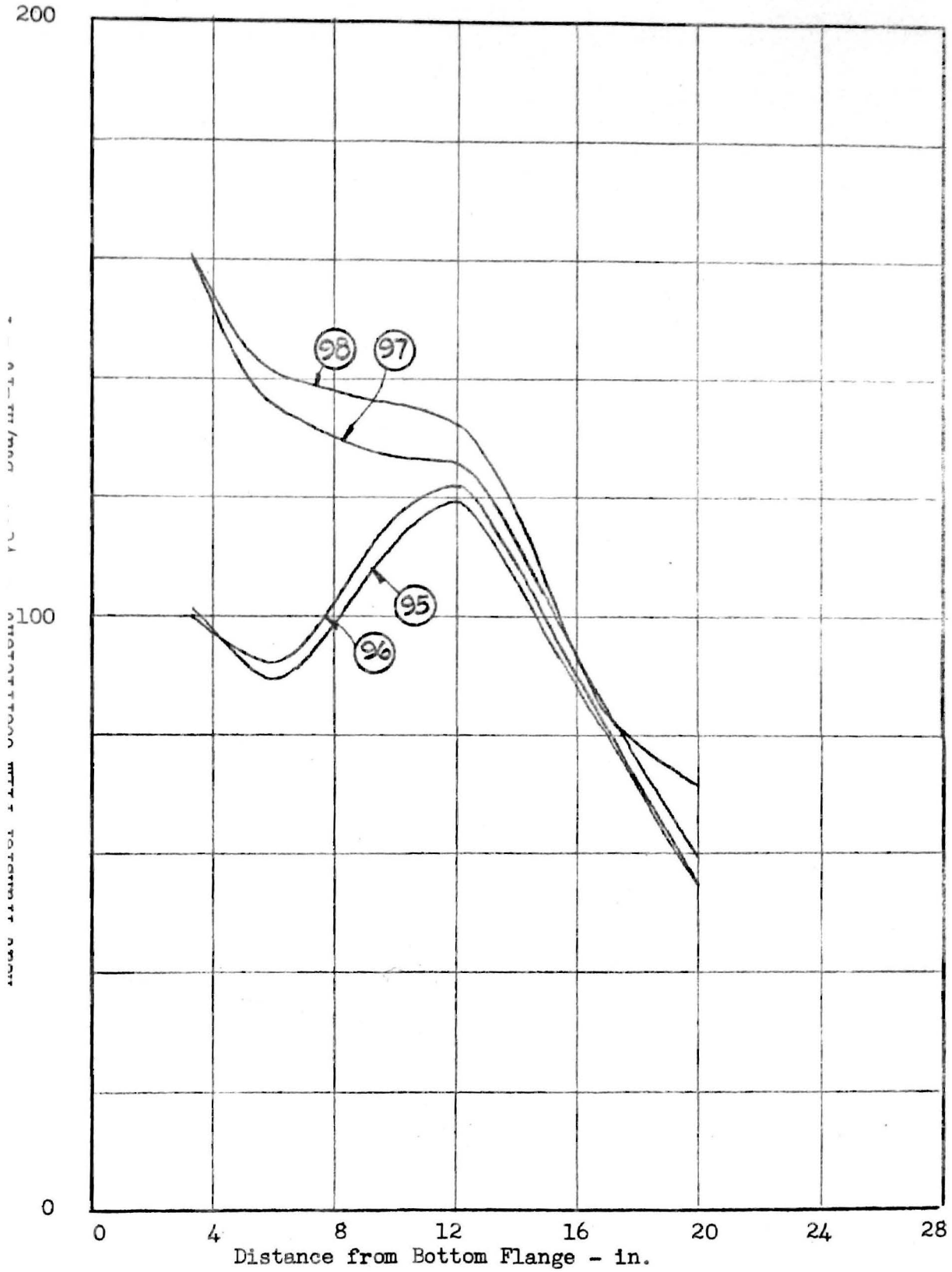

Figure 15(u). Local Heat Transfer Film Coefficients
Runs 95-98, V_R = 1.550

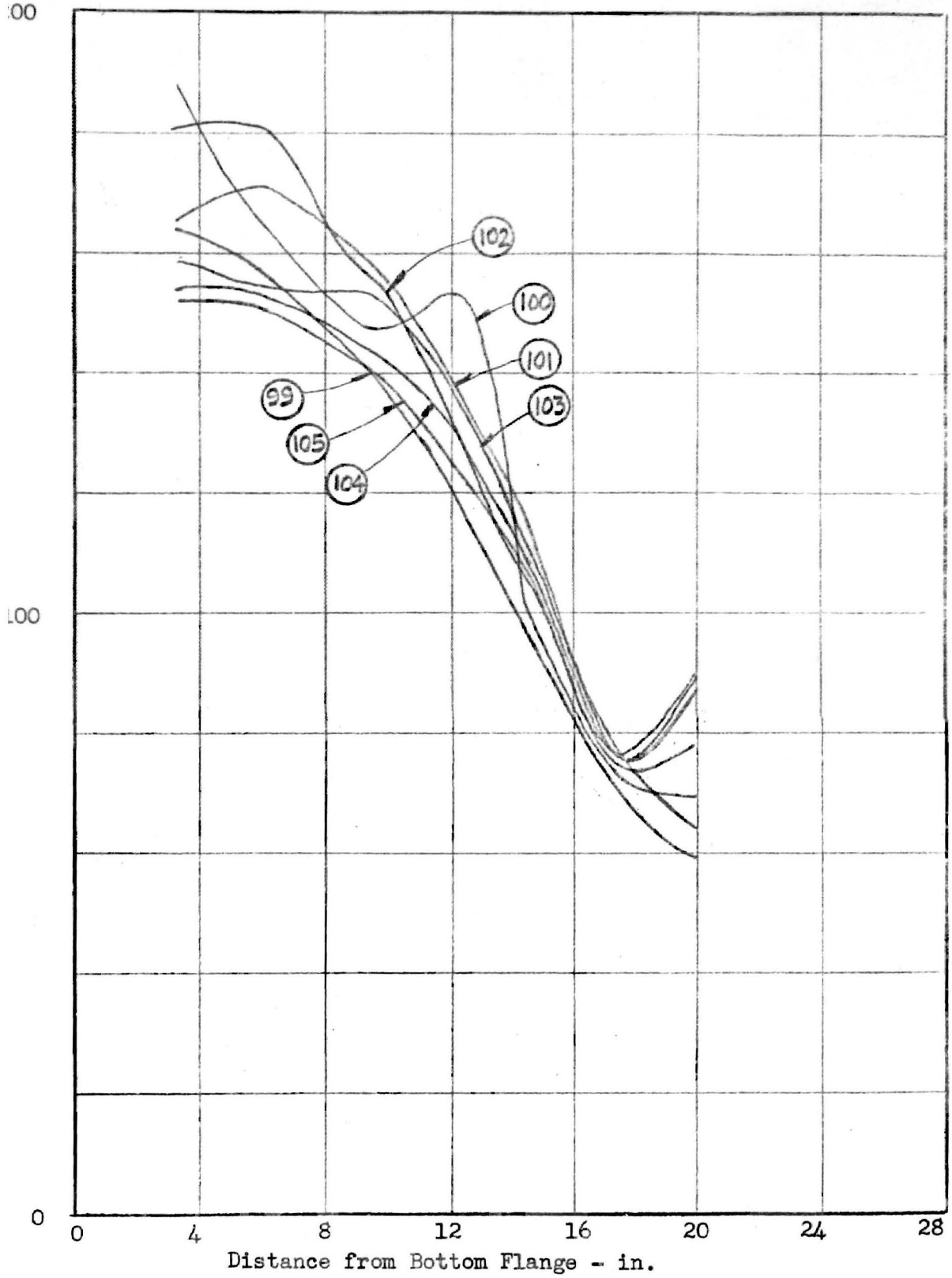

Figure 15(v). Local Heat Transfer Film Coefficients
Runs 99-105, V_R = 1.936

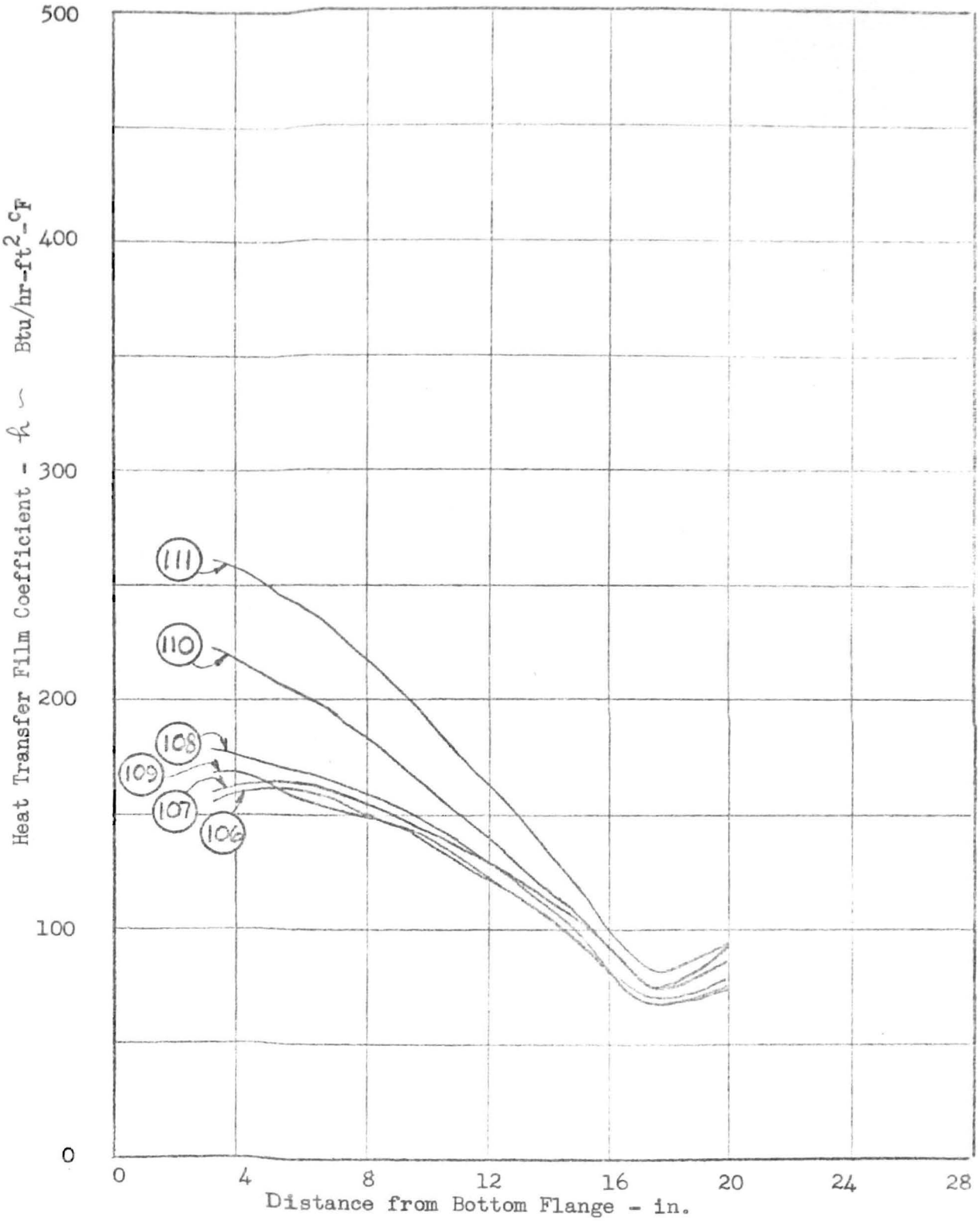

Figure 15(w). Local Heat Transfer Film Coefficients
Runs 106-111, V_R = 2.265

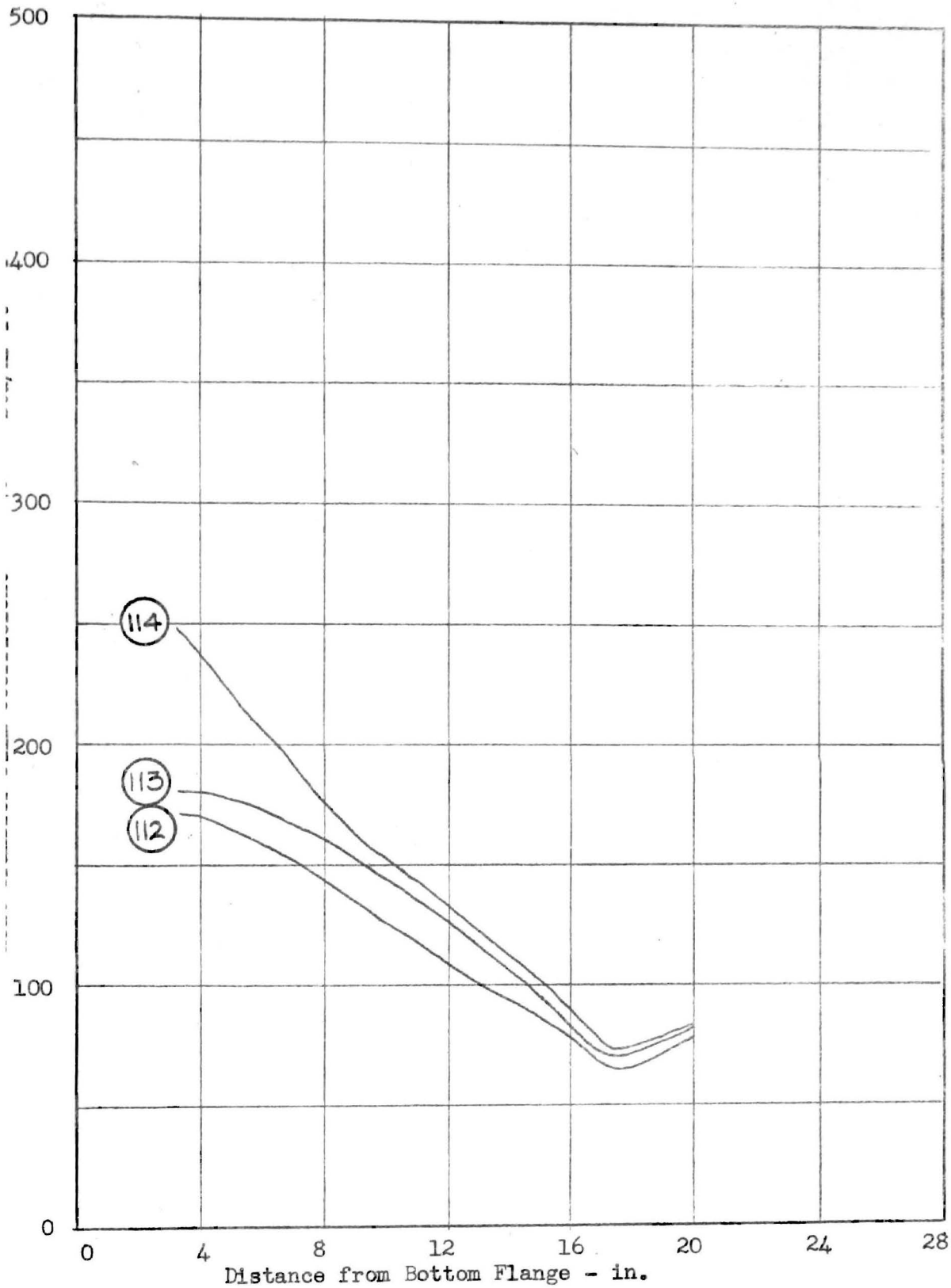

Figure 15(x). Local Heat Transfer Film Coefficients
Runs 112-114, V_R = 2.825

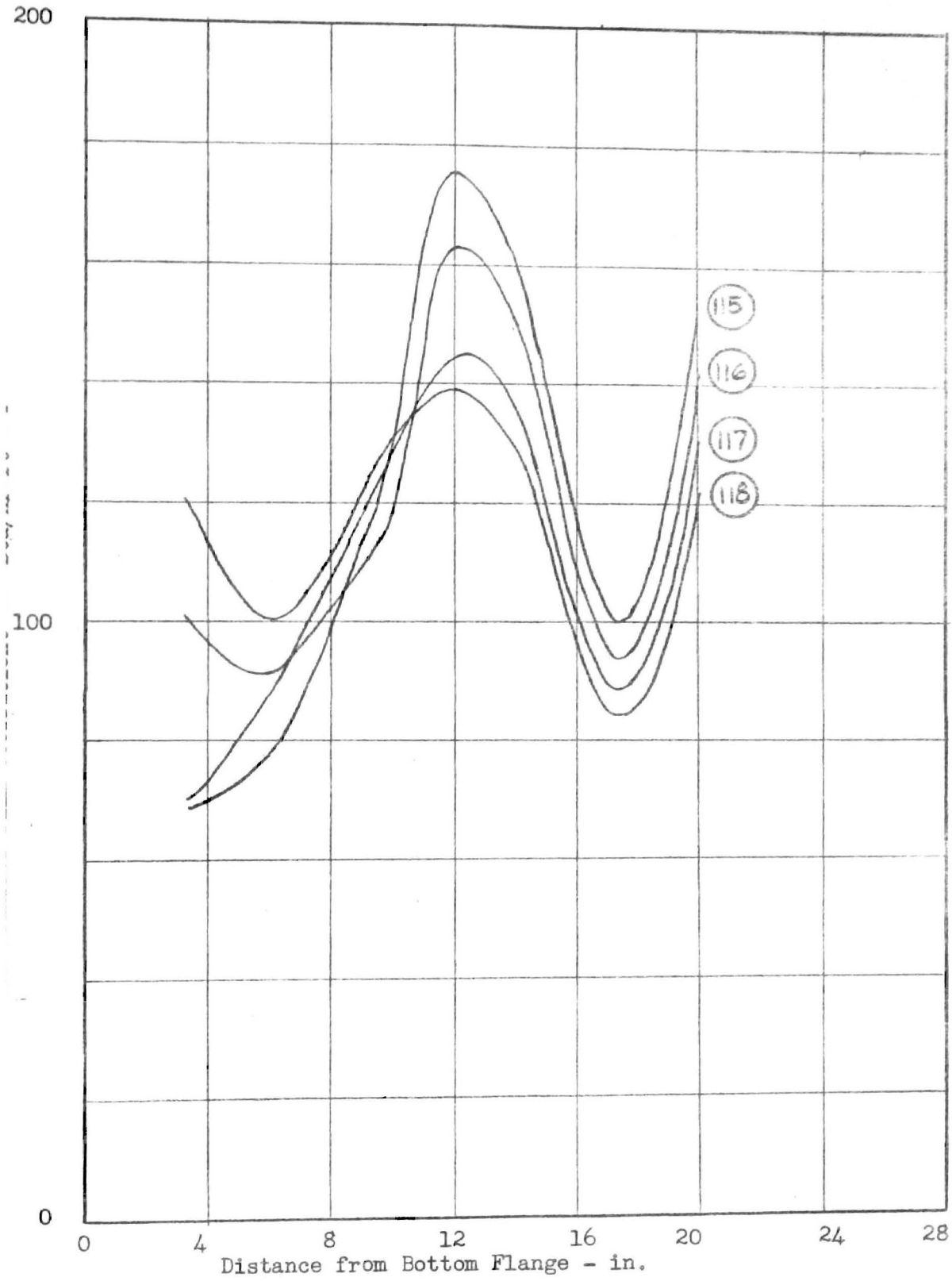

Figure 15(y). Local Heat Transfer Film Coefficients
Runs 115-118, V_R = 0.728

APPENDIX B

SOLUTIONS TO KREITH-SUMMERFIELD EQUATION

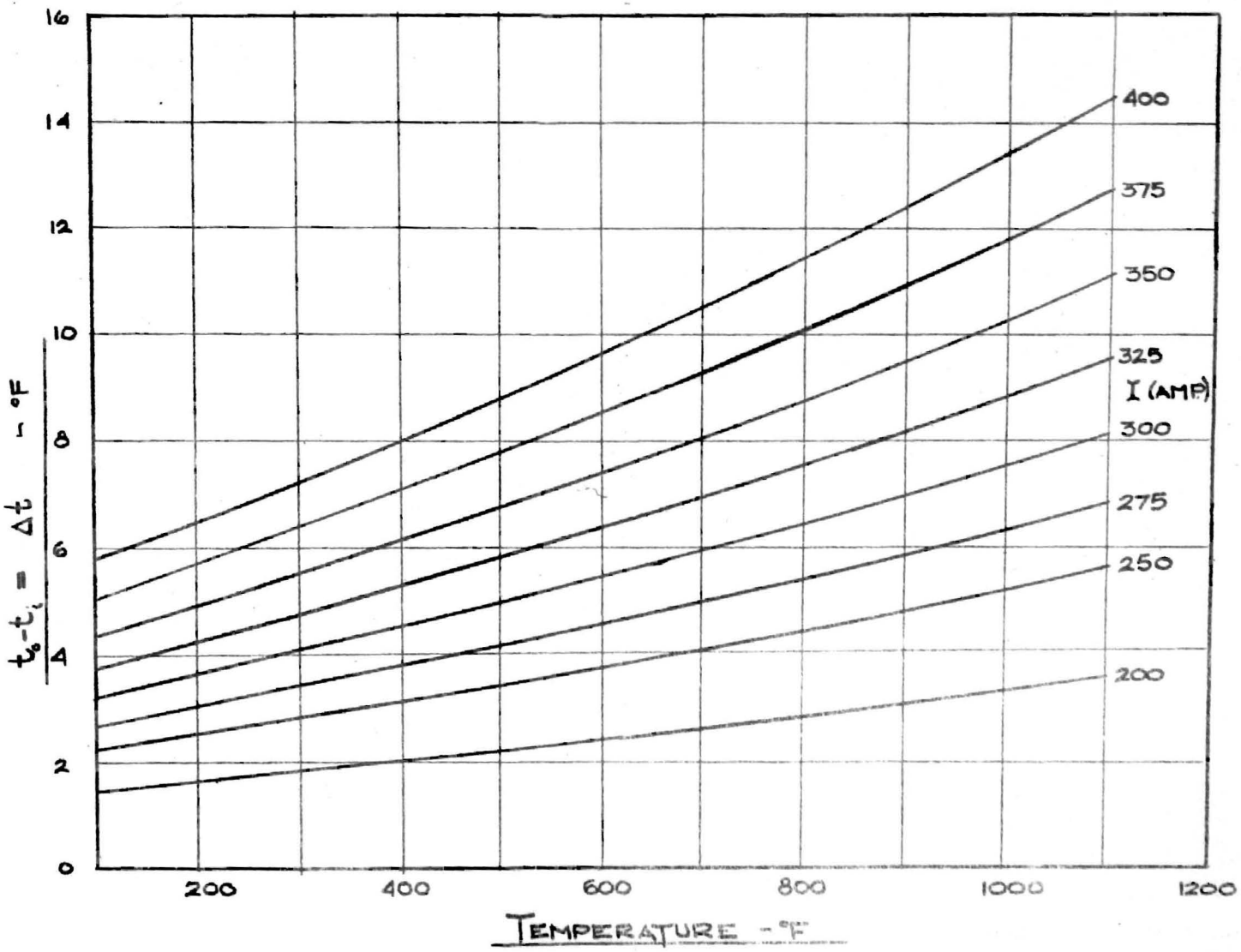

Figure 16. Solutions of Kreith-Summerfield Equation

APPENDIX C

PROPERTIES OF FREON 12

The thermodynamic and physical properties of Freon 12 were ecessary for the analysis of the experimental data. The sources of hese properties and several estimates which were made will be described n this appendix.

Eiseman, McHarness, and Martin (10) have determined the P-V-T nd caloric properties of Freon 12 and have presented an empirical quation of state for these properties. Based on their equation of tate the E.I. du Pont de Nemours Company has published tables and harts of these properties.

Using the tabulated values for the enthalpy, the values of the pecific heat at constant pressure were calculated from the relation

$$C_p \equiv \left(\frac{\partial h}{\partial T}\right)_p \simeq \left(\frac{\Delta h}{\Delta T}\right)_p . \qquad C-1$$

he results of these calculations are shown in Figures 17 and 18. sing the tabulated values for the specific volume, the values of the olume coefficient of expansion were calculated from the relation

$$\beta \equiv \frac{1}{v}\left(\frac{\partial v}{\partial T}\right)_p \simeq \frac{1}{v_{avg}}\left(\frac{\Delta v}{\Delta T}\right)_p . \qquad C-2$$

he results of these calculations are shown in Figures 19 and 20.

Lenoir (11) has presented the thermal conductivity values for reon 12 at one atmosphere and Benning and Markwood (12) present the

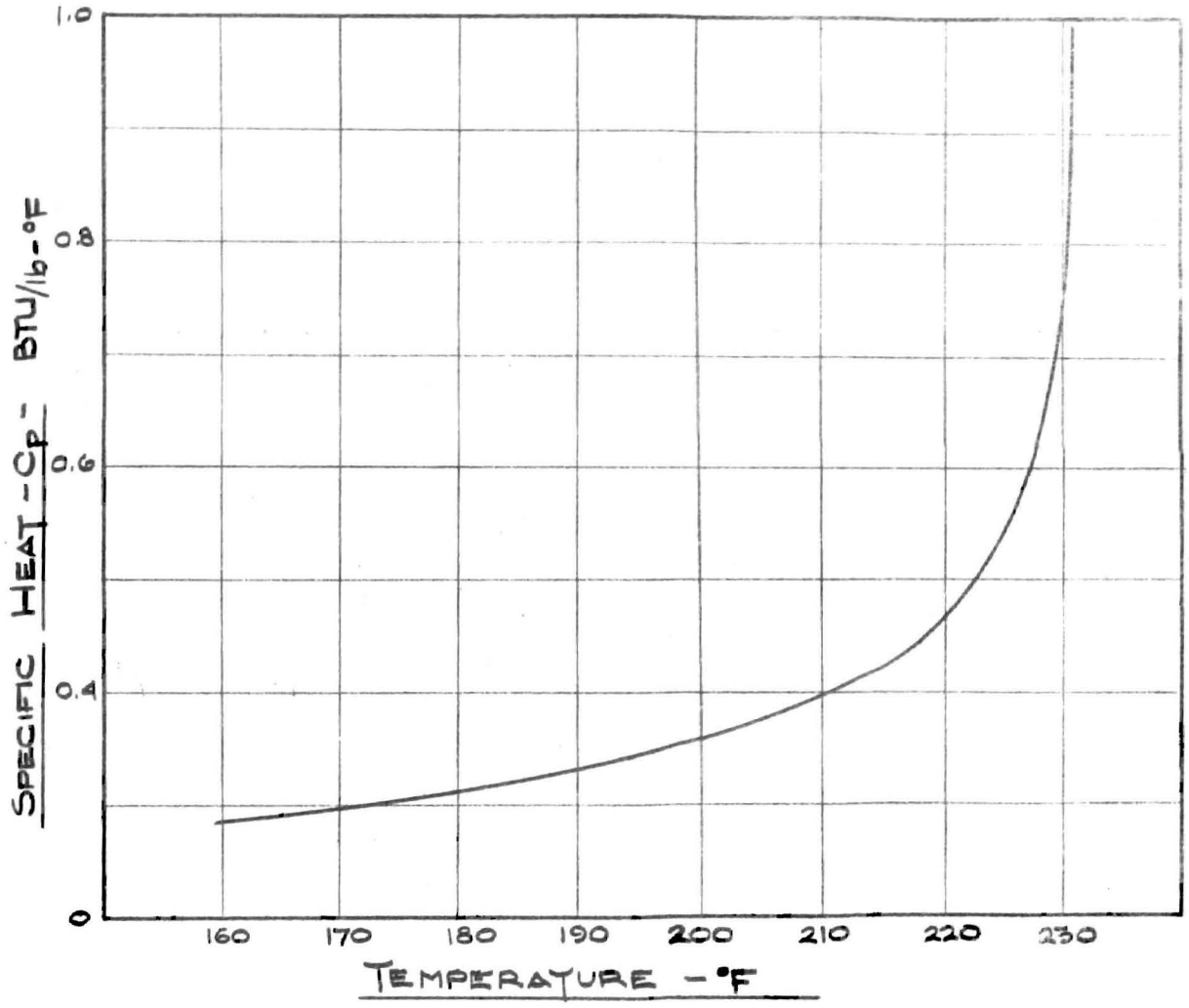

Figure 17. Specific Heat of Saturated Liquid Freon 12

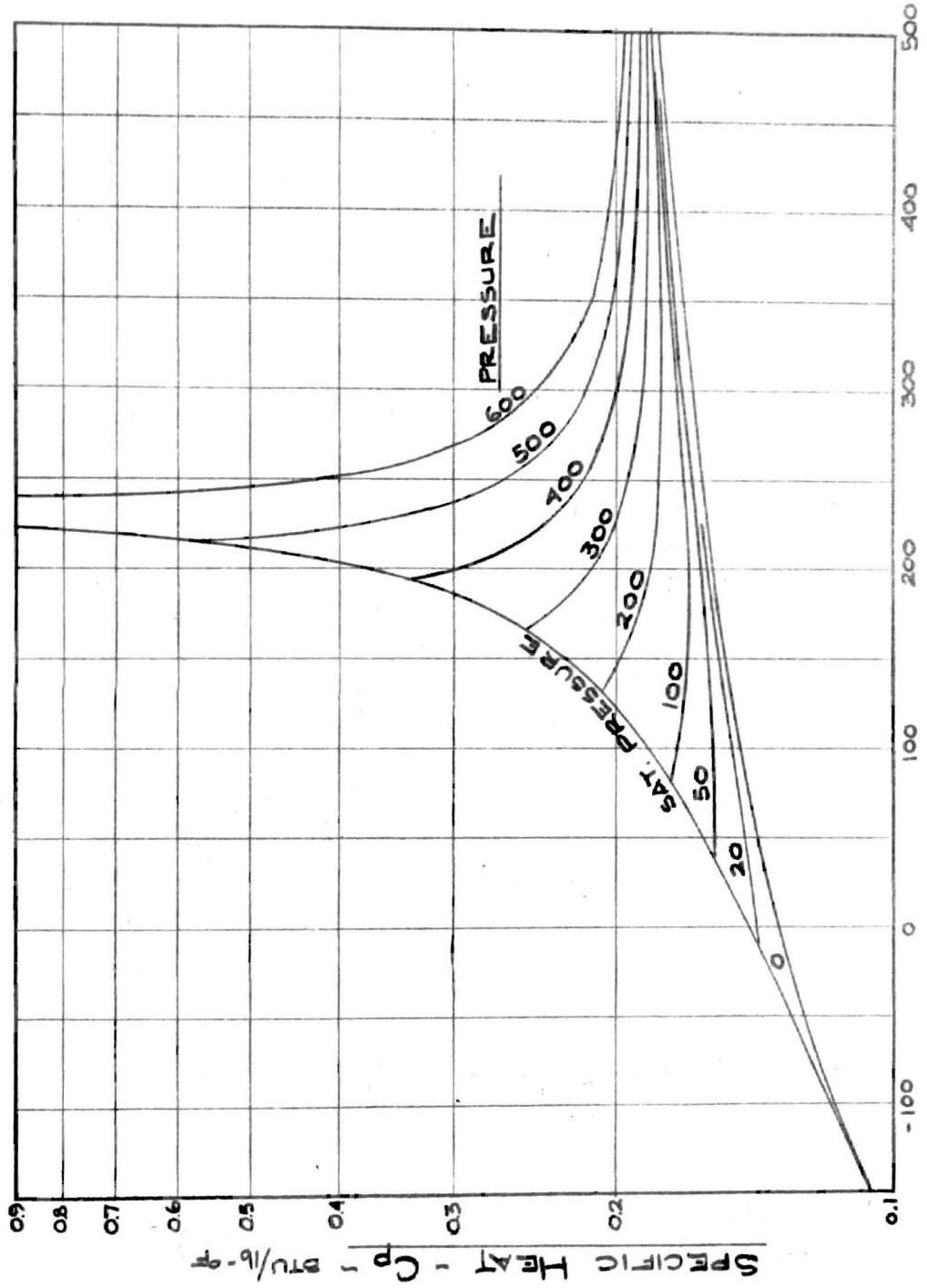

Figure 18. Specific Heat of Superheated Vapor Freon 12

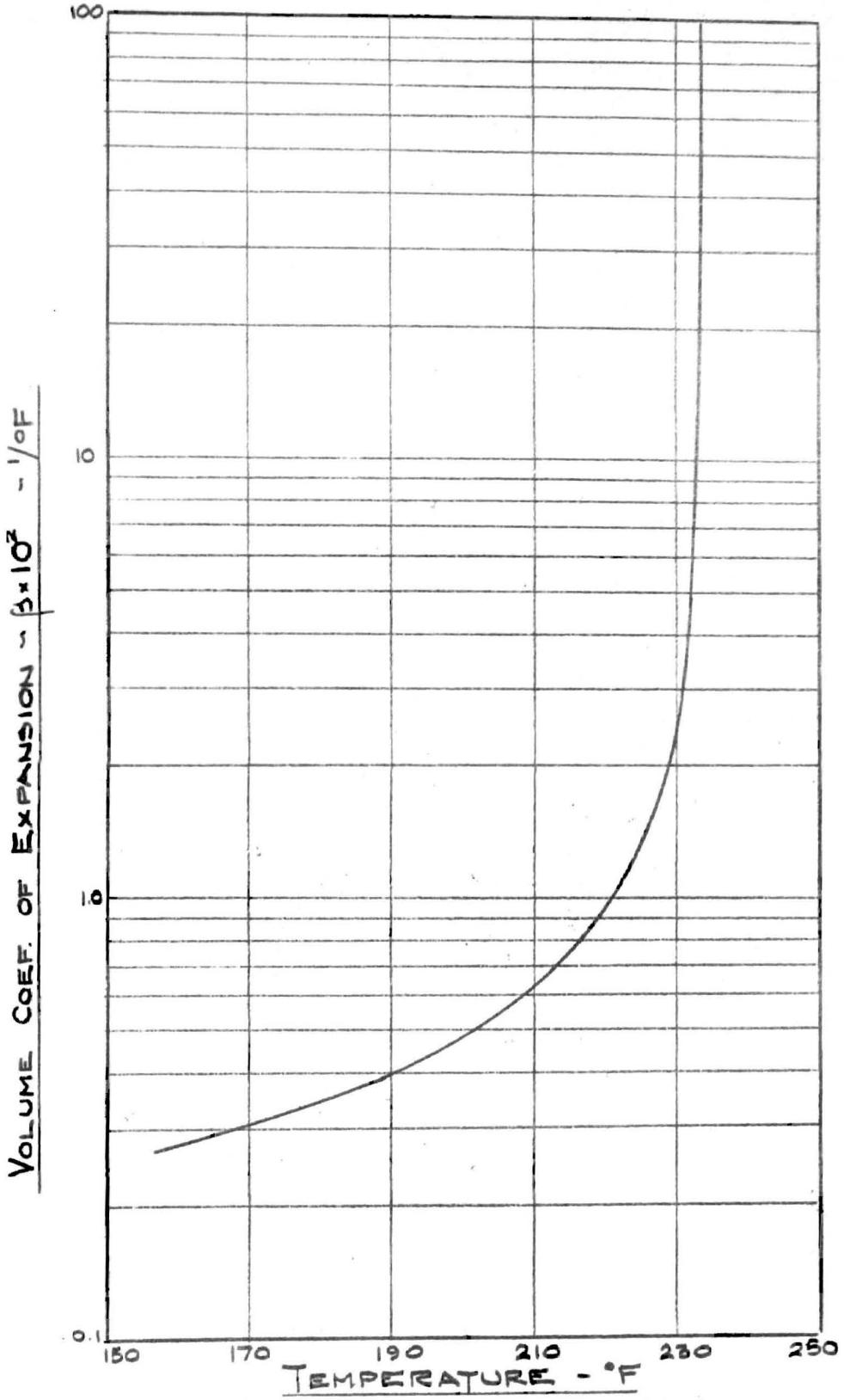

Figure 19. Volume Coefficient of Expansion of Saturated Liquid Freon 12

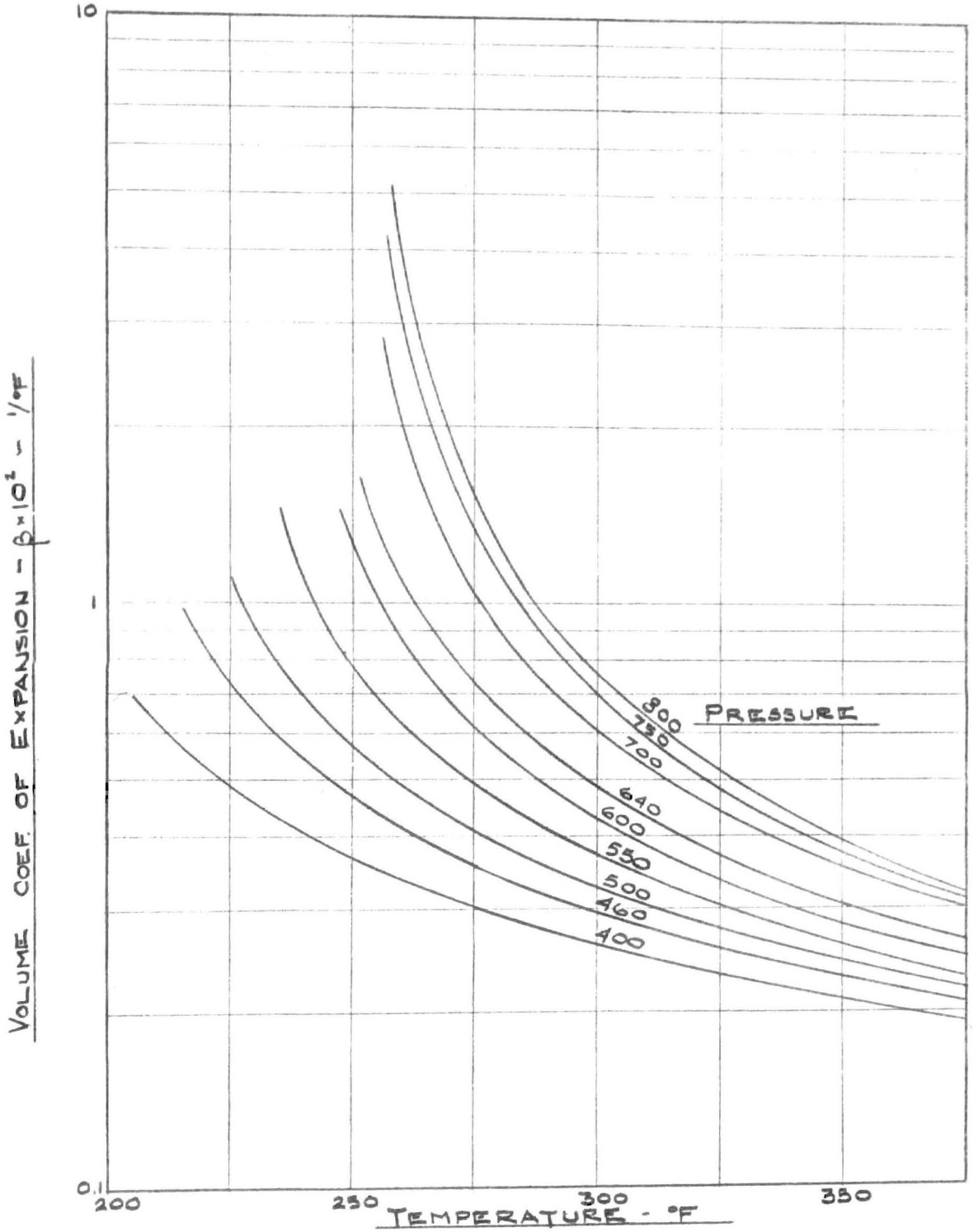

ure 20. Volume Coefficient of Expansion for Superheated Vapor Freon 12

thermal conductivity for Freon 12 at the saturated liquid conditions. The thermal conductivity values for the supercritical regions were calculated on the basis of the generalized correlation of thermal conductivity for gases presented by Comings and Nathan (7). The result of these calculations are shown in Figure 23.

Markwood and Benning (13) have presented the viscosity for Freon 1 at one atmosphere and for the saturated liquid. The viscosity for the supercritical regions was calculated on the basis of the generalized correlation of viscosity for gases presented by Comings and Egly (6). The results of these calculations are shown in Figure 26.

It must be noted that the calculations based on the generalized correlations could be in error by twenty percent in the supercritical regions. An error of one hundred percent could easily be present in the critical region. Therefore, the usefulness of these generalized correlations lies primarily in their consistency and not in their accuracy. The present writer has always felt that an estimate of this sort is better than nothing at all.

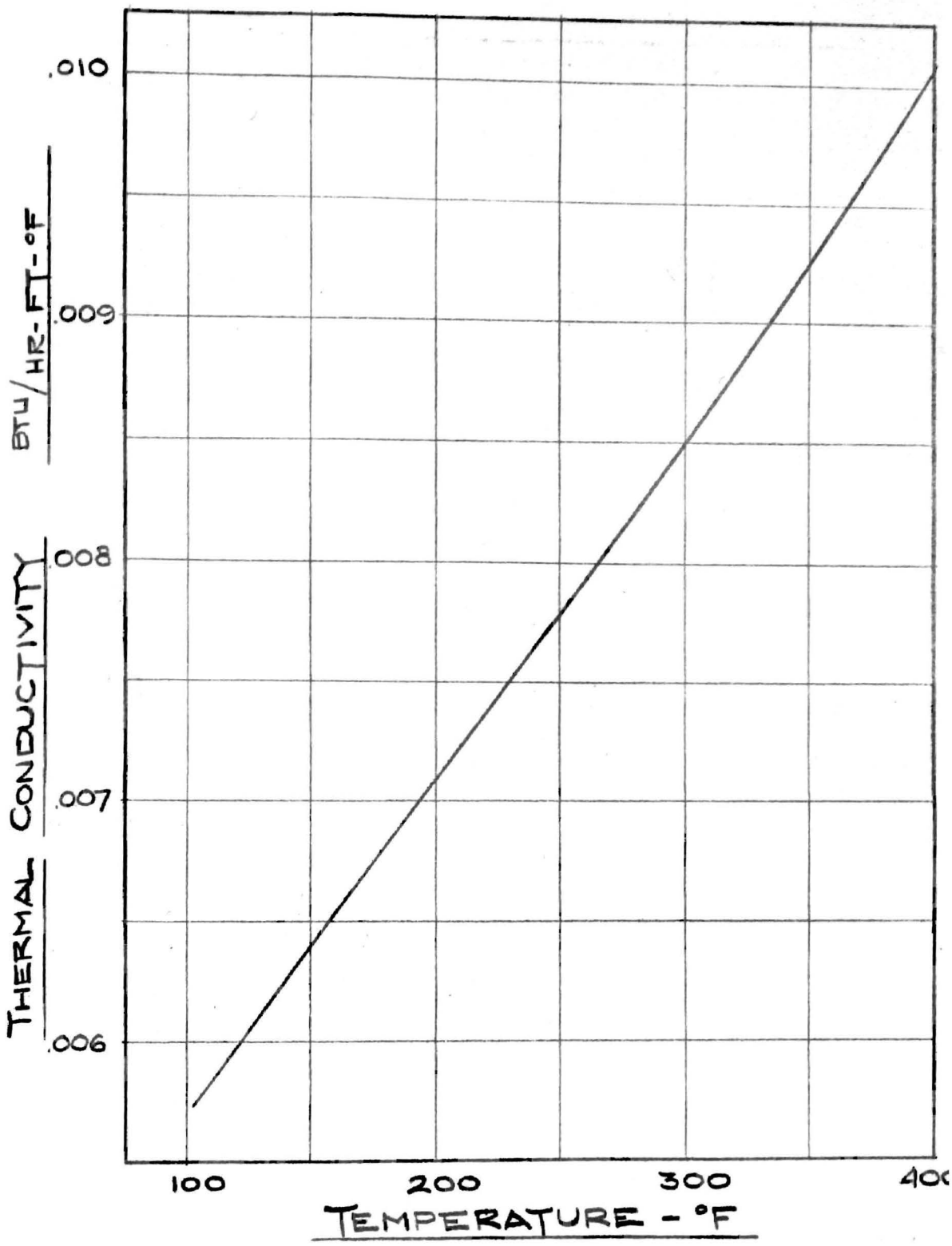

Figure 21. Thermal Conductivity at One Atmosphere for Freon 12, from Lenoir (11)

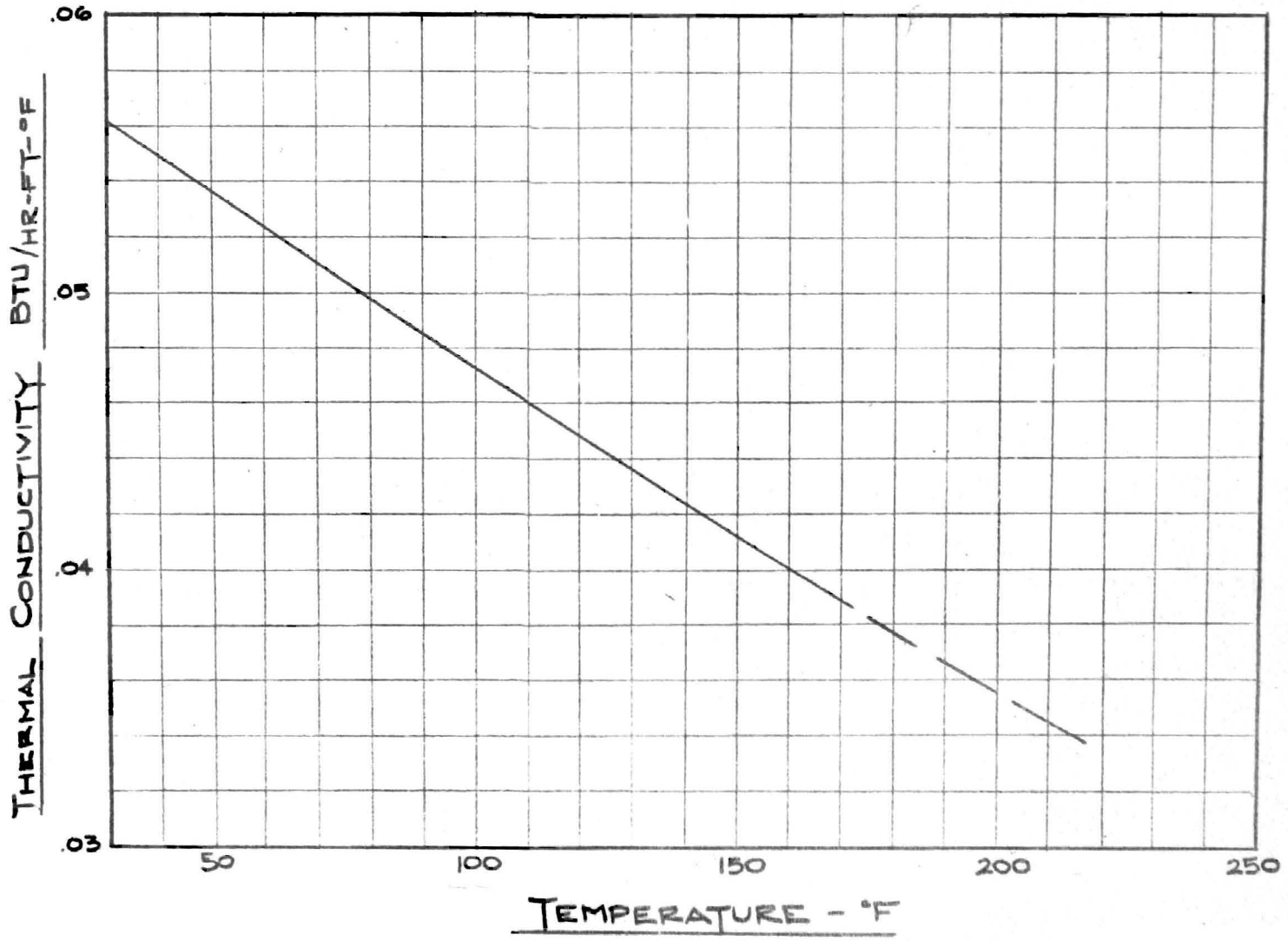

Figure 22. Thermal Conductivity for Liquid Freon 12, from Benning and Markwood (12)

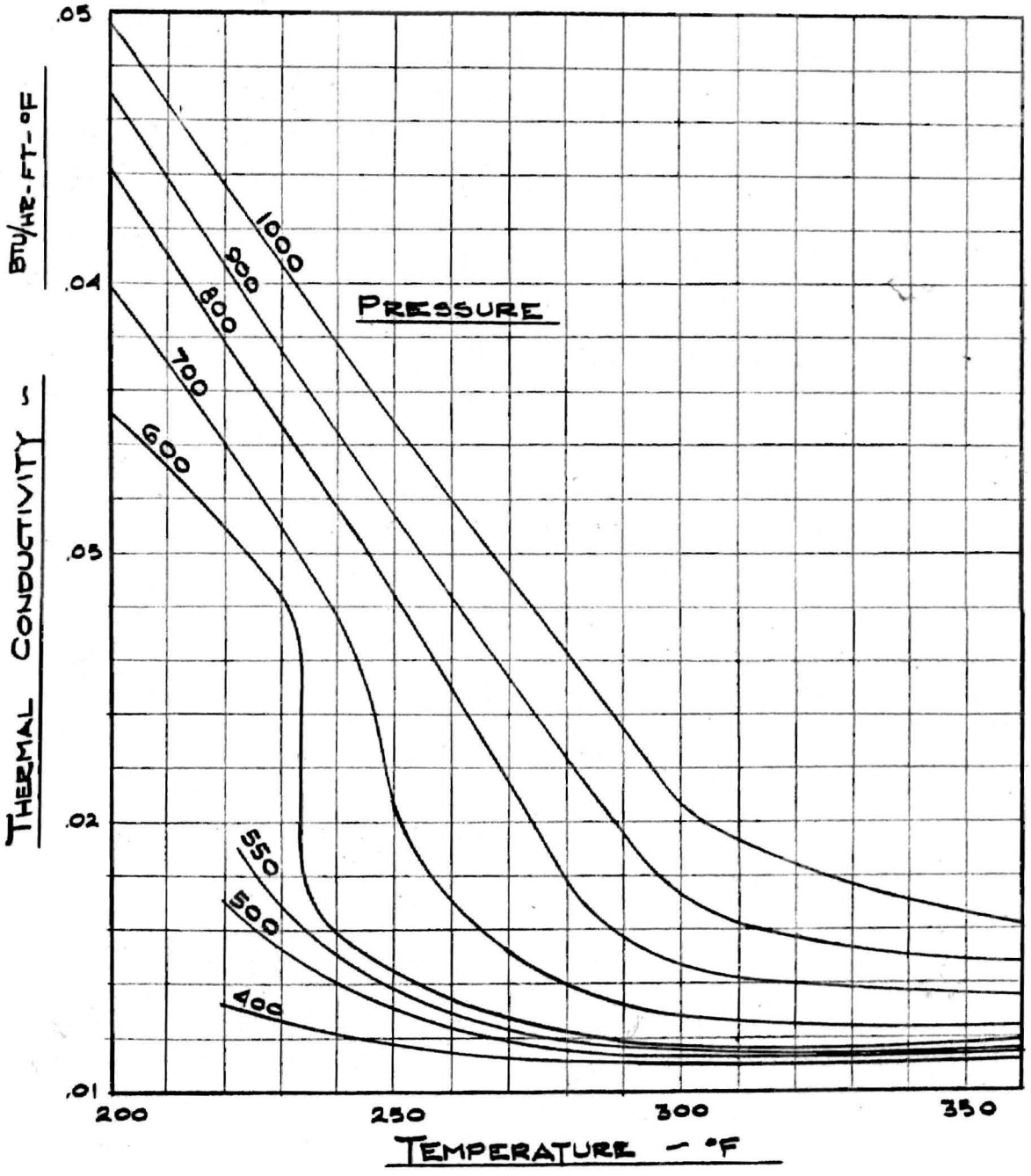

Figure 23. Estimated Thermal Conductivity for Superheated Freon 12

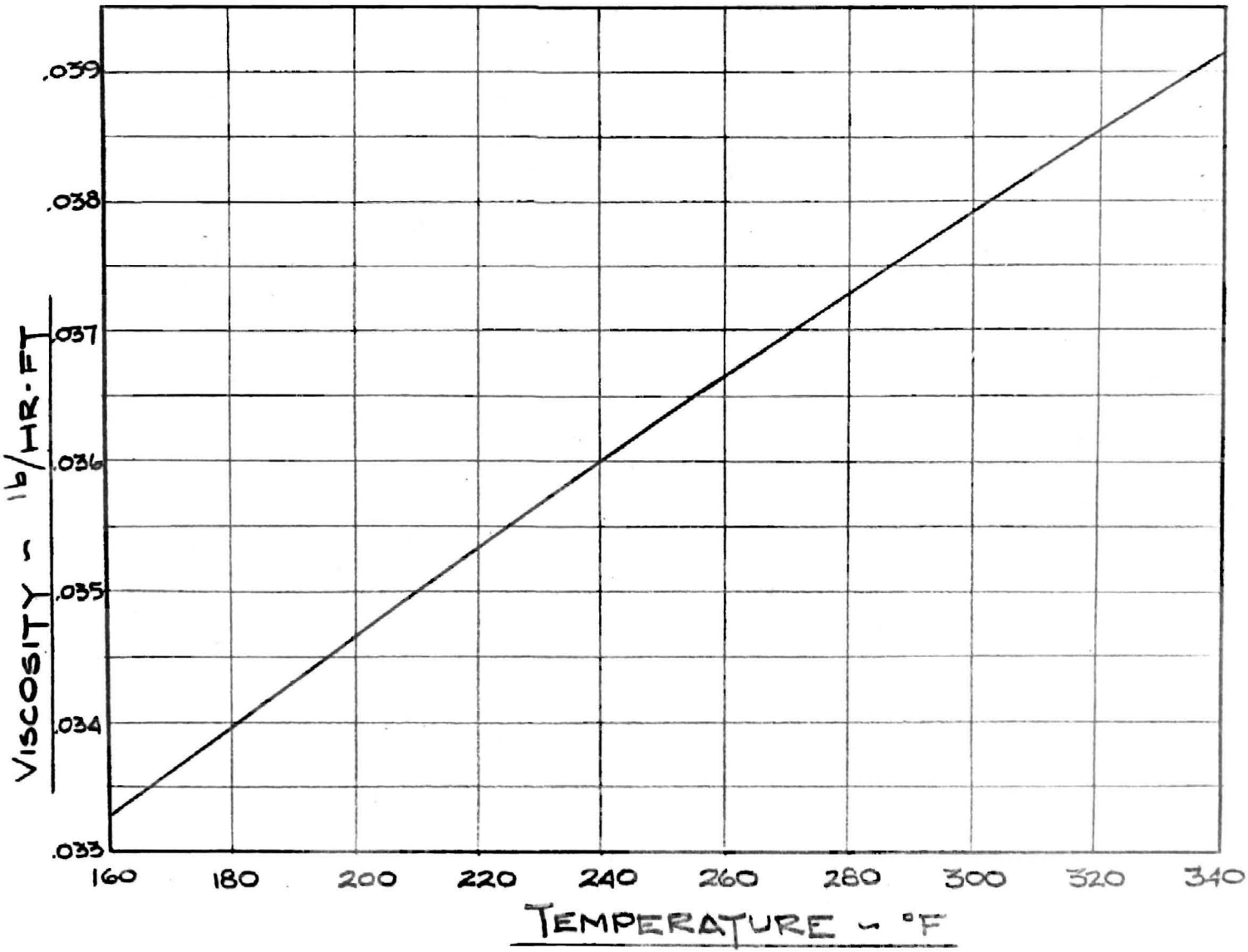

Figure 24. Viscosity of Freon 12 at One Atmosphere, from Benning and Markwood (13)

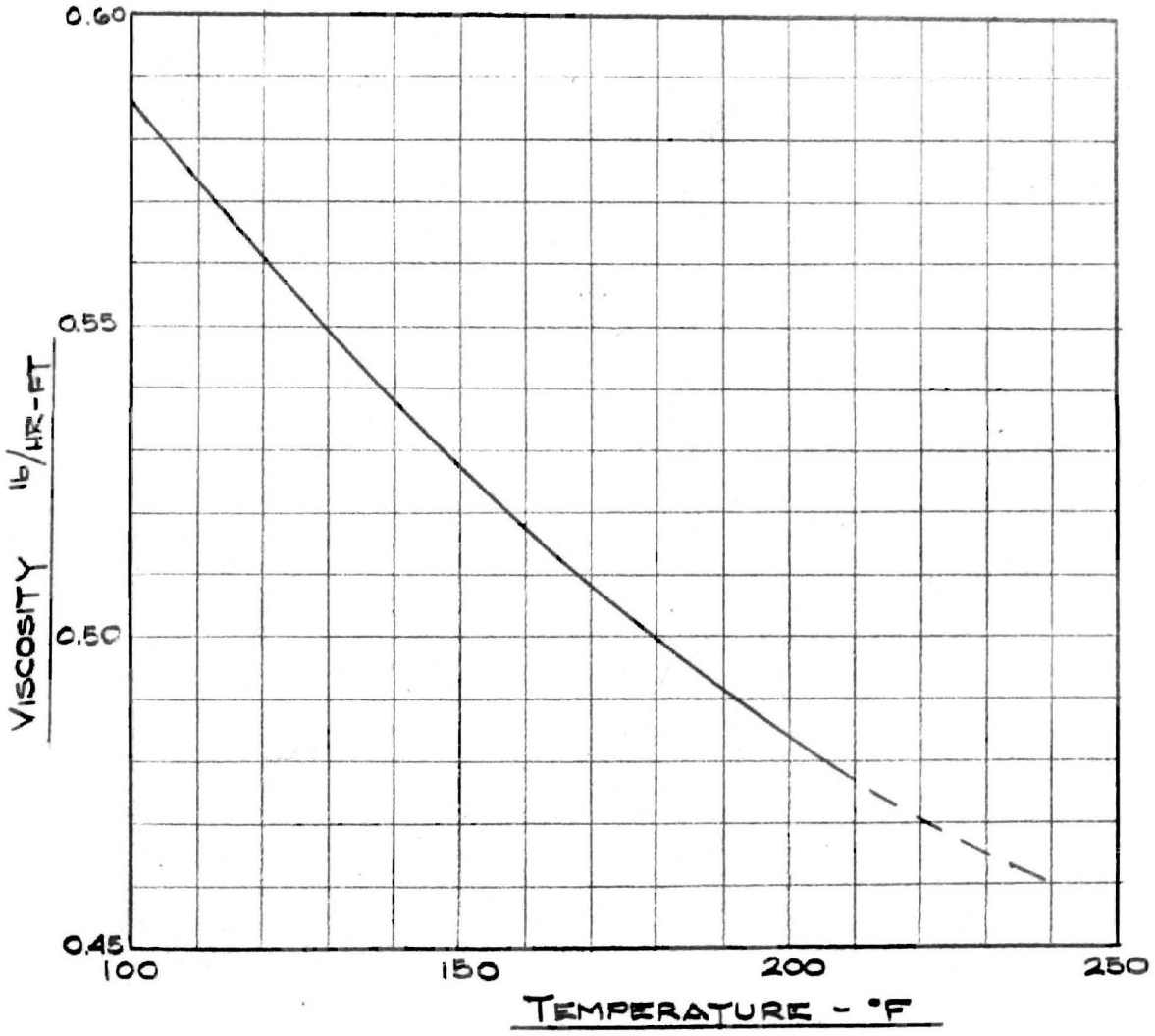

Figure 25. Viscosity of Liquid Freon 12, from Benning and Markwood (13)

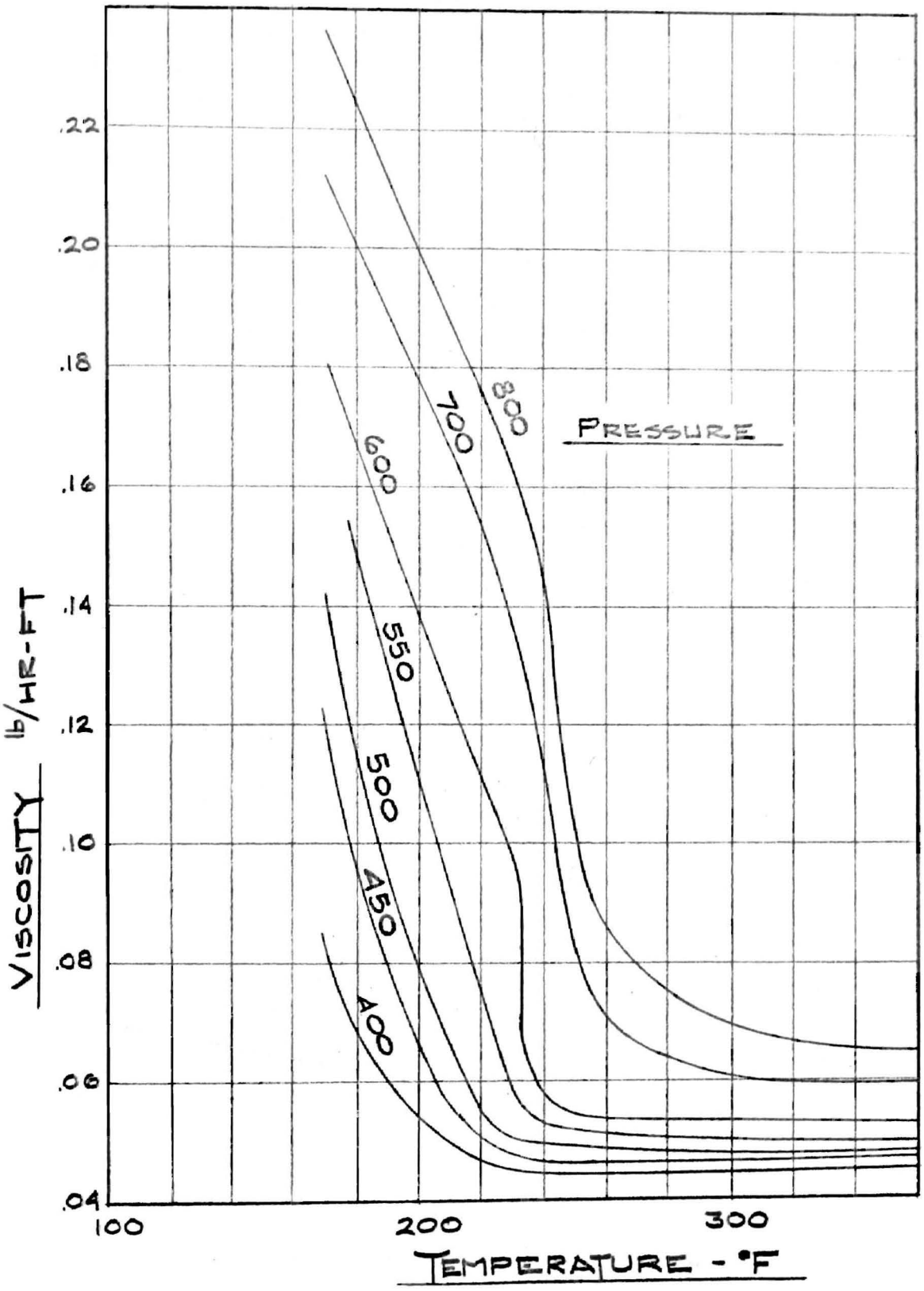

Figure 26. Estimated Viscosity for Superheated Freon 12

APPENDIX D

VENTURI CALIBRATION

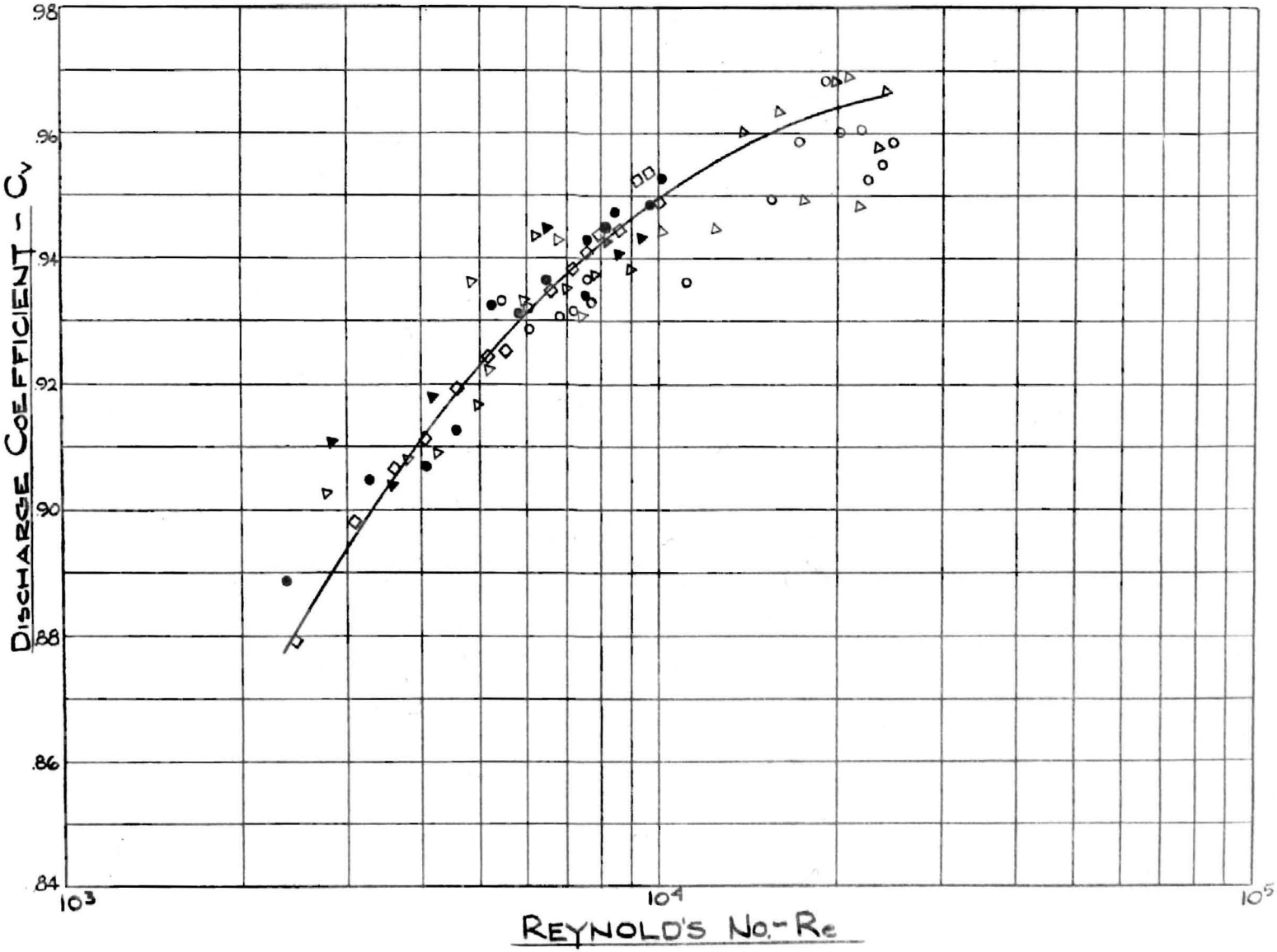

Figure 27. Venturi Calibration Curve

APPENDIX E

THERMOCOUPLE CALIBRATIONS

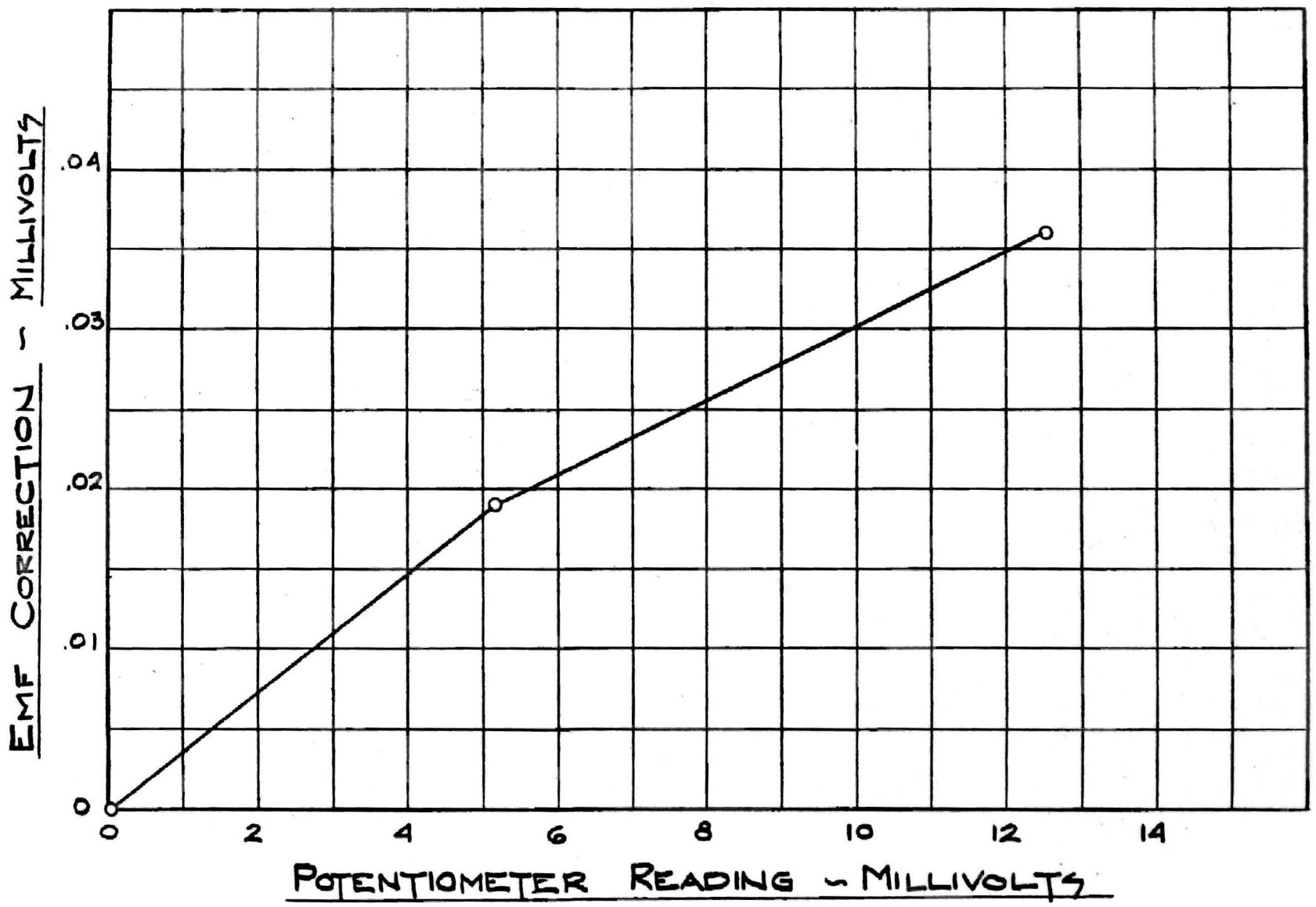

Figure 28. Bulk Thermocouple Calibration Curve

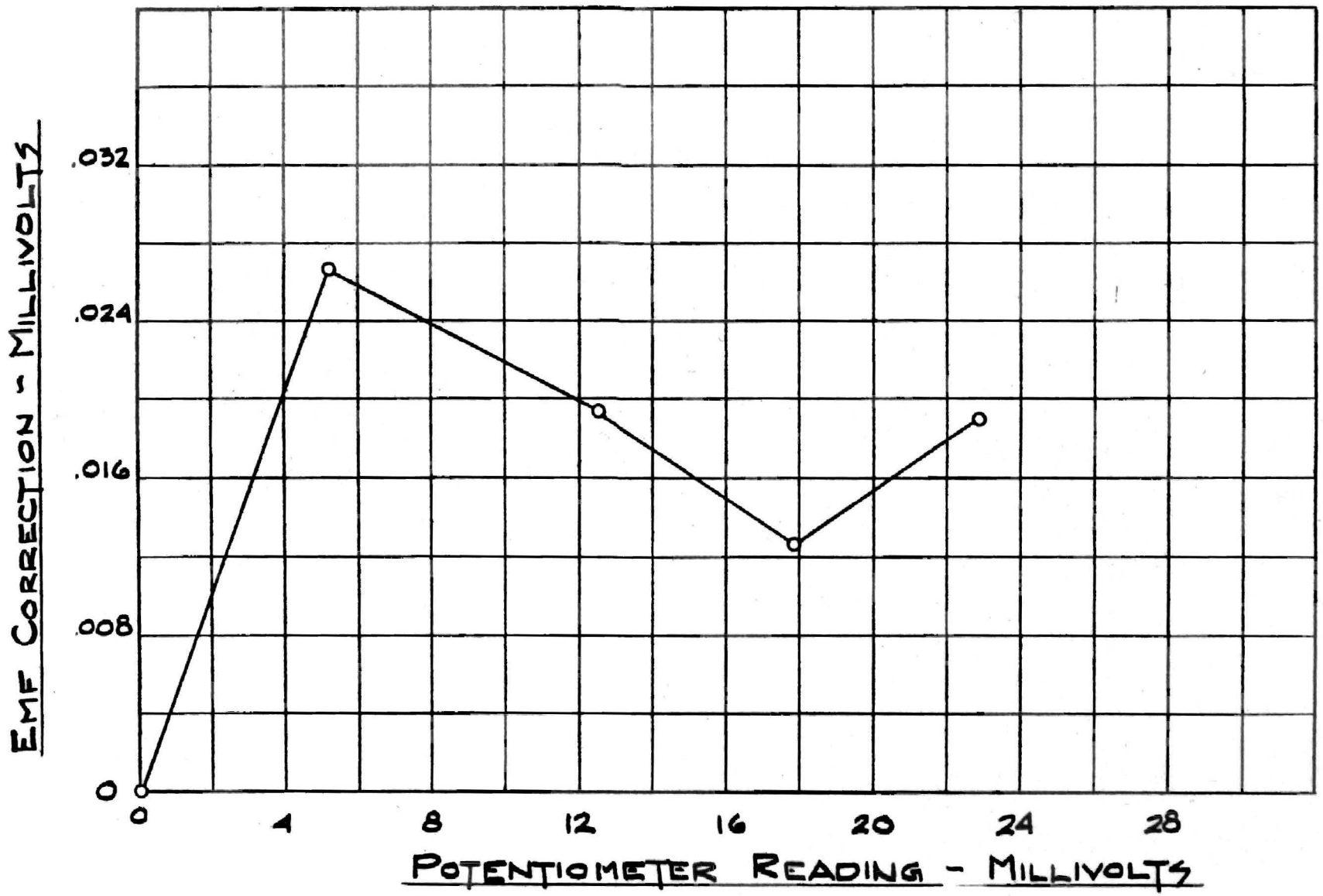

Figure 29. Wall Thermocouple Calibration Curve

APPENDIX F

PROPERTIES OF AISI TYPE 304 STAINLESS STEEL

The thermal conductivity and electrical resistivity values for the ISI type 304 stainless steel tubing were taken from reference (14). hese values are plotted in Figures 30 and 31.

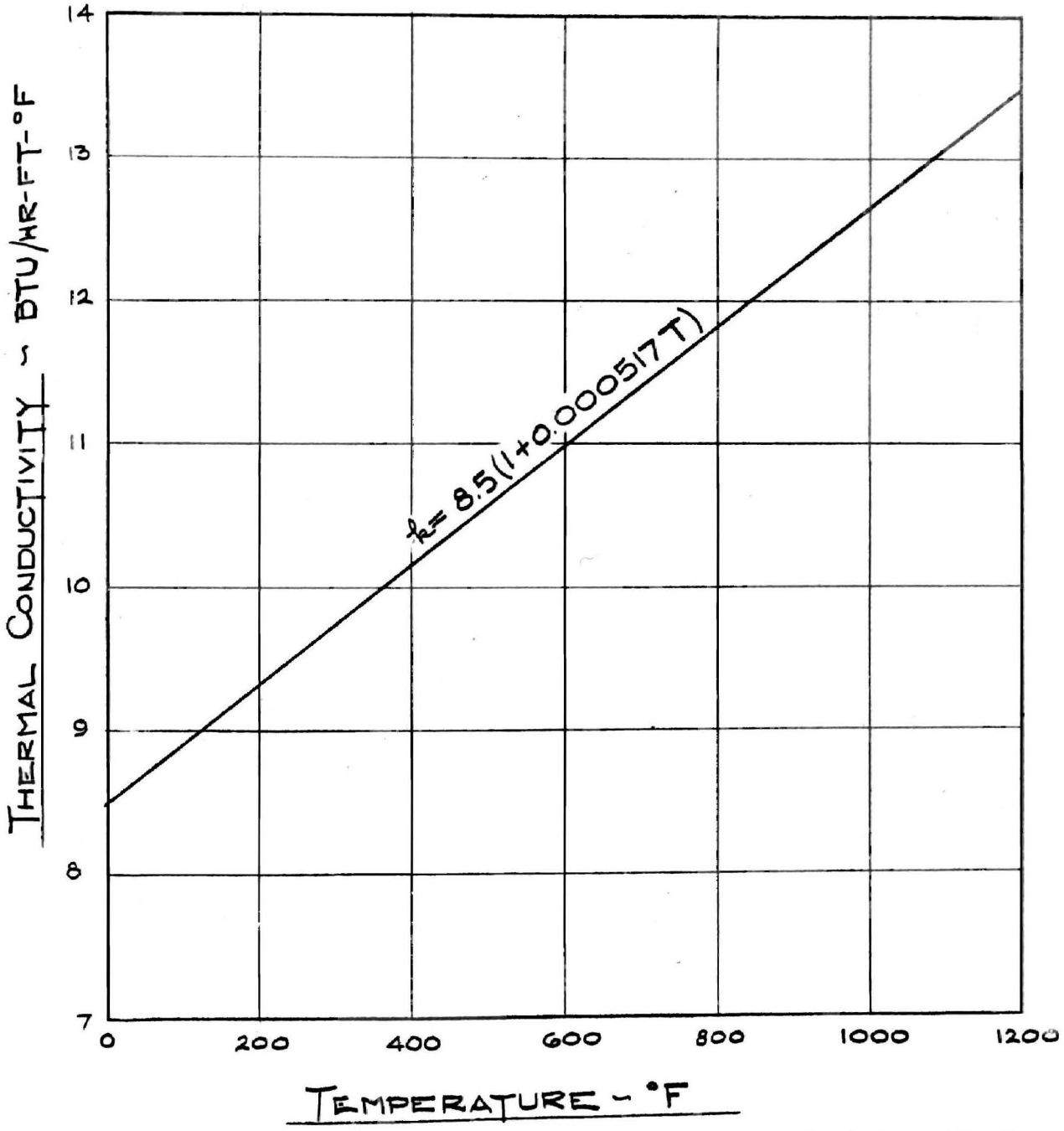

Figure 30. Thermal Conductivity of AISI Type 304 Stainless Steel

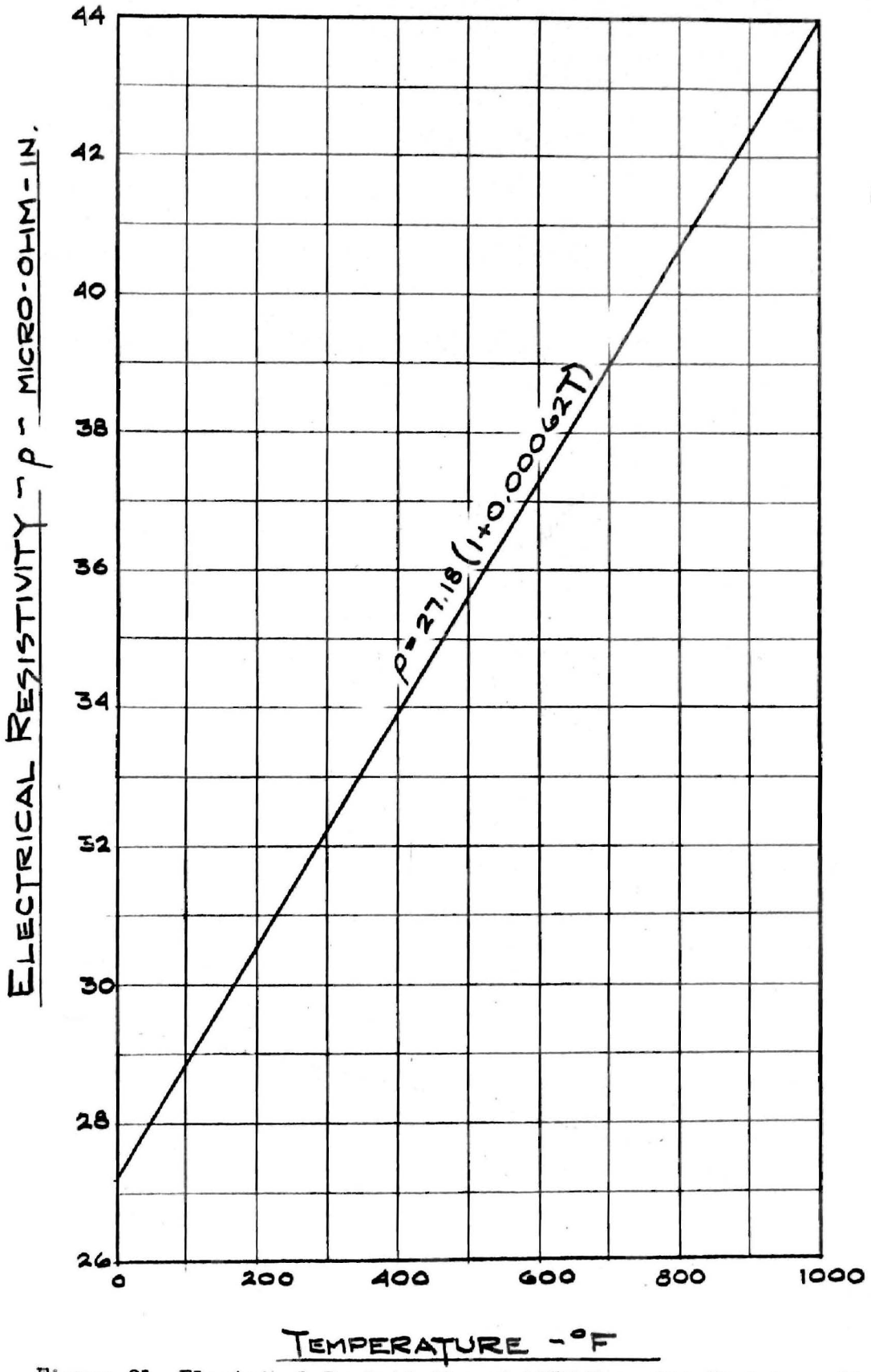

Figure 31. Electrical Resistivity of AISI Type 304 Stainless Steel

APPENDIX G

SYMBOLS

A	Area, ft^2.
A_d	Surface area of heat transfer element, ft^2.
A_i	Cross sectional area of tube, ft^2.
C_p	Specific heat capacity at constant pressure, Btu/lb_m-^oF.
d	A diameter, ft.
d_i	Inside diameter, ft.
d_o	Outside diameter, ft.
g	Gravitational constant, ft/hr^2.
h	Enthalpy, Btu/lb_m.
h	Heat transfer film coefficient, $Btu/hr-ft^2-^oF$.
I	Electric current, amperes.
k	Thermal conductivity, $Btu/hr-ft-^oF$.
k_a	Apparent thermal conductivity defined by equation IV-5, $Btu/hr-ft-^oF$.
l	A length, ft.
l_t	Length of test section, ft.
m	A variable defined by equation VII-4.
p	Pressure, consistent units.
q	Heat flow per unit time, Btu/hr.
r	A radius, ft.
r_i	Inside radius, ft.
r_o	Outside radius, ft.

t Temperature, °F.

t_b Bulk temperature, °F.

t_f Film temperature, °F.

t_n Temperature at a designated location, °F.

t_s Surface temperature, °F.

u Velocity, consistent units.

v Specific volume, ft^3/lb.

w Weight rate of flow, lb/hr.

x A distance, ft.

y Vertical distance between center of test section and center of heat exchanger, ft.

α Temperature coefficient of electrical resistivity, $1/°F$.

β Temperature coefficient of thermal conductivity, $1/°F$.

β Volume coefficient of expansion, $1/°F$.

γ Specific weight, lb/ft^3.

ρ Electrical resistivity, ohm-ft.

μ Dynamic viscosity, lb/hr-ft.

Dimensionless Groups

Gr Grashof number, $\frac{g d^3 \Delta t \beta \gamma^2}{\mu^2}$

Nu Nusselt number, $h d / k_e$

Pr Prandtl number, $c_p \mu / k_e$

Re Reynolds number, $\gamma u d / \mu$

St Stanton number, $h / c_p u \gamma$

Subscripts

b	Bulk conditions.
c	Critical conditions.
m	Mean conditions.
f	Film conditions.
s	Surface conditions.

VITA

Jack Philip Holman

Candidate for the Degree of

Doctor of Philosophy

Thesis: HEAT TRANSFER TO FREON 12 NEAR THE CRITICAL STATE IN A THERMAL SYPHON TYPE APPARATUS

Major Field: Engineering

Biographical:

Born: The writer was born in Dallas, Texas, July 11, 1934, the son of John H. and Bessie M. Holman.

Undergraduate Study: He graduated from Woodrow Wilson High School, Dallas, Texas, with honors, in January 1951. At that time he entered the School of Engineering at Southern Methodist University. He received the Bachelor of Science in Mechanical Engineering degree, with honors, from that institution in August, 1955.

Graduate Study: In September, 1955 the writer entered the Graduate School of Southern Methodist University. He received the Master of Science in Mechanical Engineering degree from that institution in August, 1956. In September, 1956 he entered the Graduate School of Oklahoma State University, where he completed the requirements for the Doctor of Philosophy degree in August, 1958.

Experience: The writer worked in the Industrial Engineering department of Collins Radio Company for four eight-weeks cooperative sections while at Southern Methodist University. He also worked as an engineer for Burden Air Conditioning Company for three eight-weeks cooperative sections. While working on the M.S. in M.E. degree at Southern Methodist University he served as a graduate teaching assistant and later a full time instructor. He taught courses in heat power laboratory, thermodynamics and analytic mechanics. While working on the Ph.D. degree at Oklahoma State University he also served as a graduate teaching and research assistant. He taught courses in various heat power laboratories and wind tunnel laboratory. He worked on research projects in heat transfer and two-phase, two-component flow. During the summer of 1957 the writer served as a senior propulsion analyst for Chance-

Vought Aircraft Inc. He also taught a thermodynamics couse for Southern Methodist University during the summer of 1957.

Professional Organizations: The writer is an Engineer-in-Training (Texas) and a member of the following professional organizations: American Society of Mechanical Engineers, Society of Automotive Engineers, Sigma Tau, and Kappa Mu Epsilon.